Final Technical Report

Stress-Assisted Corrosion in Boiler Tubes
(DE-FC36-02ID14243)

Project Period (03/01/2002 – 02/28/2006)

Preet M. Singh, (404) 894 6641, preet.singh@ipst.gatech.edu
School of Materials Science and Engineering
Georgia Institute of Technology
500, 10th Street, NW
Atlanta, GA, 30332

Steven J. Pawel, (865) 574 5138, pwl@ornl.gov
Oak Ridge National Laboratory
Bethel Valley Road
P.O. Box 2008
Oak Ridge, TN 37831-6156

04/30/2006

Acknowledgments

This report is based upon work supported by the U. S. Department of Energy Industrial Materials of the Future Program under Award No. **DE-FC36-02ID14243** ".

Authors would also like to thank Dr. W.B.A. Sharp from MeadWestvaco, Dr. Ray Vasudevan from International Paper, John Hainsworth from B&W, and Dr. Peter Gorog from Weyerhaeuser Company for their advise and support in this project. Representative boiler tubes from the Weyerhaeuser Longview mill were provided by D. Rittenbach (Weyerhaeuser). A. Willoughby (ORNL) managed photography and specimen handling for the SAC investigation. Tube panels were flame cut longitudinally into manageable sections for handling by L. Smarsh (ORNL). Circumferential wave inspections were performed by M. Cooper, J. Gustafson, and S. Shankles (Longview Inspections). Longitudinal wave inspections were performed by M. Quarry (Lawrence Livermore National Laboratory) and J. Brignac (Alstom Power). Radiographic inspections were performed by R. Sweet and C. Culbertson (Longview Inspections). Following the various inspections, tubes were saw cut into sections to facilitate visual inspections and metallographic sampling by B. Gaskin (ORNL). H. Longmire (ORNL) prepared and photographed the metallography specimens. L. Walker (ORNL) performed the SEM and microprobe analyses. Along with P. Singh (Georgia Institute of Technology), D. Wilson and P. Tortorelli (ORNL) reviewed the draft manuscript, and F. Stooksbury and K. Choudhury (ORNL) helped prepare the final document. Help of Mr. Jamshad Mahmood, and Dr. Jorge Perdomo and other researchers at IPST @ GaTech, who worked on this project, is greatly appreciated.

Content

LIST OF TABLES

LIST OF FIGURES

magnification view of the deepest penetration associated with this particular attachment weld (bottom). A decarburized layer is marked with an arrow in the lower photograph. Note the weld-rounded features of the SAC indication and the fact that it is almost as wide as it is deep.

Figure 3.2.6. Cluster of SAC indications on the ID of a boiler tube showing that only one indication appears to be propagating. The attachment weld in this case is just out of the photograph at the upper left. All of the indications are bulbous, rounded at the tip, and filled with oxide. Note also the thick oxide accumulation on the ID surface that tends to obscure the SAC indications from visual detection.

Fig. 3.2.7. SAC indications that appear to be propagating from a pit on the tube ID. As-polished.

Fig. 3.2.8. Backscattered electron microscopy of a typical SAC indication on the tube ID. The top photograph shows the entire SAC indication, and the bottom photograph is a higher magnification view of a portion of the oxide in the penetration. Relatively light colored corrosion product has an Fe/O ratio consistent with Fe_3O_4, and the relatively dark product has an Fe/O ratio consistent with Fe_2O_3.

Figure 3.2.9. Pictures showing a tube section with external attachment weld removed from a boiler. Removal of oxide scale from internal surface reveled clear signs of SAC cracks in the area of attachment weld.

Figure 3.2.10. Pictures showing a tube section with external attachment weld removed from a boiler. Removal of oxide scale from internal surface reveled clear signs of SAC cracks in the area of attachment weld.

Figure 3.2.11. Micrographs showing a typical SAC crack. Micrograph also shows clear signs of grain growth and de-carburized layer at the inner surface of tube.

Figure 3.2.12. Micrograph also shows clear signs of very prominent grain growth and de-carburized layer at the inner surface of tube. This is not a typical case but was seen in a few tubes examined at Corrosion Lab and Georgia Tech.

Figure 3.2.13. Micrographs showing grain growth and de-carburized layer at the inner surface of the failed boiler tube. Notice that the crack seems to have stopped at the interface of decarburized layer and typical pearlitic microstructure of the carbon steel tube. This is very common feature found on most of the tubes showing grain growth.

Figure 3.2.14. Typical microstructure difference for the tubes showing grain growth and de-carburized layer at the inner surface.

Figure 3.2.15. Micrographs showing microhardness indents in the areas of grain growth and de-carburized layer as well as normal carbon steel tube structure. Notice that the indent size decreases away from the tube surface.

ABBREVIATED TERMS

ASTM	American Society for Testing and Materials
CW	circumferential wave
EPRI	Electric Power Research Institute
ESP	emergency shutdown procedure
ID	inside diameter
LW	longitudinal wave
NDE	non-destructive evaluation
ORNL	Oak Ridge National Laboratory
SAC	stress-assisted corrosion
TC	thermocouple
CF	Corrosion Fatigue
SCC	Stress Corrosion Cracking
AFM	Atomic Force Microscope
FEM	Finite Element Modeling

EXECUTIVE SUMMARY

Water touched surfaces of industrial boiler tubes are susceptible to blunt discontinuous cracking generally referred to as stress-assisted corrosion (SAC). SAC is generally observed on the waterside of carbon steel boiler tubes at locations exhibiting the combination of a substantial external attachment weld, at tube bends, or at other areas with high stress. SAC under the weld-attachment are generally associated with a significant internal oxide accumulation compared to a thin protective magnetite (Fe_3O_4) film found on the internal surface of boiler tubes. Non-destructive evaluations were not effective for detecting SAC, but metallographic evaluations revealed wall penetrations up to 30% of the tube thickness that were transgranular with bulbous features, rounded tips, and filled with a relatively dense oxide. These oxides were found to have alternating layers of Fe_2O_3 and Fe_3O_4.

An autoclave with recirculation-loop was set up to simulate boiler-waterside environment in laboratory to systematically evaluate the role of key industrial boiler design and environmental parameters in initiation and propagation of SAC in the laboratory. Parameters like stress amplitude, water chemistry (i.e. oxygen concentration, pH or conductivity, etc.) can be individually studied in a controlled environment. Effect of these parameters individually was quantified to help develop mitigation strategies to avoid SAC in industrial boilers. This setup was designed and put-together to help us carryout required experiments to understand the SAC mechanism.

A Hastelloy-C autoclave with three liters capacity and design pressure of 3500 psi and design temperature of 350^{o}C was used for corrosion tests. A specially designed slow strain rate test rig was fitted on the autoclave such that the test samples could be exposed to the test water and strained at slow strain rate. Fixtures were made to allow tensile and compact samples to be tested in this facility. Low frequency fatigue loading could be applied to the test samples by controlled reversing of stroke direction.

Recirculation loop is designed to allow monitoring and control of water chemistry during the test. A 100-liter storage/makeup tank was used to control dissolved oxygen level and to add other chemicals needed to simulate different boiler chemistries. A high pressure pump with pressure valve controlled the recirculation loop pressure between the autoclave and the makeup-tank. Water exiting the autoclave is further cooled by using a series of heat exchangers where the temperature of water is controlled below 50^{o}C. Various sensors are used to monitor and control the water chemistry which includes oxygen concentration, pH, redox potential, and conductivity. Water samples are taken to test water for dissolved chemicals. Metal concentration is monitored by using inductively coupled plasma spectroscopy (ICP). Concentrations of other added chemicals to control oxygen levels can be

regularly measured by electrophoresis, colorimetric and/or titration based methods.

Use of carbon steel for the service of high temperature water applications strongly depends upon the formation and stability of the protective magnetite film, Fe_3O_4, on the waterside surface of boiler tubes. Tests were carried out in a recirculation autoclave under industrial boiling water conditions. Boiler water chemistry was controlled during a series of tests to keep the dissolved oxygen in the range of 10 ppb - 10 ppm. Tests were conducted to develop the magnetite film on carbon steel tube samples under different test conditions. Results have indicated that the water chemistry and ratios of anode/cathode have an effect on the magnetite film morphology. Film characterization by atomic force microscopy (AFM) and scanning electron microscopy (SEM) has shown that the magnetite film changes from a fine-grained porous film with tetrahedral crystals at the surface to an irregular-grained compact and protective film when the anode to cathode area is decreased. Corrosion fatigue crack initiation and growth mechanisms involved in boiler water environments include magnetite film damage as an important step. Slow strain rate tests were carried out in simulated boiler water environments, using smooth carbon steel samples, to investigate the role of temperature and water chemistry on crack initiation. Results from the tensile samples tested in boiler water with oxygen and oxygen below 5-ppb have shown that the percentage area reduction & fracture strain of the tensile specimen decrease with an increase in the stress amplitude. The results from SSRT and low-frequency tests indicate that the strain rate affect SAC initiation and growth in boiler water environments.

An operating recovery boiler was instrumented with strain gages and thermocouples near/around an attachment weld associated with a manway to assess the relative magnitude and frequency of strain events in the boiler. The data from this boiler suggest that the strains associated with shutdown/restart events, including emergency shutdown procedures (ESPs), are of a magnitude potentially associated with the initiation of SAC at a few locations close to the attachment weld. The strains associated with steady-state operation and the minor perturbations thereof are very modest and unlikely to be associated with SAC initiation or propagation.

A finite element model has been developed to perform thermal and mechanical analyses of tube wall panels containing attachment welds in order to examine the effect of the attachment weld on the stress/strain distribution in the tubes. Consistent with field observations of SAC, the results of the analyses show that effects of the attachment weld are confined to a short section of the tube close to the attachment weld and that the constraint from the weld on the free expansion of the tube alters the stress distribution near the weld. The variation in hoop stress at the waterside surface during a normal operating cycle is different for tubes with and without an attachment weld, and provides a possible explanation for the observation of SAC

limited to regions very near the attachment welds. Modeling results for tube wall panels made of co-extruded composite tubing suggest these may be less susceptible to SAC than their plain carbon steel counterparts due to more favorable distribution of stresses. In the present state of model development, variations in the attachment weld parameters and the properties of the base metal (e.g. a decarburized layer) have relatively little effect on the trends indicated by the model.

The goal of this project was to clarify the mechanism(s) of stress-assisted corrosion (SAC) of boiler tubes for the purpose of determining key parameters in its mitigation and control. To accomplish this, the R&D partners and industry contributors used information gathered across multiple industries, and by making in-situ measurements of boiler tube-strain in operating boilers, and perform laboratory simulations of SAC. Through these activities, significant environmental, operational, and material characteristics were identified to reduce the frequency and severity of SAC. Results from this project can be used to control SAC in boilers and increase operating efficiencies represented by decreased downtime (greater intervals between inspection and maintenance cycles) with associated energy and cost savings.

1. INTRODUCTION

Stress-assisted corrosion (SAC) is a broad term given to waterside corrosion of carbon steel boiler tubes that occurs as a result of a combination of stress and corrosion. In the simplest sense, the mechanism can be described [1-4] as a localized failure of a nominally protective magnetite (Fe_3O_4) film resulting from mechanical and/or thermal stresses on the tube, thus permitting the corrosive medium – in this case, high temperature water/steam inside the boiler tubes – access to the substrate to advance steel corrosion at the location of film failure. Significant general thinning of the tubes from the waterside is not typically a factor in SAC – only localized corrosion in/around locations of frequent film failure. Depending on the water quality and heat transfer conditions during the periods of film failure, the resulting corrosion may be relatively modest with rapid repassivation or sufficiently severe to cause significant penetration of the tube wall.

Experience with SAC in boiler tubes suggests that internal surfaces immediately adjacent to external (non-pressure) attachment welds on the boiler tubes are particularly susceptible to development of SAC, due to thermal or mechanical effects concentrated at the attachment location [1,2,5,6] or perhaps relative anodic behavior of the stressed region at/near the attachment [7]. Most commonly, SAC tends to be manifested in short clusters of indications resembling cracks perpendicular to the associated attachment weld. Because of the myriad of stress and water composition variables involved, no specific rate (or even bounding rate) has been determined for the SAC processes. In the strictest sense, the occurrence of SAC may be independent of the boiler age [8], but it tends to be a relatively slow process and is most commonly found in boilers that have been operating for at least ten years [3,7].

Based largely on discussions and findings associated with a boiler-industry-wide colloquium in July 2000, Sharp [9] published an extensive overview of the history of SAC in boilers representing the full range of industries. In his overview, Sharp noted that the Electric Power Research Institute (EPRI) took a leading role in research to explain and control boiler tube problems of this type in the utility industry in the late 1980s. Over the next ten years, EPRI developed a detailed mechanism and control scheme to avoid formation and growth of crack-like waterside indications termed corrosion fatigue in the utility industry. While the corrosion fatigue identified by the utility industry was no doubt similar to what the pulp and paper industry termed SAC, the colloquium attendees were not convinced that EPRI's mechanism and feedwater chemistry recommendations were necessarily relevant to recovery boilers. In particular, attendees cited significant differences in water treatment issues between utility boilers and recovery boilers (very large make-up water fraction in recovery boilers, different chemicals and treatment strategies) and the wide range of microstructural characteristics ascribed to SAC and corrosion fatigue as evidence that the details of the phenomenon and the EPRI recommendations might not apply to all boilers.

This research project was initiated to examine details of the initiation and propagation of SAC in recovery boiler tubes. One of the objectives of this project was to develop a pressurized test facility for simulating boiler tubing waterside conditions to duplicate SAC in steel specimens and to manipulate critical variables to understand the mechanisms associated with this phenomenon. Other project objectives included failure analysis of boiler tubes to understand the role of microstructure on SAC initiation and propagation, to examine non-destructive detection schemes for SAC in recovery boilers, to understand the reason for failure localization near attachment weld through measurements and to initiate a modeling effort to identify the role of attachment welds in the predominance of SAC.

Although the corrosion fatigue studied by EPRI and SAC in industrial boilers may be limiting cases of the same phenomenon, the cause(s) of SAC were not understood and the magnitude of industrial problem required a research program to understand this connection and develop general guidelines to mitigate it.

The goal of this project was to clarify the mechanism(s) of stress-assisted corrosion (SAC) of industrial boiler tubes for the purpose of determining key parameters in its mitigation and control. To accomplish this, the R&D partners and industry contributors initially used the information gathered across multiple industries. Later, in-situ measurements of strain and finite element method (FEM) were used to understand the localization of this failure near attachment welds. A laboratory simulation facility was developed in this project to simulate boiler environment and stress conditions in laboratory for SAC. Through these activities, significant environmental, operational, and material characteristics will be identified to select parameters for each which reduces the frequency and severity of SAC.

This project used a team approach including industry contributors and research organizations to bring together the required experience, information, and financial and technical resources to accomplish the proposed tasks. The project was coordinated and managed by the Georgia Institute of Technology whereas a industrial advisory committee was formed for directing the project, with members from among the participating (in-kind) companies and experienced individuals who monitored progress and provided information and materials as appropriate. Technical execution of the project was accomplished primarily by Oak Ridge National Laboratory (ORNL) and GaTech.

Results from this project are relevant to the wide range of industry, including the chemical, petrochemical, and pulp and paper companies that operate boilers, the manufacturers of these boilers, the water treatment firms that are responsible for water quality; and the consultants and failure analysis experts that address boiler problems.

1.1 References for Introduction:

1. Electric Power Research Institute, EPRI-TR-100455, "Corrosion Fatigue Boiler Tube Failures in Waterwalls and Economizers – Volume 4: Summary Report and Guidelines for Corrosion Fatigue Evaluation," prepared by Ontario Hydro, Toronto, Canada, December 1993.
2. Sylvester, W. R., "Waterside Corrosion Fatigue Cracking – Is There a Single Cause and Solution?" ABB C-E Services TIS 8318, Combustion Engineering, Inc, Windsor, CT, 1987.
3. Sylvester, W. R. and Sidla, G., "Waterside Stress-Assisted Corrosion Cracking in Boilers," Pulp and Paper Canada, Vol. 91, No. 6 (1990) p.T248.
4. Schoch, W. and Spahn, H., "On the Role of Stress-Induced Corrosion and Corrosion Fatigue in Water-Wetted Boiler Components," in Corrosion Fatigue: Chemistry, Mechanics, and Microstructure, NACE, Houston, TX (1972) p.52.
5. Dooley, R. B., "A Vision for Reducing Boiler Tube Failures," Power Engineering, Vol. 96 (1992) p. 33.
6. Gabrielli, F., "An Overview of Water-Related Tube Failures in Industrial Boilers," Materials Performance, Vol. 27, No. 1 (1988) p.51.
7. Esmacher, M. J., "Stress-Enhanced Corrosion of Boiler Tubing," Materials Performance, Vol. 26, No. 5 (1987) p. 17.
8. Masterson, H. G., Castle, J. E., and Mann, G. M. W., "Waterside Corrosion of Power Station Boiler Tubes," Chemistry and Industry (1969) p. 1261.
9. Sharp, W. B. A., "An Overview of Stress-Assisted Corrosion in the Pulp and Paper Industry," National Association of Corrosion Engineers 2004 Annual Conference and Exhibition, March 28-April 1, 2004, New Orleans, LA, *Corrosion2004* Paper 04513.

2. BACKGROUND

Casing-side tube leaks in water-filled utility boiler tubes were first reported in the 1960's[1]. At that time the leaks were attributed to "outside-in" cracks. Increasing awareness of similar leaks in both furnace and economizer sections was documented in some publications in the late 1970's. In the late 1980's, the two major US manufacturers of black liquor recovery boilers issued notices to alert the pulp and paper industry about the problem. The service bulletin from Babcock and Wilcox called it "stress-assisted corrosion" and the paper industry continued to use this term. In the utility industry, a related phenomenon entitled corrosion fatigue cracking had been recognized as a major cause of tube failures and reduced availability in utility boilers since 1983. In the utility industry the mechanism of cracking of boiler and economizer tubes from the waterside is generally referred as corrosion fatigue cracking of boiler tubes and has been recognized as a major cause of tube failures and reduced availability in utility boilers [1,2]. The Electric Power Research Institute (EPRI) began a research project to study the problem in the late 1980's [1]. In 1992 EPRI identified corrosion fatigue as the leading cause of availability loss in fossil fuel fired utility boilers. By then it was known to occur on the water side of pressure/non-pressure attachments in water-filled tubes, e.g. at windbox attachments, tie bars, scallop bars, seal plates and other locations that are solidly welded together. EPRI noted that these failures had often been incorrectly identified as weld defects or stress-corrosion cracks. The waterside corrosion fatigue found in utility boilers was found to be strongly influenced by boiler water chemistry, particularly oxygen content, pH, chloride and sulfate content, as well as by number of start-ups, operating hours and chemical cleans.

Waterside corrosion problems are also experienced by industrial boilers where the temperatures, resulting boiler pressures, and water chemistries can be significantly different. In the pulp and paper industry, any water leak into the boiler can potentially cause smelt/water explosion and has led to a number of fatal accidents. In the late 1980's, US manufacturers of black liquor recovery boilers for the pulp and paper industry realized this potential problem and a number of publications came out describing this type of cracking as stress assisted corrosion (SAC) [3-6]. In May 1991, the fatal rupture of a floor tube in a recovery boiler in a Missoula, MT paper mill initiated increased concern about SAC in the US paper industry.

During the last 20 years, a number of US paper companies needed to replace lower furnace tubes or decommission many recovery boilers due to stress-assisted corrosion (SAC) on the waterside of boiler tubes. In fact, more than half of the power and recovery boilers that have been inspected reveal SAC damage, which portends significant energy and economic impacts. SAC is indicated by crack-like fissures that initiate and propagate on the waterside

of boiler tubes, typically near external attachment welds. Such cracks potentially violate most state boiler operation laws and codes, and are very difficult to detect and quantify. However, propagation of SAC (with or without concomitant external corrosion) can lead to de-rating of boilers and tube failures, possibly resulting in potential smelt-water explosions and extended downtime for maintenance or repairs.

SAC is typically associated with pressure/non-pressure attachments in boiler waterwalls and economizers. Such locations are windbox attachments, tie bars, scallop bars, seal plates and locations solidly welded together like areas with thick attachment welds from the cold-side of tubes are most common sites for SAC failures. Boiler operation guidelines or best practices to avoid corrosion fatigue in the utility power industry came out of EPRI projects and are typically followed in the utility industry [1, 2].

Studies by Schoch and Spahn [7] showed that the morphology of SAC produced in controlled corrosion fatigue tests depended critically on the oxygen content of the water environment. This research was concerned with corrosion fatigue cracking in the low-pressure environments of industrial deaerators. Esmacher [8] reported five case histories on the effect of residual stresses (from fabrication or welding) on the water-side corrosion performance of carbon steel boiler tubing. Cases are reviewed in which tube swaging or bending operations producing high forming stresses in deformed zones resulted in the formation of stress-enhanced corrosion cells. The phenomenon of accelerated corrosion in welded support zones, membrane-welded panel sections, and weld-repaired areas was discussed. A number of publications described corrosion fatigue problem in carbon steel tubes in utility boilers [8-11].

Although SAC has been reported in industrial boilers in other parts of the world, the small amount of research that has been done elsewhere has focused more on the related phenomenon of deaerator cracking. Studies by Scooch and Spahn in Germany showed that the morphology of SAC produced in controlled corrosion fatigue tests depended critically on the oxygen content of the water environment. This research was concerned with corrosion fatigue cracking in the low-pressure (with occasional water hammer) environments of industrial deaerators. It did not produce guidelines for boiler water quality to eliminate SAC. Paper mills in other parts of the world generally inspect less for SAC than do US mills. As far as we have been able to learn, no other country is developing technology to control SAC.

SAC in recovery boilers appears to have some similarities to the waterside corrosion fatigue cracking previously studied in fossil fuel power boilers by the EPRI, but the hazards associated with leaks in recovery boilers and the differences in feed water chemistry and operation make it difficult to extrapolate the results of the EPRI research to recovery boilers.

While no specific factors have been universally associated with SAC, some elements that appear to have a significant influence on SAC include (a) local operational and residual stresses, particularly associated with attachment welds, (b) corrosive conditions in the boiler feed water, including temporary upset conditions, and (c) cyclic thermal stresses. Work from our study also indicates the initiation of cracking may also be associated with local variations in properties of the boiler tube material. Non-destructive testing experts agree that new/advanced techniques show promise for detecting and quantifying SAC in early stages.

Boiler tube leak in utility boilers may lead to lower energy efficiency. However, some of the industrial boilers like recovery boilers in the pulp and paper industry may experience a smelt/water explosion, if water leaks into the furnace. In some boilers, where SAC is expected or is detected, boiler pressures have to be reduced to avoid failures or the boiler has to be shut down to remove and replace affected tubes. In all above stated scenarios, there is significant energy loss and safety risk to the boilers. Radiographic techniques for semi-quantitative estimation of the depth of stress-assisted cracks, originally developed by Buckeye Cellulose and INDT, were widely used to survey recovery boilers for SAC in the 1990s.

Use of carbon steel in high temperature water applications strongly depend upon the formation and stability of protective magnetite, oxide film on the waterside surface of boiler tubes. A significant volume of work was published on the mechanisms of magnetite growth and resulting oxide film morphology under different high temperatures in high purity water or caustic solutions [12-15].

Dooley [1] reported that the corrosion fatigue of carbon steel tubes is strongly influenced by water chemistry where the oxygen is the major factor. Results from phosphate chemistry water tests indicate that a two-orders-of-magnitude increase in dissolved oxygen from 10 ppb to 1000 ppb may decrease the number of thermal cycles required to initiate corrosion fatigue cracks by an order of magnitude (from about 1000 to about 100) [1]. This type of increase is associated with boiler startup when the thermal strains are also greatest. Dooley also reported that the decreasing pH and increasing boiler chloride or sulphate levels have a secondary effect on corrosion fatigue failures where the corrosion fatigue susceptibility increases. Other factors that may influence the corrosion fatigue behavior of boiler tubes are number of unit starts, operating hours, and number of chemical cleanups. Depending upon the water chemistry operating parameters, the stress range needed to cause corrosion fatigue changes. As the water chemistry deviates from the optimum boiler water chemistry, the stress required to initiate corrosion fatigue decreases. This may explain a large variation of corrosion fatigue or SAC occurrence from one boiler to another or from one area in boiler to another due to possibilities of variation in water chemistry as well as stress due to attachment welds or other

sources [1] .

This present project is aimed at developing an understanding of SAC in industrial boilers with special emphasis on the recovery boilers in the pulp and paper industry. Water chemistry and other operating parameters for industrial boilers can be significantly different from the fossil fuel boilers in the utility industry. A number of variables related to the boiler operation, environment and stress may influence the occurrence of SAC in industrial boilers. However, individual parameters cannot be easily controlled or studied in a working boiler to evaluate their effect on SAC. Control can be achieved in a constructed laboratory environment. The first step to do so is to establish a setup to simulate boiler conditions in laboratory. A recirculation-loop autoclave facility was developed to simulate industrial boiler environments. This equipment was used to investigate the effects of water chemistry and stress parameters on the overall SAC initiation and propagation in carbon steel tubes.

Mechanisms of SAC in boiler water environment can be identified and duplicated in a laboratory. This was done so that appropriate environmental (water treatment and chemical cleaning), operational (thermal stresses, attachment weld design/location), and material (mechanical properties, composition of base material and oxide films) options can be selected to reduce the severity and frequency of SAC. Further, identification of boilers with certain "risk factors" for SAC could lead to risk-based inspections which encompass frequency and scope for individual boilers.

Simulation of boiler water conditions permitted systematic evaluation of the role of key design and environmental parameters in a laboratory system. Their individual or combined effects on SAC could then be quantified and mitigation strategies can be developed to avoid SAC. For example the effect of stress amplitude, water chemistry (i.e. oxygen concentration, pH or conductivity, etc.) can be individually studied. Under normal operation, boiler tubes are protected by a magnetite film on the steel surface.

Previous work has suggested that damage to the magnetite film plays an important role in SAC initiation and growth. A series of tests were carried out to characterize formation and growth of oxide film under different environmental conditions in the autoclave system. It was found that the stability of protective magnetite film on steel surface depends on various environmental factors including "oxidation potential" of water, pH, temperature, anode to cathode ratios and other variables. Results from the lab simulations as well as from the strain measurements have indicated that the stress assisted corrosion in boilers may occur due to "upsets" in the boiler water chemistry and especially during boiler shutdown and startup periods.

Corrosion resistance of the boiler tube material on the waterside is fundamentally controlled by the stability of the oxide film formed on the surface. A number of factors influence the oxide film stability, such as base composition and microstructure (including carbide and inclusion distribution) and, as a result, these material properties are expected to contribute significantly to the occurrence of SAC. Further, resistance to cracking of the material at disruptions in the oxide film is influenced by a number of physical properties of the material, such as strength and grain size, as well as by the changes in microstructure developed during fabrication, such as welding and bending. It was found that that properties and condition of the tube material is a significant variable in SAC.

To evaluate the key material characteristics associated with SAC and to support laboratory simulation efforts, information from past inspection reports and failure studies was analyzed for relevant patterns implicating the prominence of particular material features or properties related to SAC. Further, tube specimens representing boilers with evidence of SAC as well as boilers with little or no evidence of SAC were examined using metallography, surface analytical techniques, and mechanical tests to find features of the base material and/or oxide film correlating with SAC. In addition, inspection records were evaluated to attempt to quantify the rate of SAC propagation as a function of material and operating variables. However, it was found that the record with water treatment and boiler inspection companies was not complete to be useful for understanding all factors involved in SAC in boilers.

Previous experience with SAC in recovery boilers indicates that suspect regions are typically associated with attachment welds on the cold side of the furnace, although SAC also has been identified on the fire side of tubes near hanger welds associated with construction. Although no theory had earlier been developed to account for specific weld designs and features but the combination of residual and operating stresses (>0.2% strain identified as significant) associated with the welds, as well as perhaps increased restraint associated with thermal excursions, contribute to cracking in these locations. To support this information, strain gages were placed on the cold side of a operating boiler to measure total strains and nominal fluctuations for over one year. Modeling to determine stresses/strains on the inside of the tubes was undertaken to relate the external measurement to the value of interest and to assess potential for the propagation of cracks.

Results from this project were reported to the U. S. companies, for whom SAC is a significant issue, via a number of publications, presentations and meetings. Audience for these publications and presentations included personnel from the chemical, petrochemical, and pulp and paper companies that operate boilers; the manufacturers of these boilers; the water treatment firms that are responsible for water quality; and the consultants and failure analysis experts that address boiler problems.

3. RESULTS AND DISCUSSION

Overall project was divided into five main tasks which were carried out at GaTech and ORNL. Main tasks for this project are following:

- Laboratory Simulation of SAC
- Material Characterization
- Evaluation of Stress Effects
- Finite Element Modeling
- Evaluation of Environmental Effects

Results from every task have been discussed separately along with the appropriate, background, literature review, experimental details, results and discussions. Related references have been given at the end of each result section to make it easy for the reader to find a relevant reference.

3.1. LABORATORY SIMULATION OF SAC

Autoclave with recirculation-loop was used to simulate industrial boiler environments. A series of tests were carried out to investigate the effect of water chemistry and stress parameters on the overall SAC initiation and propagation in carbon steel tubes. Effect of parameter, individual or combined effect, on SAC initiation and propagation was quantified.

As stress is an important component of SAC, stresses can either be applied as constant strain, as in U-bend or rigid-fixture tensile samples. However, these techniques are less reproducible than constant extension rate tests or slow strain rate tests (SSRT). Therefore, along with the recirculation-loop autoclave, a tensile test rig was also designed and manufactured to test materials in boiler water environment. Low frequency cyclic loading could be applied on test samples by reversing the motor direction.

Simulation of boiler water conditions permitted systematic evaluation of the role of key design and environmental parameters in a laboratory system. For example the effect of stress amplitude, water chemistry (i.e. oxygen concentration, pH or conductivity, etc.) can be individually studied. Under normal operation, boiler tubes are protected by a magnetite film on the steel surface. Previous work has suggested that damage to the magnetite film plays an important role in SAC initiation and growth. A series of tests were carried out to characterize formation and growth of oxide film under different

3.1.1 Closed-loop Autoclave for Boiler environment simulation

An autoclave with recirculation-loop was set up to simulate boiler-waterside environment in

laboratory to systematically evaluate of the role of key industrial boiler design and environmental parameters in initiation and propagation of SAC in the laboratory. Parameters like stress amplitude, water chemistry (i.e. oxygen concentration, pH or conductivity, etc.) can be individually studied in a controlled environment. Effect of these parameters individually or in select combinations on the initiation of SAC can then be quantified to help develop mitigation strategies to avoid SAC in industrial boilers. Figure 3.1.1 shows a schematic of the recirculation-loop along with the autoclave. This Hastelloy-C autoclave, as shown in Figure 3.1.2, has a capacity of three liters with the design pressure of 3500 psi and design temperature of 350^{o}C. Recirculation loop is designed to allow monitoring and control of water chemistry during the test, as is shown in Figure 3.1.3. A 100-liter storage/makeup tank is used to control dissolved oxygen level and to add other chemicals needed to simulate different boiler chemistries. A high pressure pump with pressure valve controls the recirculation loop pressure between the autoclave and the makeup-tank, as shown in Figure 3.1.3. Water exiting the autoclave is used in a heat exchanger to pre-heat the water entering the autoclave. Water flow rates can be controlled up to 10 liters per hour.

Water exiting the autoclave is further cooled by using a series of heat exchangers where the temperature of water is controlled below 50^{o}C. Various sensors are used to monitor and control the water chemistry which includes oxygen concentration, pH, redox potential, and conductivity, as shown on the control panel in Figure 3.1.4. Water samples are taken to test water for dissolved chemicals. Metal concentration is monitored by using inductively coupled plasma spectroscopy (ICP). Concentrations of other added chemicals to control oxygen levels can be regularly measured by electrophoresis, colorimetric and/or titration based methods.

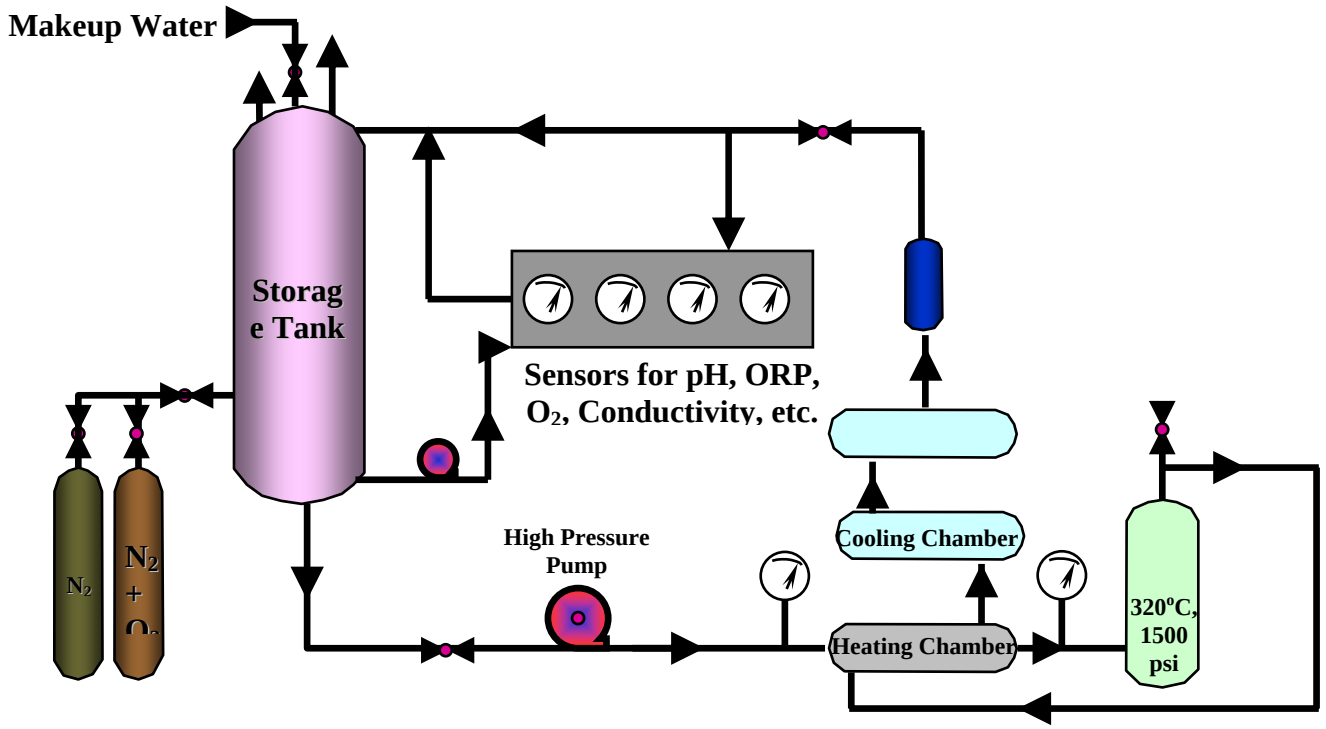

Figure 3.1.1. Schematic of the recirculation loop and autoclave used to simulate boiler environments to study SAC.

Figure 3.1.2. Autoclave used for boiler water environment simulation

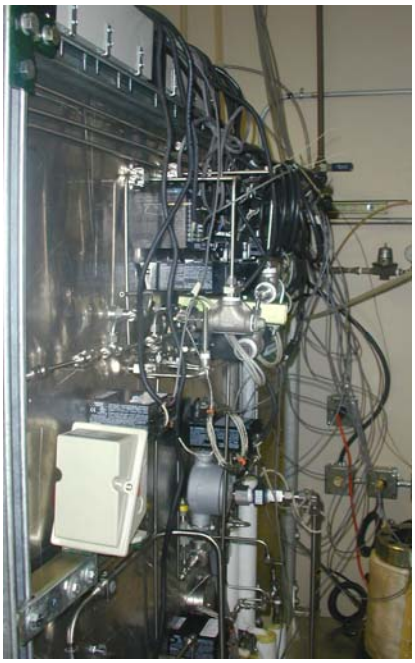

(a) (b)

Figure 3.1.3. (a) Autoclave, heat exchangers and make-up tank within protection shield (b) Sensors and controllers for measuring pH, redox potential, temperature, conductivity, and dissolved oxygen in boiler water simulations.

Figure 3.1.4. Control panel and protection shield for autoclave and recirculation loop. Data from sensors was recorded in a data acquisition system.

3.1.2 Application of Stress for SAC Simulation

Initial SAC tests consisted of carbon steel tensile samples strained to a constant value in a rigid fixture and exposed to the high purity water environments, as is shown in Figure 3.1.5. The tests coupons were electrically isolated from the vessel body by use of ceramic fixtures. The carbon steel samples were polished to 600 grit finish, after which they were cleaned with acetone, weighed, and prepared for exposure. The samples were introduced into the autoclave, and the vessel was sealed. Once the required water chemistry was achieved in the recirculation loop, heating was started to obtain initial test conditions. Pressure was determined by the test temperature and was not controlled.

Figure 3.1.5. Constant strain tests where samples could be loaded to a strain equivalent to predetermined stress values using a calibrated load-cell.

However, these tests did not reproduce stress conditions experienced by the boiler tubes. Boiler tubes undergo a series of dynamic loading, especially during startup and shutdown. To simulate these conditions, constant extension rates test rig was designed where the tensile samples or compact tension samples could be exposed to the boiler water environment and be tested under different strain rates and under low frequency fatigue conditions. Test rig developed is shown in Figure 3.1.6. Special moving seals were designed to prevent any leak during the test and still be able to strain the tensile sample at a variety of slow rates. Load train and sample holder is shown schematically in Figure 3.1.7. Recirculation-loop and autoclave was tested for maximum temperature and pressure and under static and flow conditions before actual tests were started in this facility. Safety shield was used to

protect users against any unexpected steam leak or circulation line failure. All sensors were placed outside this shield such that the operator did not have to enter the safety shield for any control or measurement.

Figure 3.1.6. A constant extension rate or slow strain rate test rig fitted with autoclave and recirculation loop was used for SAC tests.

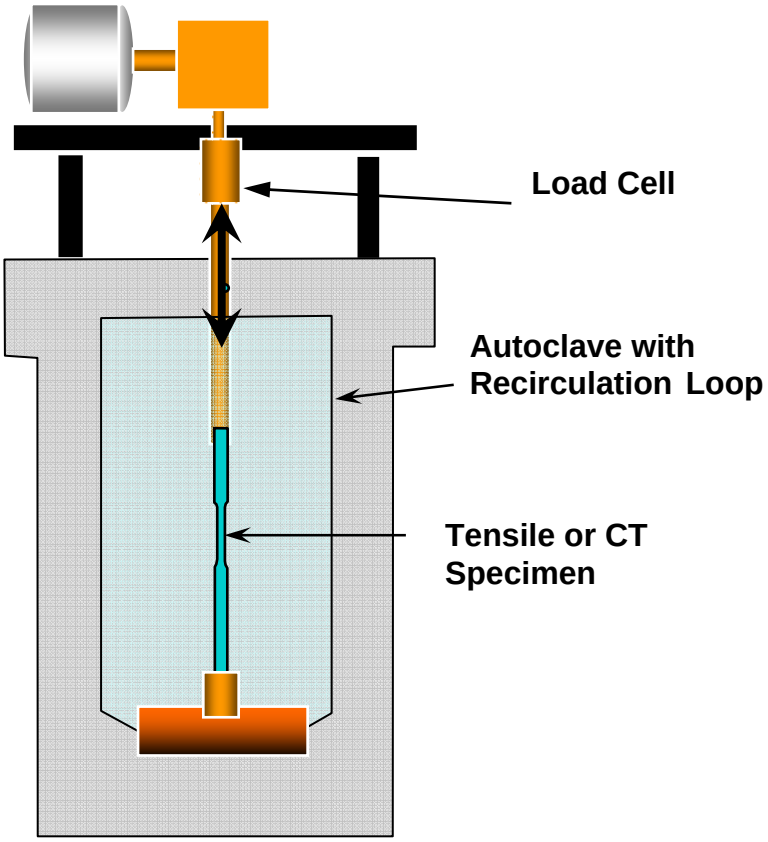

Figure 3.1.7. Schematic of the autoclave showing the load-train and tensile sample fixtures. Load on the test sample was measured outside the autoclave

3.1.2.1 Coupon Tests for Magnetite Characterization

Some polished coupons were exposed to the boiler water environment to check if the conditions were correct to develop magnetite scale similar to the one found on the surface of boiler tubes in the field. At the end of each test, the coupons were removed without disturbing the surface film on carbon steel samples. Surface film was first examined using an optical microscope and then characterized using X-ray diffraction method. X-ray diffraction pattern provided information on the type of oxide film and phases present but did not provide information on the morphology of the film. The film morphology will be characterized by use of SEM/EDS on sectioned and polished samples. The next series of tests planned for this study include stressed carbon steel samples simulating the effect of operating and residual stresses on oxide film damage during boiler operation or during boiler shutdown.

Under normal operation, boiler tubes are protected by a magnetite film on the steel surface. Previous work has suggested that damage to the magnetite film plays a major role in SAC initiation and growth [6, 7, 8, 11, 18]. Initial tests were conducted in pure water where the medium carbon steel, ASME SA-210, samples were exposed to the test environments with temperatures ranging from 250°C to 320°C for time periods of up to 72 hours. Industrial

boilers typically operate with water temperature in this selected range. Figure 3.1.8 shows an unexposed carbon steel SA-210 coupon and a coupon of the same steel exposed to pure water at 250^{o}C for 24 hours. The surface film was black in color with a few areas where the film texture was powdery instead of shinny-black. Removal of this thin powdery layer revealed shinny black surface layer underneath. A series of tests were carried out to characterize the formation and growth of oxide film under different environmental conditions in the autoclave system.

Surface film on the exposed samples was characterized using x-ray diffraction method. Figure 3.1.9 shows a x-ray diffraction pattern for an unexposed SA-210 carbon steel sample. As is expected, prominent peaks in this diffraction pattern correspond to iron (BCC). Figure 3.1.10 and 3.1.11 are x-ray diffraction patterns of films developed at 250^{o}C for 4 and 24 hours respectively and the composition for both samples was predominately magnetite, Fe_3O_4.

Further tests were carried out at 320^{o}C, simulating industrial boilers operating at pressures around 1500 psi. As shown in Figure 3.1.10, the film is again magnetite. Comparison of diffraction pattern for the samples tested so far indicates that the samples exposed to pure water at 250^{o}C and 320^{o}C for 24 hours showed iron peaks along with the magnetite peaks. Whereas the sample exposed at 250^{o}C for 24 hours had more prominent magnetite peaks. One possible explanation for this is spalling of thicker oxide film formed on samples exposed for longer times or at higher temperatures.

Test results from the recirculation-loop autoclave indicate that the laboratory test conditions were similar to industrial boilers. Under typical power boiler or industrial boiler conditions, the iron in mild steel is thermodynamically unstable in the presence of high temperature water and tends to form magnetite film with liberation of hydrogen [17]. The reaction product, magnetite, in slightly alkaline water forms a protective layer at the surface which ensures that thinning of the tube wall is negligible under normal operating conditions. Use of carbon steel for high temperature water applications strongly depends upon formation and stability of protective oxide film of magnetite, Fe_3O_4, on the waterside surface of boiler tubes. Above about 230^{o}C, iron reacts with oxygen-free neutral or slightly alkaline water to form magnetite film, which can be summarized by following reaction.

$$3\ Fe + 4\ H_2O \rightarrow Fe_3O_4 + 4\ H_2$$

A number of investigators have studied morphology and mechanism of magnetite film growth on iron/carbon steel surface [12-18]. Some investigators used strong alkaline solutions to develop thicker oxides, but have reported that the morphologically of the magnetite

developed under these conditions was similar to the magnetite film formed on boiler tube surfaces under normal operating conditions. There is some discrepancy between the results from magnetite growth experiments reported [17]. Magnetite film grown under very similar conditions can either be thick and relatively porous or it may be thin and compact. Marsh[17] concluded that depending upon the cathodic area in contact with the test sample, the morphology of magnetite can be changed. A mild steel sample oxidized in high temperature alkaline solutions and in electrical contact with a suitable area of magnetite (or noble metal like gold) in the same solution will, in general, produce a fine-grained porous film with a wide array of surface tetrahedral crystals at the film surface, as shown by Potter and Mann [13, 15]. Generally film growth rates may be higher for this type of porous oxide film. However, if the mild steel sample has no contact with a suitable cathodic surface, then an irregular, non-porous film is formed in high temperature water environment. This film may provide greater protectiveness and is also significantly thinner. Bloom [12] reported that this type of film eventually may also form pits on the surface due to film rupture/damage. Once the film is locally disrupted, the remaining intact magnetite on the sample may act as a cathodic surface and the oxide growth in the damaged areas may become anode sites as reported by Potter and Mann [13, 15]. Marsh [17] showed that indeed the morphology of oxide developed on carbon steel samples isolated from other surfaces had a thin compact film similar to the one reported by Bloom[12], whereas the film morphology in pits on the same sample was similar to the ones reported by Potter and Mann[13, 15].

Magnetite film thickness increases with time in boilers and may typically reach 10-15 μm. This is almost 10^4 times thicker than a typical "passive" film on iron [17]. Magnetite film stability is the most important requirement for corrosion resistance of carbon steel in high temperature water. In normal boiler conditions, protection by magnetite film formation is achieved and this is verified by the good performance of most boiler systems and boiler tubes. However, when magnetite film is disrupted, either mechanically or chemically and in presence of excess oxygen, anodic activity at the disruption sites leads to accelerated loss of the carbon steel at these local areas.

With application of stress, the oxide film cracks perpendicularly to the stress direction as well as to the metal/oxide interface. There is critical strain required for the magnetite film to fracture. However, the value of critical strain will depend upon the film properties which in-turn depends upon the environmental parameters, cyclic stress and temperature [11]. During boiler operation, the tubes are subjected to tensile stresses, which may vary depending upon the residual and applied stresses in local areas. However, the magnetite film on the tube surface grows stress-free under constant temperature and pressure conditions. During boiler operation, tube metal stresses vary locally, therefore during shutdown the oxide film on metal surface will experience compressive stresses depending upon the magnitude of stress change

in the base metal. Similarly, during startup, reverse stress cycle may be experienced by the base metal as well as oxide film. Westwood and Lee [10] have suggested that the operational stresses may be insufficient to cause damage in the magnetite film during normal boiler operation. However, failures are generally associated with external attachment welds, which may produce localized stresses sufficient to disrupt the magnetite film on the tube surface. In areas of high stresses like attachment welds, oxide film may get damaged frequently during operation or during shutdown and new oxide will be developed locally. This may cause buildup of oxide in these areas.

Pawel et. al [20] have shown that areas of tubes with SAC cracks typically had thicker magnetite film then the other parts of the tube. This may either be due to the differences in the local heat transfer in areas with attachment welds or may be due to disruption of the protective magnetite film and subsequent local oxidation reaction producing thicker deposits. Schoch and Sphan [7] proposed a mechanism of crack initiation where the thick magnetite film may contain structural defects which may result in an initiation of fatigue failure of the thick magnetite film and thereby exposing underlying metal to further localized corrosion attack. This repeated action will locally consume metal creating oxide notch. Subsequent load cycles will cause progressive growth of this "chemico-mechanical" notch. They also proposed that in areas where the film is thinner, the damage does not initiate by film cracking but by a slip process in the substrate alloy [7]. Once the crack is effectively nucleated, stress concentration at the tip may favor rapid chemical/mechanical growth of localized failure.

Magnetite film stability is the most important requirement for corrosion resistance of carbon steel in high temperature water. When magnetite film is disrupted, either mechanically or chemically and in presence of excess oxygen, anodic activity at the disruption sites leads to accelerated loss of the carbon steel at these local areas. Initial results from the recirculation-loop autoclave show that industrial boiler conditions can be simulated successfully in laboratory.

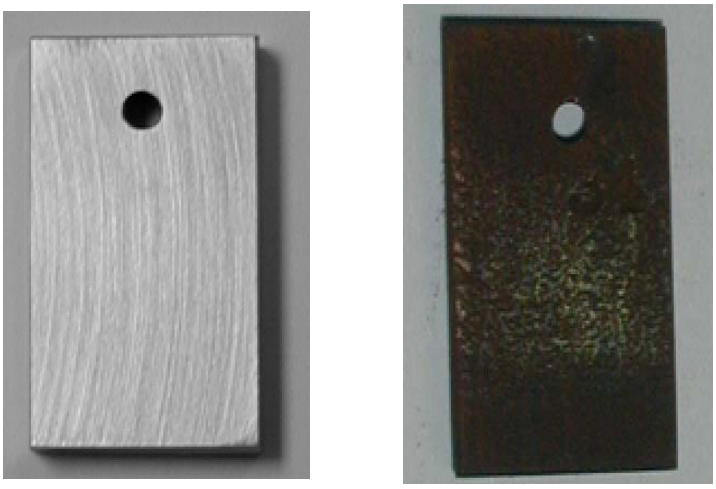

Figure 3.1.7. SA-210 carbon steel samples (a) unexposed and (b) exposed to pure water at 250^{o}C for 4 hours.

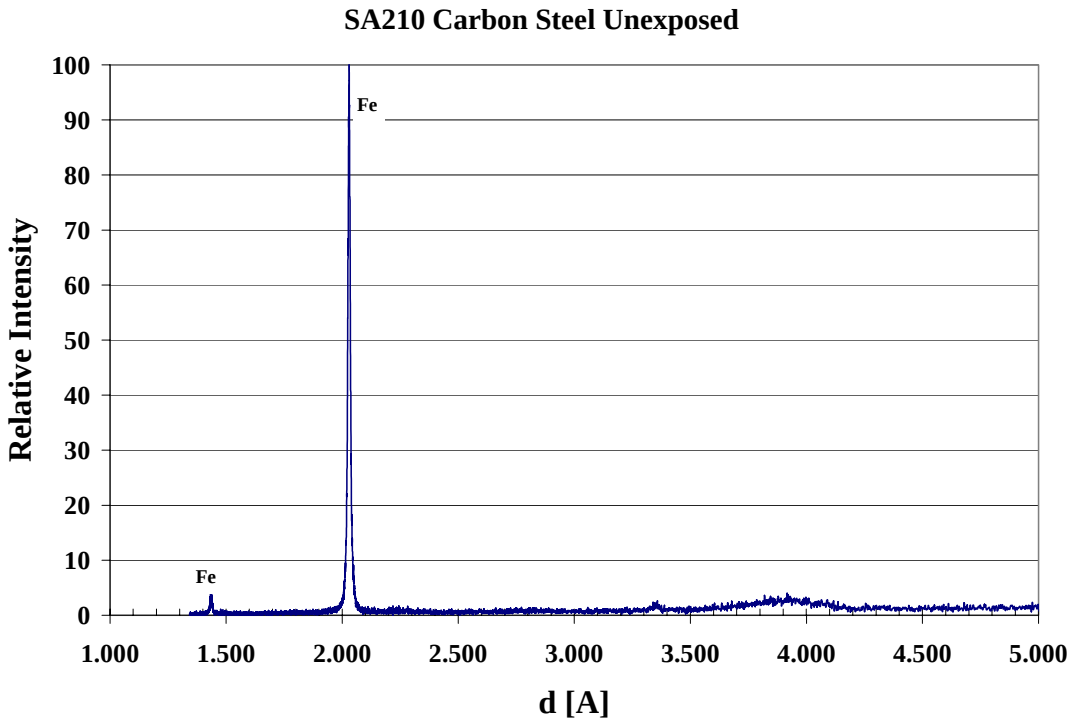

Figure 3.1.8. X-ray diffraction pattern for unexposed SA-210 carbon steel sample.

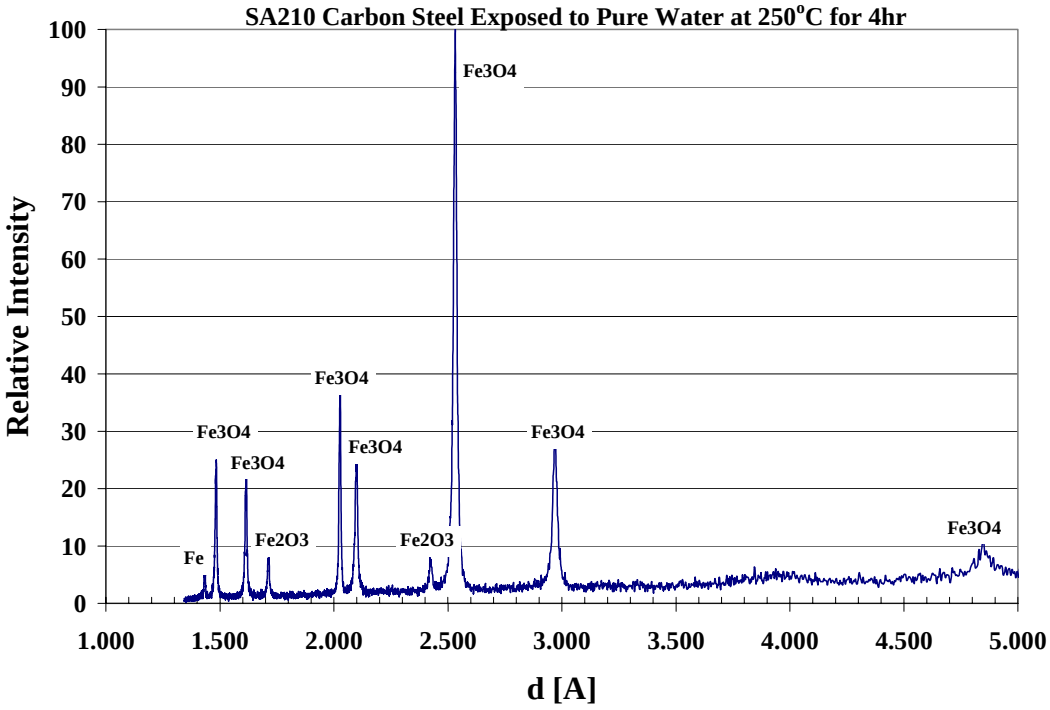

Figure 3.1.9. X-ray diffraction pattern for SA-210 carbon steel sample exposed to pure water at 250°C for 4 hours.

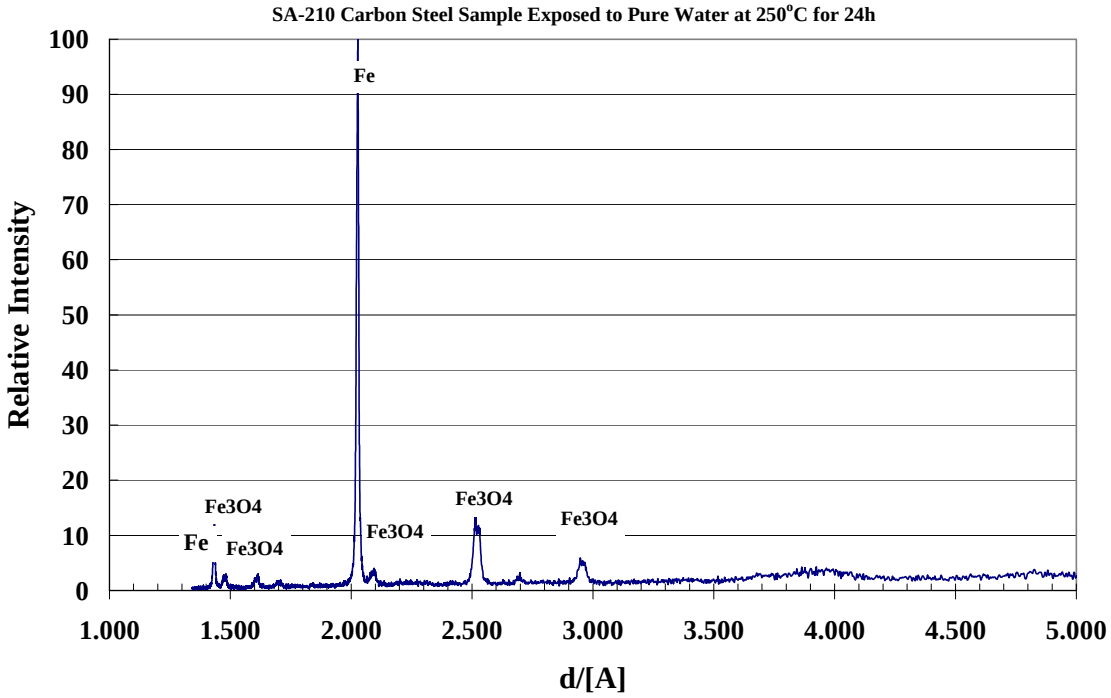

Figure 3.1.10. X-ray diffraction pattern for SA-210 carbon steel sample exposed to pure water at 250°C for 24 hours.

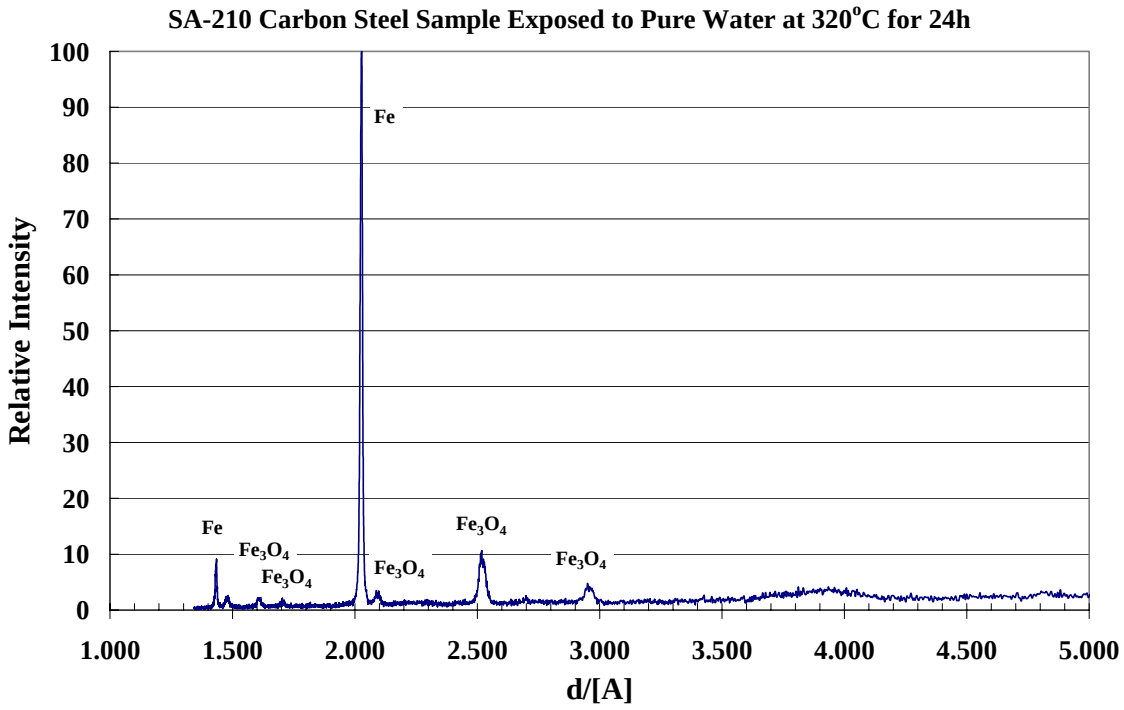

Figure 3.1.11. X-ray diffraction pattern for SA-210 carbon steel sample exposed to pure water at 320°C for 24 hours.

3.1.2.2 References for Laboratory Simulation of SAC

1. Dooley, R. B., A vision for reducing boiler tube failures, Power Engineering, March, 1992, pp. 33-37.
2. Dooley, R. B., A vision for reducing boiler tube failures - part II, Power Engineering, March, 1992, pp. 41-42.
3. Sylvester, W.R. and Sidla G., "Waterside Stress-Assisted Corrosion Cracking in Boilers", *Pulp and Paper Canada*, 91:6 (1990) p. T248-T252
4. C-E Service Information Letter # 388, "Waterside Corrosion Fatigue Cracking (In Recovery Boilers)", 1988.
5. ABB Service Information Letter # 6-92, "Waterside Stress-Assisted Corrosion Cracking in Chemical Recovery Boilers", 1992
6. Sylvester, W.R., "Waterside Corrosion Fatigue Cracking – Is There a Single Cause and Solution?," ABB C-E Services, Inc., TIS 8318, Combustion Engineering, Inc., Windsor, CT, 1988.

7. Schoch, W., and H. Spahn. "On the Role of Stress-Induced Corrosion and Corrosion Fatigue in Water-Wetted Boiler Components." In *Corrosion Fatigue: Chemistry, Mechanics, and Microstructure.* Houston, TX: NACE, 1972, pp. 52-64
8. Esmacher, M. J. Materials Performance (1987), 26(5), 17-20.
9. Bloom M. C. and Krulfeld M.. *Journal of the Electrochemical Society*, Vol. 104, 1957, p 264.
10. Westwood H. J. and Lee W. K. "Corrosion fatigue cracking in fossil-fueled boilers" J. Materials Engineering, Vol. 9, No. 2, 1987.
11. Crouch A. G., Dooley R. B., Corrosion Science, Volume 16, 1976, p. 341.
12. Bloom M. C., Newport G. N., and Fraser W. A., *Journal of the Electrochemical Society*, Vol. 111, 1957, p 1343.
13. Potter, E.C. and G.M.W. Mann, "Oxidation of Mild Steel in High-temperature Aqueous Systems", *Proc. 1st Int. Cong. Metall. Corrosion,* London, Butterworks, 1961, p. 417
14. Field E. M., Stanley R. C., Adams A. M., and Holmes D. R. *Proc. 2nd Int. Cong. Metall. Corrosion,* London, Butterworks, 1963, p. 829.
15. Potter, E.C. and G.M.W. Mann, "Mechanism of Magnetite Growth on Low-Carbon Steel in Steam and Aqueous Solutions up to 550 Degrees C.", *Proc. 2nd Int. Cong. Metall. Corrosion,* London, Butterworks, 1963, p. 872.
16. Castle J. E. and Mann G. M. W., Corrosion Science, Vol. 6, pp 253-262, 1966.
17. Marsh T. F. *Journal of the Electrochemical Society*, Vol. 113, April 1966, pp 313-318.
18. Robertson, J., "The Mechanism of High Temperature Aqueous Corrosion of Steel", *Corrosion Science,* Vol. 29, no. 11/12, 1989, pp. 1275-1291
19. Seifert, Hans-Peter; Ritter, Stefan; Ineichen, Ulrich; Tschanz, Urs; Georodetti, Bruno. Labor fur Werkstoffverhalten, Gruppe Bauteilsicherheit, Forschungsbereich Nukleare Energie und Sicherheit, Germany. PSI-Bericht (2003), (03-10), 1-106.
20. Pawel S. J., Willoughby A. W., Longmire H. F., and Singh P. M. , CORROSION-2004, Paper # 04517, New Orleans, NACE, March 2004.

3.2 MATERIAL CHARACTERIZATION

Experience with SAC in boiler tubes suggests that internal surfaces immediately adjacent to external (non-pressure) attachment welds on the boiler tubes are particularly susceptible to development of SAC, due to thermal or mechanical effects concentrated at the attachment location [1 to 6] or perhaps relative anodic behavior of the stressed region at/near the attachment [7]. Most commonly, SAC tends to be manifested in short clusters of indications resembling cracks perpendicular to the associated attachment weld. Because of the myriad of stress and water composition variables involved, no specific rate (or even bounding rate) has been determined for the SAC processes. In the strictest sense, the occurrence of SAC may be independent of the boiler age [8], but it tends to be a relatively slow process and is most commonly found in boilers that have been operating for at least ten years [3,7].

Based largely on discussions and findings associated with a boiler-industry-wide colloquium in July 2000, Sharp [9] published an extensive overview of the history of SAC in boilers representing the full range of industries. In his overview, Sharp noted that the Electric Power Research Institute (EPRI) took a leading role in research to explain and control boiler tube problems of this type in the utility industry in the late 1980s. Over the next ten years, EPRI developed a detailed mechanism and control scheme to avoid formation and growth of crack-like waterside indications termed corrosion fatigue in the utility industry. While the corrosion fatigue identified by the utility industry was no doubt similar to what the pulp and paper industry termed SAC, the colloquium attendees were not convinced that EPRI's mechanism and feedwater chemistry recommendations were necessarily relevant to recovery boilers. In particular, attendees cited significant differences in water treatment issues between utility boilers and recovery boilers (very large make-up water fraction in recovery boilers, different chemicals and treatment strategies) and the wide range of microstructural characteristics ascribed to SAC and corrosion fatigue as evidence that the details of the phenomenon and the EPRI recommendations might not apply to all boilers.

3.2.2 Non Destructive Inspection of Boiler Tubes

Due in part to recurring corrosion problems that included SAC, the bottom 16 m (53 ft.) of the recovery boiler at the Weyerhaeuser Longview paper mill near Longview, Washington, was recently replaced. A large sampling of representative panels and pieces of tubing – almost 300 linear meters (about 1000 feet) in total – was delivered to ORNL for evaluation of SAC via non-destructive evaluation (NDE) techniques as well as standard metallography. The results of this evaluation have been reported in detail previously [10] but are summarized in this section.

Four different NDE techniques were applied to the tubes/panels removed from the Longview boiler. Each technique is briefly described in the paragraphs that follow, along with the general results from each type of inspection.

3.2.2.1 Circumferential Wave Inspection

In the circumferential wave (CW) technique, ultrasonic waves are generally introduced and detected from the process side of the boiler tubing with a transducer embedded in plastic. The working surface of the transducer has the same curvature as the outside surface of the boiler tubes – in this case, about 38 mm (1.5 in.) radius – and is coupled to the tube surface with a standard viscous gel. To develop adequate coupling, adherent accumulations of oxide as well as any loose rust/debris were removed, primarily with a power wire brush. The CW technique detects longitudinally oriented flaws via analysis of the waves that travel around the tube circumferentially. The approximate size/penetration depth of any flaws can be estimated by comparing the signal fraction reflected from a flaw with that which travels the entire circumference, and the relative position of the flaw can be determined by analysis of the reflected signal travel time.

Potential advantages of this relatively new technique include that it detects longitudinally oriented flaws best (because they are perpendicular to the direction of wave travel), which is consistent with the predominant orientation of SAC indications in boiler tubes. Also, since ultrasonic waves are not sent over long distances, power and attenuation issues are relatively minor for this technique. In addition, the precise location of any indication in the ultrasonic wave circuit is not critical, since only a limited length of tubing (roughly, the length of the transducer) is under evaluation at any given time. A disadvantage is that the technique works best from the process (fire) side of the boiler tubing – directly opposite the external attachment of interest – because this location places the expected SAC location in the center of the detection range (halfway around the tube from the transducer). Working from the fireside can happen only during shutdown when the inside of the boiler is a very busy place, and also may require substantial surface preparation to remove studs. [The studs are segments of steel rod, typically 2.5 cm long and 1 cm diameter, welded to the fireside tube and membrane surfaces in a dense, close-packed array. In general, the purpose of the studs is to encourage the formation of a solid smelt layer on the fireside surfaces, which provides some corrosion protection from the relatively aggressive molten/splashing smelt that tends to form in the lower portions of recovery boilers.]

It was not possible to evaluate the entire lot of 300 m of boiler tubing for SAC using the CW technique, as the equipment and personnel to operate the gear were available to the project for only a limited time. As a result, effort was concentrated on regions considered

susceptible to SAC and which required a minimum of surface preparation to remove extensive scale or fireside studs on the tube surfaces. About a dozen wall tubes with floor attachments (filler blocks) were examined in greatest detail, as this region has been found historically susceptible to SAC in recovery boilers, and does not require the removal of fireside studs (one of few locations in a boiler in which the examination can practically take place from the cold side). Only a few wall tubes with lateral (transverse) scallop-type attachment welds were examined due to the extreme effort (heavy grinding) to remove the studs to facilitate use of the CW technique. None of the locations examined were found to generate significant indications of SAC, which was subsequently confirmed with metallographic examination. As a result, no direct conclusions regarding the utility of the CW technique can be drawn from this investigation. However, it is suspected that the extreme proximity of SAC to attachment welds would tend to mask potential indications due to attenuation issues associated with discontinuous wall thickness at these locations.

3.2.2.2 Longitudinal Wave Inspection

In the longitudinal wave (LW) technique, which is also referred to as the guided wave method, ultrasonic waves are introduced on the cold side of boiler tubes with a transducer array embedded in plastic machined with a curve to fit the outside surface of the tube. The waves travel primarily longitudinally down a length of tubing and are detected by a separate receiver or, alternatively, reflected from circumferentially oriented flaws and detected with the same unit as the input transducer. Like the CW technique, flaws can be located and sized by analysis of the pitch/catch time for reflected waves and the fraction of the input energy collected at the receiver. Similar to the CW technique, appropriate surface preparation and coupling was required.

Potential advantages of the LW technique relate primarily to its potential use in the field. For example, it can be used from the cold side of the boiler, so entry into the boiler during very busy outage time is not required, nor is the removal of fireside studs for surface preparation. Further, the LW technique may be developed in the future to the extent the boiler could be operating during the inspection. In addition, the LW technique is not necessarily a localized technique – it is theoretically possible to scan relatively large areas/lengths of boiler tube between small areas with the required surface preparation to introduce/detect waves. Potential disadvantages of this technique are that circumferentially-oriented SAC indications are not common, and that more development on issues related to surface preparation and attenuation are required to make long-distance assessments of tubing condition practical.

Similar to the situation for the CW technique, it was impractical to attempt to assess all of the available boiler tube specimens for SAC using longitudinal waves. Therefore, effort was

concentrated on tubes with longitudinal weld attachments and/or tubes with a "corner" attachment resulting from the intersection of a longitudinal and a transverse weld as representing areas potentially susceptible to SAC and having a circumferential flaw orientation detectable with the LW technique. After considerable effort, which included detailed examination of about a dozen tube panels meeting the above criterion, no significant indications of SAC were detected. Since several tubes with SAC (found by subsequent destructive analysis) were among those examined with longitudinal waves, it seems likely that the longitudinal orientation of all of the SAC indications among the Longview boiler tubes masked these from detection with this technique.

3.2.2.3 Radiographic Inspection

Select portions of tube panels were radiographed using two techniques. The first, which is similar to that which is possible in a field evaluation of a boiler, utilized the double wall/double image technique in which the x-ray source and film were both outside of the tube/weld being investigated. The second takes advantage of the fact the tubes were cut into manageable pieces and utilized the single wall/single image technique, in which the film was placed inside the tube of interest. The latter technique is not routinely used in a field inspection because it requires sections of tubing to be cut/removed.

The sections subjected to radiography were selected from among those with substantial scallop-type attachment welds deemed high probability areas for SAC based on experience. In total, eight panels (with several tubes each) were extensively examined with these radiographic techniques. A few small indications were identified, but none were judged by the radiographer to be significant and each was associated with the external attachment weld (not the tube ID). None of the radiographed tubes were subsequently found to exhibit significant SAC indications via visual and/or metallographic examination.

3.2.2.4 Visual/Borescope Inspection

All of the boiler tube sections were examined internally with a borescope. The borescope had an adjustable power light at the tip of an approximately 1 m probe length and an optics system capable of approximately 5x magnification. This process was quite slow and tedious and did not reveal any direct indication of SAC, although there were a few observations of areas where the normally smooth and uniform oxide film seemed somewhat rough/graveled with scattered debris (discussed in more detail in a later paragraph).

3.2.3 Metallography and Microhardness Evaluation

Following the borescope inspection, all of the boiler tube panels with an indication of any kind, however minor, resulting from any of the inspection techniques, as well as many with no indications, were split longitudinally with a band saw to facilitate visual inspection of the waterside of the tubing. [Tube panels and/or individual tubes were cut in a plane adjacent and parallel to the plane containing the tube membrane(s); in this fashion, the tube crowns were unscathed and available for visual assessment and metallography.] The internal tube surfaces were found, almost without exception, to be a very smooth, uniform gray with only very isolated spots of red/orange rust (no doubt resulting from the extensive handling since the removal from the boiler months earlier).

An example of the only significant exceptions to smooth/uniform oxide on the waterside of the tubes is shown in Figure. 3.2.1. Viewed at right angles (light and view port on the borescope perpendicular to the tube surface), locations like these appear slightly graveled, but with oblique lighting it is obvious that the oxide at these locations is significantly thicker than the nominal oxide thickness. Oxide accumulations almost 500 μm (20 mils) thick were observed in a few of these positions, which invariably were located on the tube waterside directly adjacent to an external attachment weld. Not every attachment weld exhibited such an oxide accumulation on the tube waterside, but no accumulations were observed that were not immediately adjacent to an attachment weld. When several tubes from a panel were examined together (such as the four-tube panel shown in Figure 3.2.2), oxide accumulations were observed on the ID of the tube crown associated with each attachment weld location, but the degree of oxide accumulation typically varied somewhat among the attachment welds in the group.

The cause of the oxide accumulations is perhaps related to subtleties of the internal heat transfer conditions at the attachment weld locations. For example, depending on the efficiency (in the thermal sense) of the weld attachment, the attachment may act as something of a cooling fin to encourage heat transfer from the tube and thereby precipitation from the water on the internal surfaces of the tube at these locations. Alternate thermal conditions at the attachment might lead to slightly increased temperatures at the attachment locations encouraging more rapid growth of oxide. In any case, it is not apparent that the oxide accumulations directly cause SAC at these locations, but it is likely the thermal conditions that contribute to the oxide accumulation also contribute to the stress state and corrosion conditions at this location.

Figure 3.2.1. Typical oxide accumulation on the internal surface of a boiler tube, viewed with oblique lighting. An attachment weld (scallop-type) is located immediately adjacent to the oxide build-up on the external surface of this tube.

A sampling of tubes exhibiting the oxide accumulation was cut into short lengths and chemically cleaned with inhibited hydrochloric acid (ASTM G-1-1990 procedure C.3.5) to remove the oxide with no appreciable attack of the underlying steel. A representative result is shown in Figure 3.2.3. Directly beneath every oxide accumulation, longitudinally-oriented SAC was observed. The indications in Figure 3.2.3 are typical of all of the SAC observed among these tubes in that they appear as a cluster of short, roughly parallel indications on the ID near the tube crown, and are centered on the attachment weld location. The total longitudinal length of each cluster was less than 3 cm in every case for the tubes in this investigation.

Following the discovery of SAC under the oxide accumulations, tubes were sectioned to facilitate metallographic examination in regions with and without oxide accumulations. Figure 3.2.4 compares the nominal appearance of the internal oxide layer – observed over the entire boiler tube ID except for very limited areas adjacent to some attachment welds – with an area exhibiting the oxide accumulation. Nominally, the oxide is approximately 50 μm thick, relatively free of porosity, very adherent, and uniform in color. In locations with an oxide accumulation, the film tends to exhibit significant porosity (contributes to poor adhesion in some areas) and irregular thickness nominally near 300 μm but in some locations up to 400-500 μm. In addition, the color of the thick films is not generally uniform,

suggesting a range of oxide stoichiometries and compositions, including trace contaminants (Cu, Cl, P, and S were sporadically detected, generally near 0.1 at.%, but Cu and Cl occasionally were present up to almost 1 at.%).

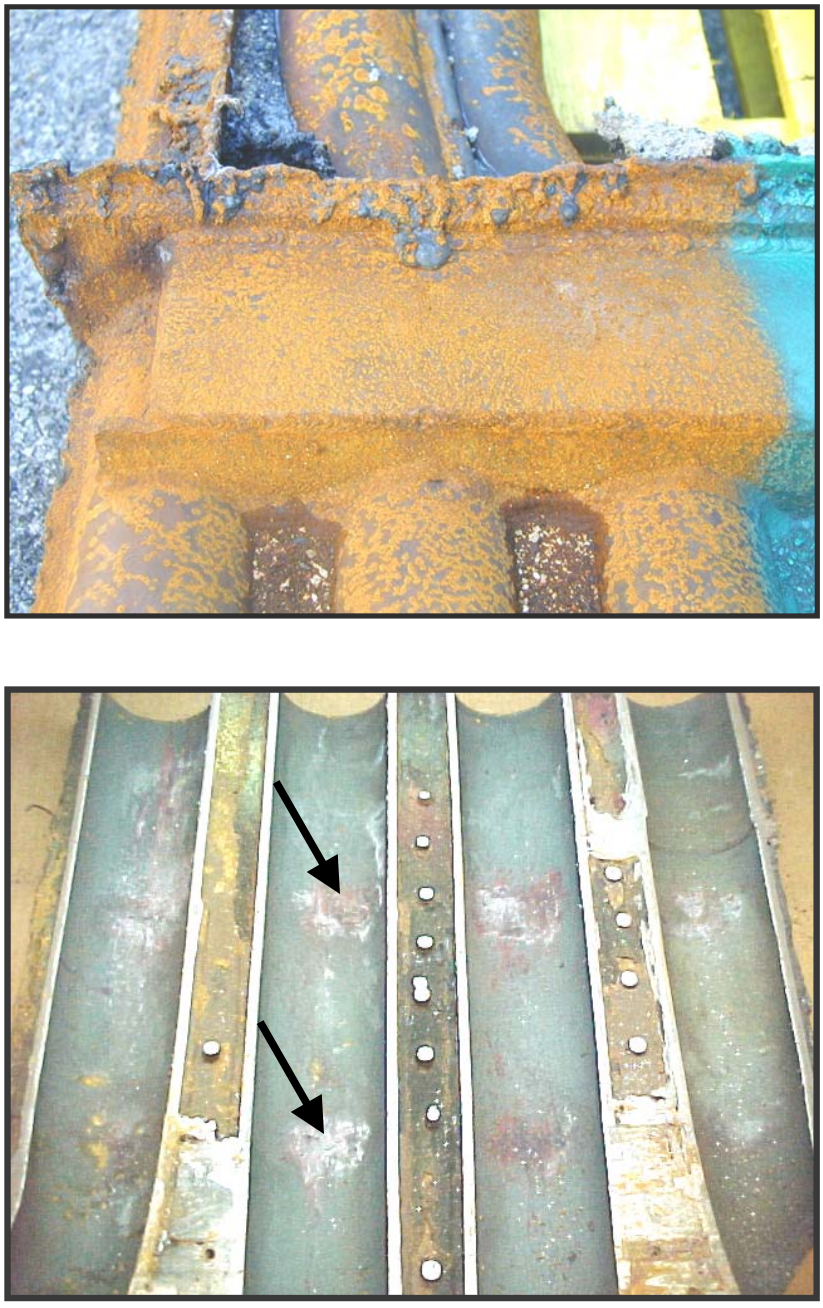

Figure 3.2.2. Top: Scallop-type fillet welds associated with a tertiary windbox. Bottom: Internal surfaces at the fillet weld locations shown above. Note variable extent of oxide accumulation opposite each weld. One pair of oxide accumulations is marked with arrows, but a similar pair of accumulations is on each tube.

Figure 3.2.3. Attachment weld (top) and appearance of the internal surface opposite the weld following acid cleaning.

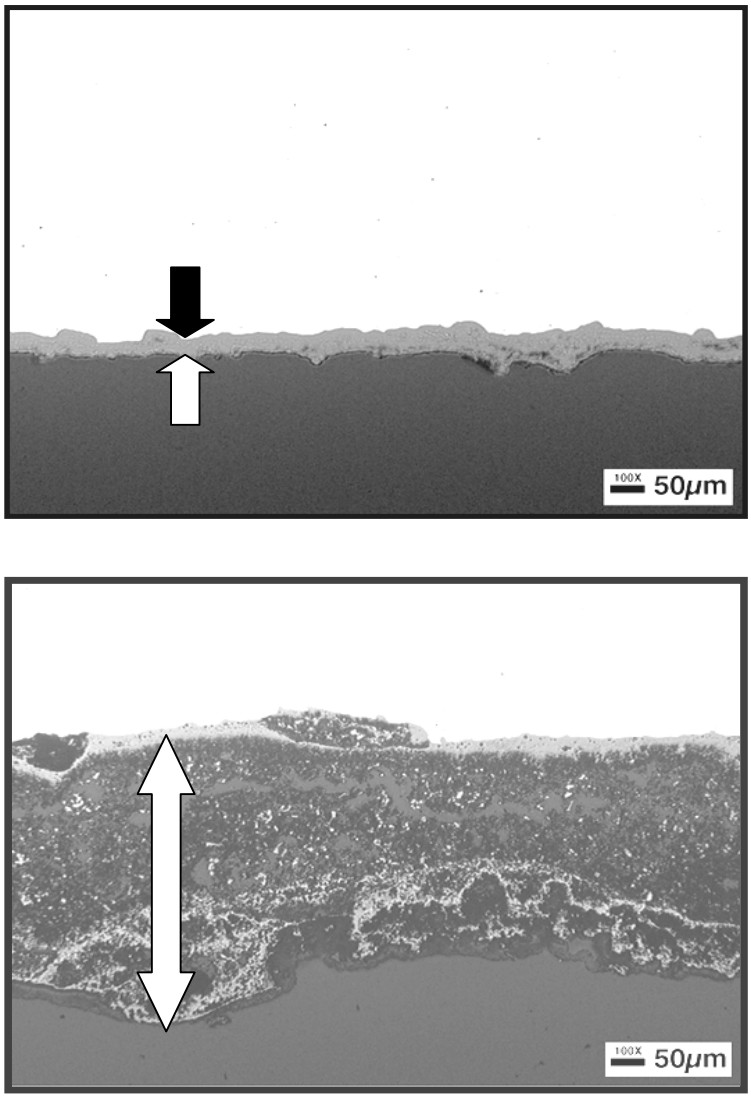

Figure 3.2.4. Comparison of the nominal oxide thickness (top) with an example of an oxide accumulation (bottom). In each photograph, the oxide is marked with arrows, and unetched steel is at the top (white) and the epoxy mount material is at the bottom.

Figure 3.2.5 is representative of the most common characteristics of the SAC indications observed in this investigation. The waterside penetrations are consistently transgranular, relatively straight (little or no branching) and wide with bulbous features and rounded tips, and filled with an adherent, layered oxide. The relative width of the deepest penetrations varies significantly, with depth/width ratios commonly in the range 1-5. The SAC penetrations are invariably located within 1 cm or so of an attachment weld location, and the deepest penetration observed among these boiler tubes was about 30% of the tube wall thickness. In some instances, the penetrations are generally narrow with somewhat bulbous features, consistent with periodic intense corrosion events. Apparently, during periods of

relatively high corrosion (probably associated with simultaneous rupture of the protective film and poor water chemistry), the penetration advances until the stress or water chemistry (or both) return to nominal levels, at which time the corrosion tends to spread laterally until full passivation is restored. In the most favorable cases, the number of "bulbs" on the penetrations can be related to the number of aggressive corrosion events [4] in the boiler.

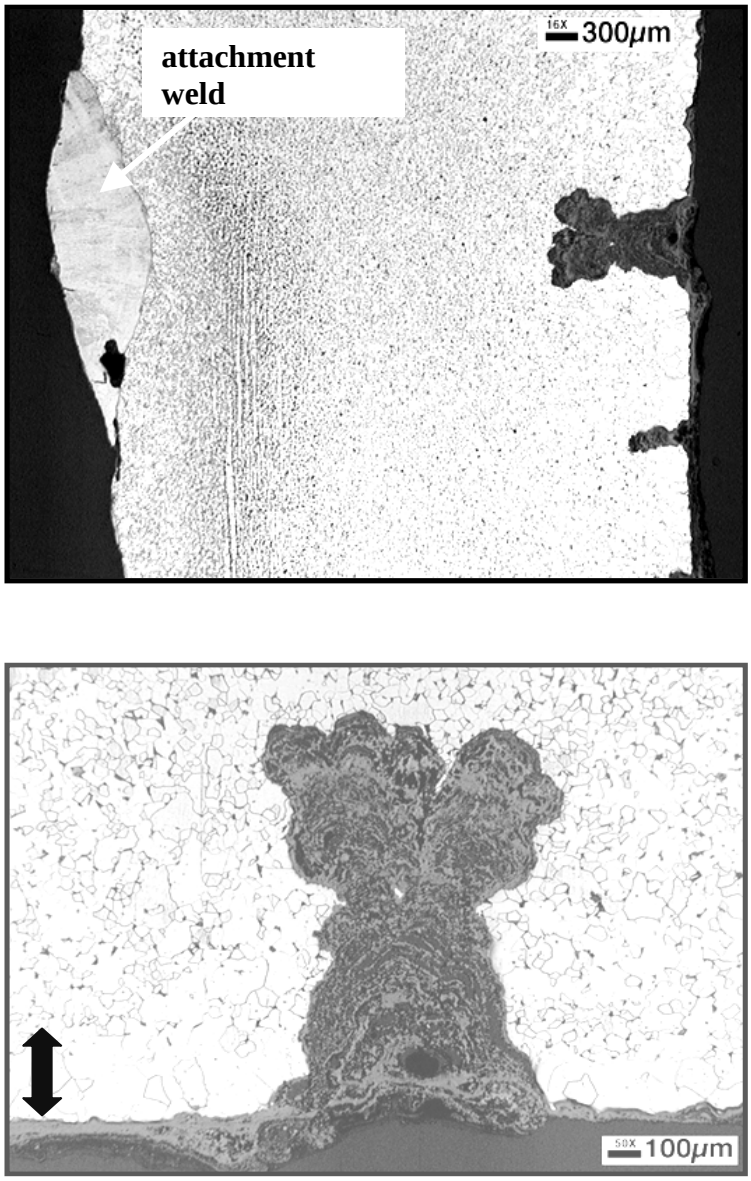

Figure 3.2.5. Representative photomicrographs of a tube cross section showing the attachment weld and adjacent SAC penetrations (top) and a higher magnification view of the deepest penetration associated with this particular attachment weld (bottom). A decarburized layer is marked with an arrow in the lower photograph. Note the weld-rounded features of the SAC indication and the fact that it is almost as wide as it is deep.

Another common feature revealed by the metallography in Figure. 3.2.5 is that the waterside surfaces rather routinely exhibit a decarburized layer approximately 200-300 μm deep in which the ferrite grains have grown significantly larger than the nominal size. Microhardness scans across the tube thickness indicate that the decarburized layer with large grains (85-100 HV) is generally somewhat softer than the nominal base material (100-115 HV). For comparison, the welds examined on these tubes exhibit somewhat higher hardness at 160-250 HV, with intermediate hardness in the weld heat-affected zone. In some regions with SAC indications, the decarburized layer was not observed on the tube waterside, suggesting sufficient general corrosion/wastage at this location to remove the thin layer of somewhat softer material. [It is also possible that tubes without the decarburization layer – potentially resulting from the original tube fabrication process – have been added in some locations as part of the periodic maintenance process.] In general, the external surfaces of the boiler tubes also exhibit the decarburized layer with some grain growth (see area adjacent to the weld at the top of Figure 3.2.5), but where extensive surface preparation for an external attachment has occurred, the decarburized layer has typically been removed by grinding.

Additional photomicrographs emphasize other common features. Figure 3.2.6 is representative of the relatively common observation that only one of a group of indications tends to propagate significantly into the tube thickness. The factors that cause a specific indication to propagate are unknown, but likely are related to the combination of mechanical load at a particular location and the stress concentration associated with the specific shape(s) at the furthest extent of the indication when loading occurs. Figure 3.2.7 is representative of the trend that many of the deepest SAC penetrations seem to propagate from a substantial pit on the ID surface of the tube. Again, specific reasons for this behavior are unknown but stress concentration at the pit and perhaps occluded water chemistry within the pit lead to this aggressive behavior.

If the SAC process is initiated when boiler tubes experience sufficient strain to fracture the nominally protective oxide [11-13] then that process is perhaps aided by boiler tubes with a slightly weakened (decarburized, large grains) internal surface. Increased resistance to SAC might be realized by utilizing boiler tubes that do not exhibit a soft layer or, alternatively, selecting a somewhat stronger tube material in general, at least for application in areas of the boiler susceptible to SAC.

3.2.4 Scanning Electron Microscopy and Microprobe Evaluation

Scanning electron microscopy of representative SAC penetrations revealed a layered oxide structure within the penetrations as well as in portions of the oxide accumulations on the internal surface of the tube. An example of the layered oxide appearance is shown in Fig.

3.2.8. While not analytically identified, the relatively dark layers of iron oxide have a uniform Fe/O ratio consistent with Fe_2O_3 and the relatively light layers have a similarly uniform Fe/O ratio consistent with Fe_3O_4. While multiple alternating layers of oxide have not been previously reported within SAC penetrations, inner and outer oxide layers (similar to that shown in Figure 3.2.5) have been observed following field and laboratory tests associated with SAC investigations [14-17]. The alternating oxide layers observed here provide visual confirmation of the concept that the corrosion conditions in the boiler tubes – and within the penetrations into the tube wall – vary periodically and that pitting/wall penetration is cyclic in nature.

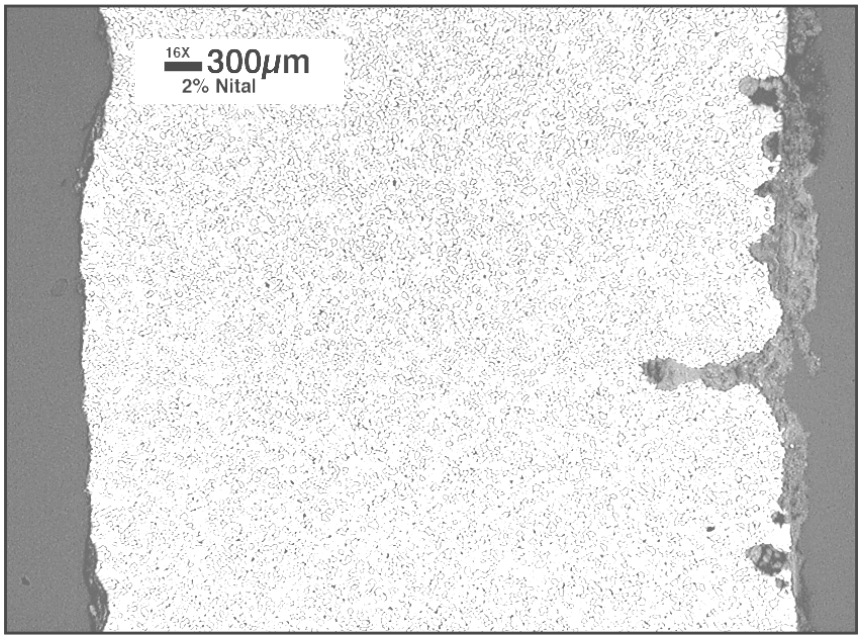

Figure 3.2.6. Cluster of SAC indications on the ID of a boiler tube showing that only one indication appears to be propagating. The attachment weld in this case is just out of the photograph at the upper left. All of the indications are bulbous, rounded at the tip, and filled with oxide. Note also the thick oxide accumulation on the ID surface that tends to obscure the SAC indications from visual detection.

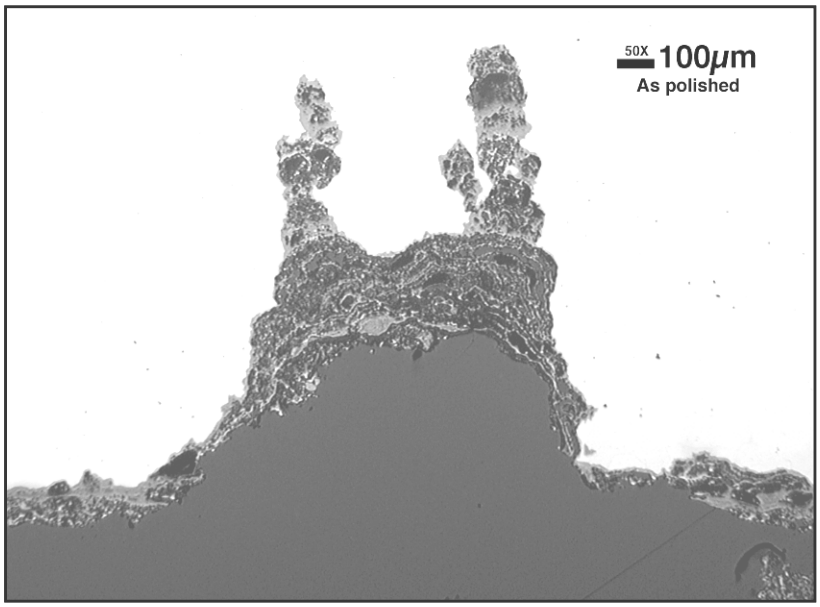

Figure 3.2.7. SAC indications that appear to be propagating from a pit on the tube ID. As-polished.

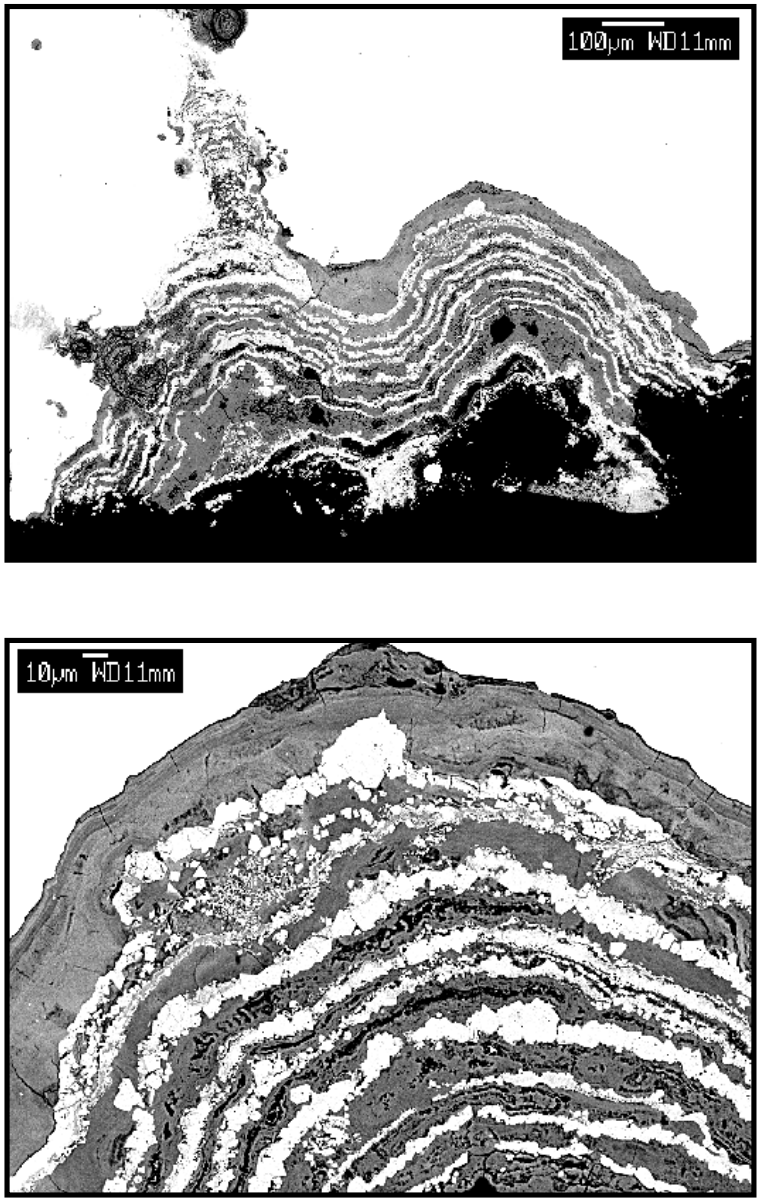

Figure 3.2.8. Backscattered electron microscopy of a typical SAC indication on the tube ID. The top photograph shows the entire SAC indication, and the bottom photograph is a higher magnification view of a portion of the oxide in the penetration. Relatively light colored corrosion product has an Fe/O ratio consistent with Fe_3O_4, and the relatively dark product has an Fe/O ratio consistent with Fe_2O_3.

Trace amounts of Cl, Cu, P, and S were detected throughout the oxide layers by microprobe chemical analysis; however, isolated concentrations of Cl and Cu were found to approximately 1 at.%. In addition, Cu tended to be located in clusters of significant concentration, with S always concentrated in the same particles/regions. The source(s) of the contamination has not been confirmed by the authors, but it seems likely that the Cu contamination results from corrosion of copper-bearing components in the steam/condensate system [18-20]. Chloride contamination typically results from in-leakage from the condenser or heat exchanger [20] or perhaps make-up water of marginal quality. The P contamination may result from the water-treatment process itself. The source of sulfur is unknown, but sulfur is typically ubiquitous in the process waters in a paper mill.

3.2.5 SAC-Failure Analysis

We received a number of boiler tubes which were removed from boilers during shutdown. The boilers were known to have SAC problem. The tubes were received at ORNL and Corrosion Lab. at Georgia Tech. for metallography. Failure analysis of boiler tubes with SAC was performed to identify any metallurgical microstructure associated with SAC. Figures 3.2.9 to 3.2.15 show some representative micrographs and macro pictures of the failed samples. Figures 3.2.9 and 3.2.10 show typical tube sections cut out of the failed boiler tubes. The samples were sectioned and cleaned chemically to remove oxide buildup from the inner surface of the tube. The sections with cracks were mounted such that the crack depth could be monitored. Samples were polished to 0.3 micron alumina powder finish and the samples were examined. Samples were also etched to reveal the microstructure of these tubes.

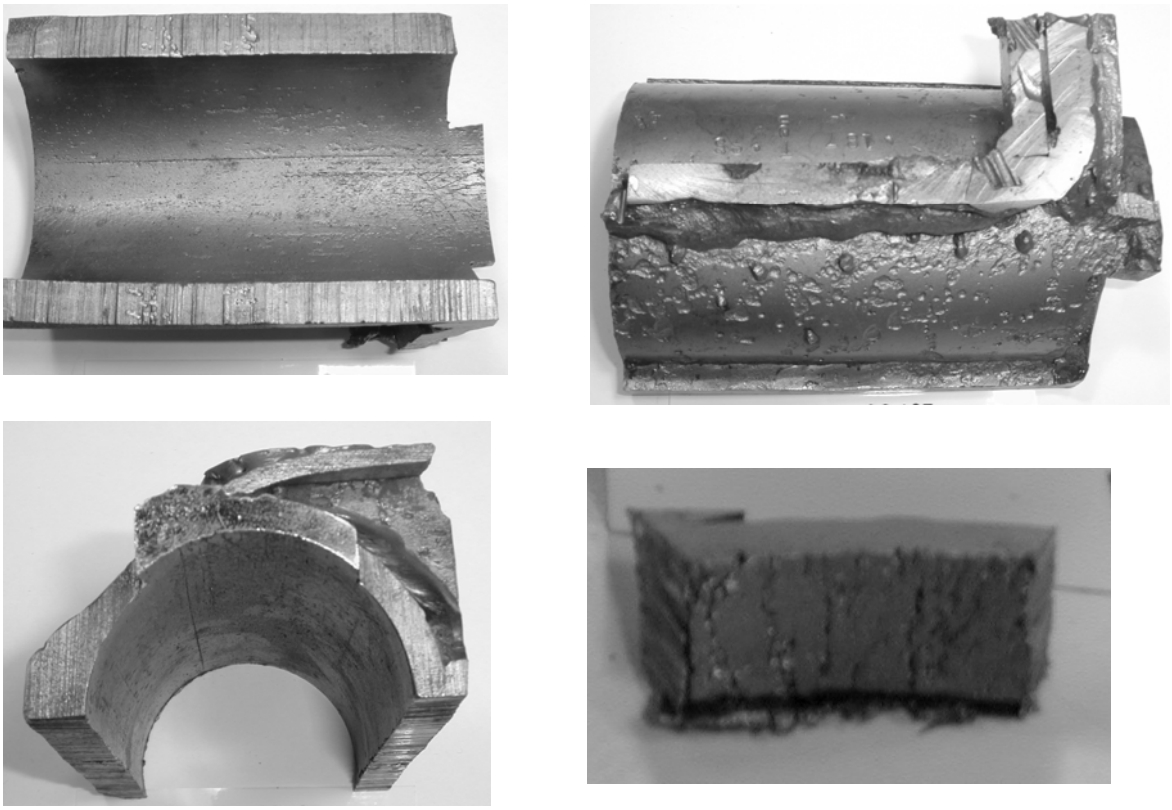

Figure 3.2.9. Pictures showing a tube section with external attachment weld removed from a boiler. Removal of oxide scale from internal surface reveled clear signs of SAC cracks in the area of attachment weld.

Figure 3.2.10. Pictures showing a tube section with external attachment weld removed from a boiler. Removal of oxide scale from internal surface reveled clear signs of SAC cracks in the area of attachment weld.

3.2.6 Microstructure of steel and crack morphology

Micrographs in Figures 3.2.11 to 3.2.15 show typical microstuctures found in these tubes. Although there were a number of tubes where the microstructure at the surface was very similar to the middle of the tube but in a significant number of tubes we saw a decarburized layer near surface which also had significantly larger grain size then the middle of the tube. Figures 3.2.12 to 3.2.15 show these layers clearly.

In sections where we found this large grained layer, we also noticed that the majority of cracks seem to stop near the interface of normal microstructure and decarburized layer. This indicates that the layer may have some role in early initiation of SAC cracks and growth.

However, when these cracks face the stoner normal materials then the cracks do not grow further in spite of fact that the stress will intensity ahead of these cracks.

Results in Figure 3.2.16 and 3.2.17 show clearly that the layers with large grain also are soft compared to the normal pearlitic microstructure in the middle of the tube. In some of the tubes, microstructure on outer surface was similar to the one at the inner surface whereas in other tubes the inner surface only had the decarburized layer. Analysis of these failed sections indicates that the grain growth occurred during tube manufacturing/processing and not during the boiler operation. This result indicates that we may be able to decrease the probability of SAC initiation through quality control and eliminating tubes with large grained microstructure at the inner surface of the tube.

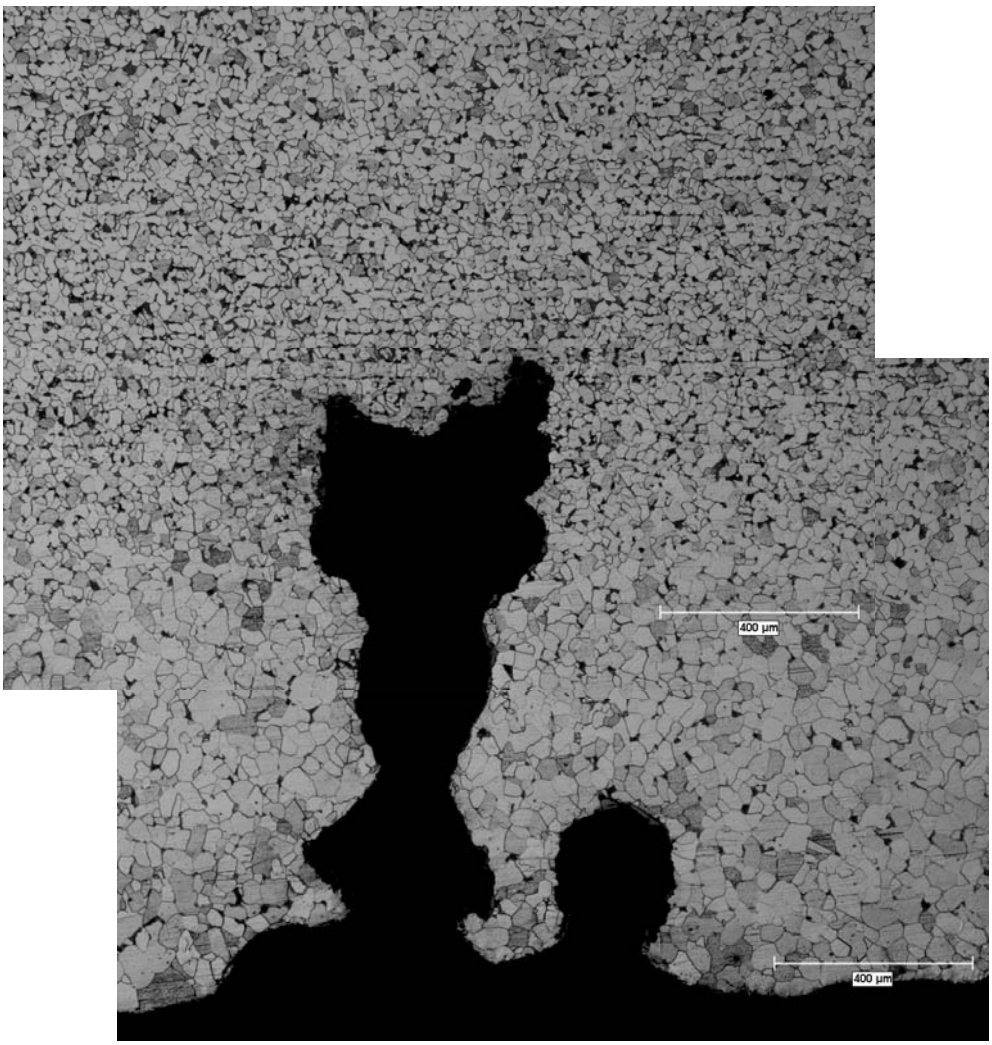

Figure 3.2.11. Micrographs showing a typical SAC crack. Micrograph also shows clear signs of grain growth and de-carburized layer at the inner surface of tube.

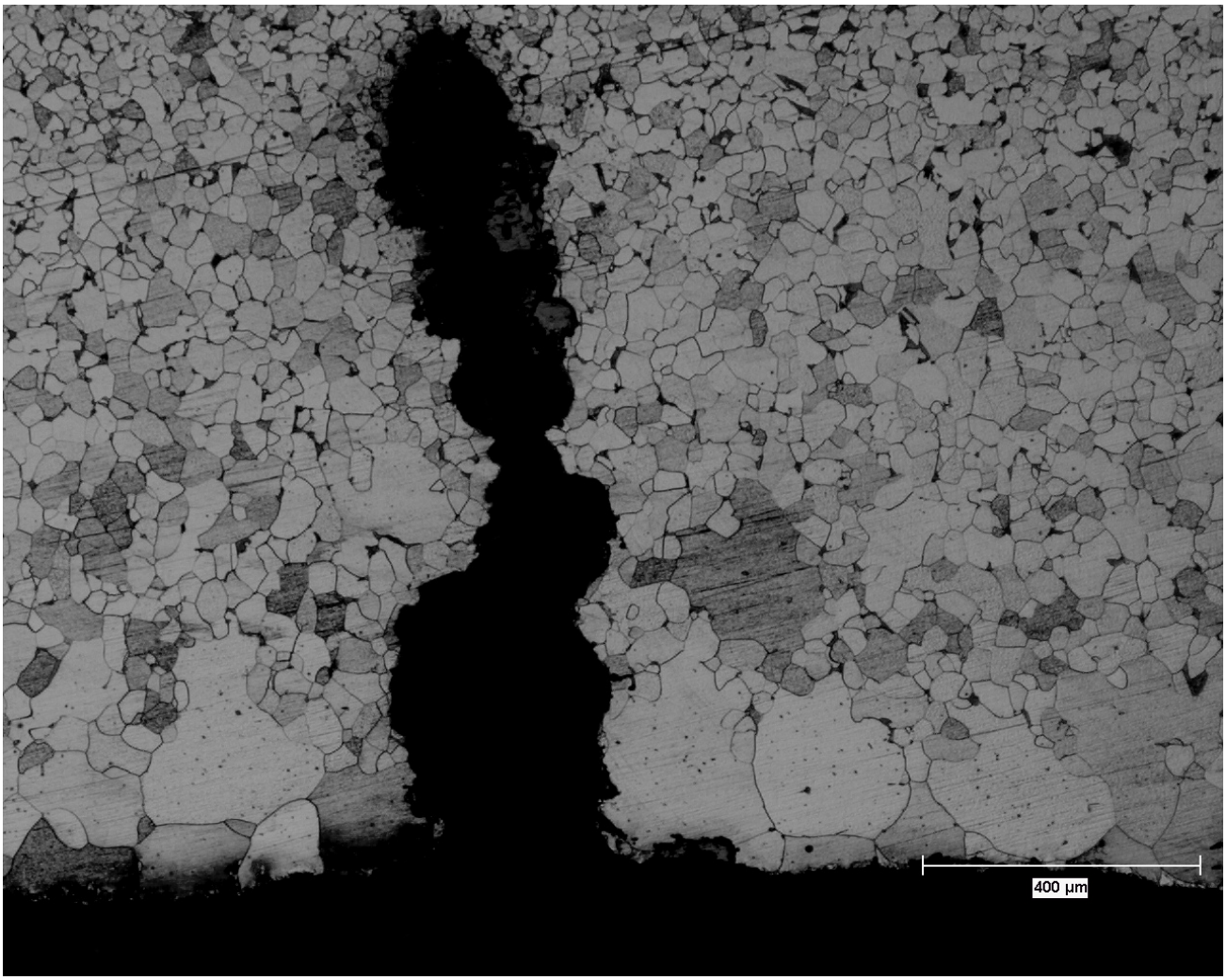

Figure 3.2.12. Micrograph also shows clear signs of very prominent grain growth and de-carburized layer at the inner surface of tube. This is not a typical case but was seen in a few tubes examined at the Corrosion Lab at Georgia Tech

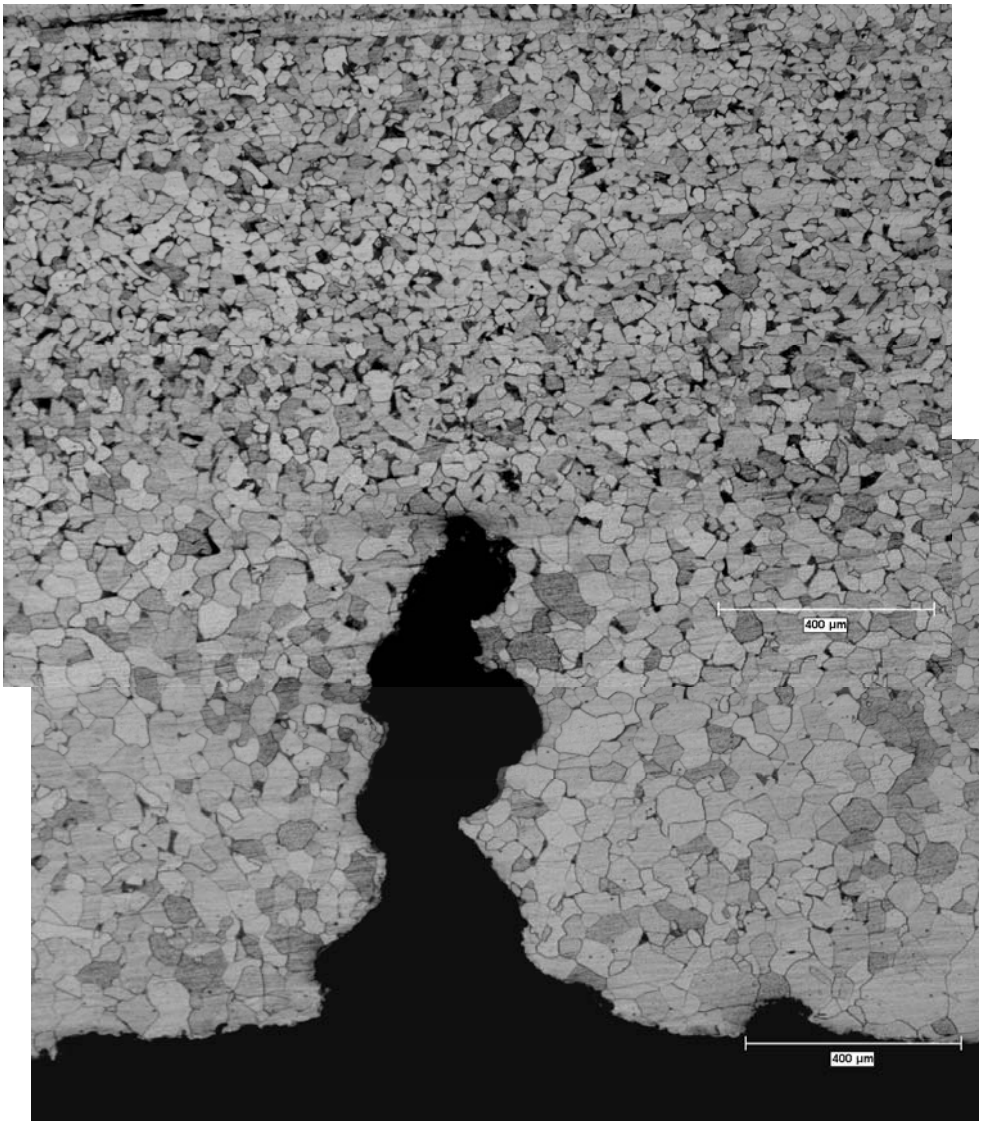

Figure 3.2.13. Micrographs showing grain growth and de-carburized layer at the inner surface of the failed boiler tube. Notice that the crack seems to have stopped at the interface of decarburized layer and typical pearlitic microstructure of the carbon steel tube. This is very common feature found on most of the tubes showing grain growth.

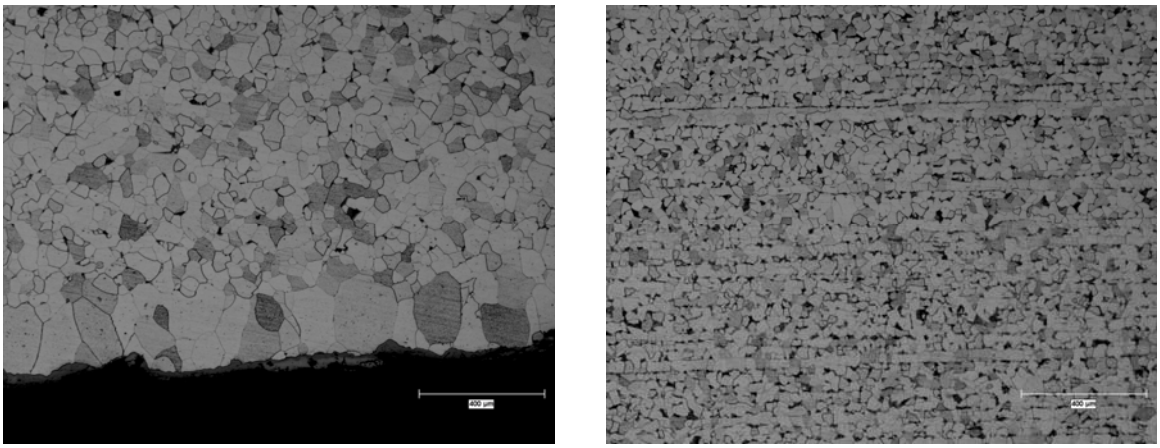

Inner Tube Surface **Middle of Tube**

Figure 3.2.14. Typical microstructure difference for the tubes showing grain growth and de-carburized layer at the inner surface.

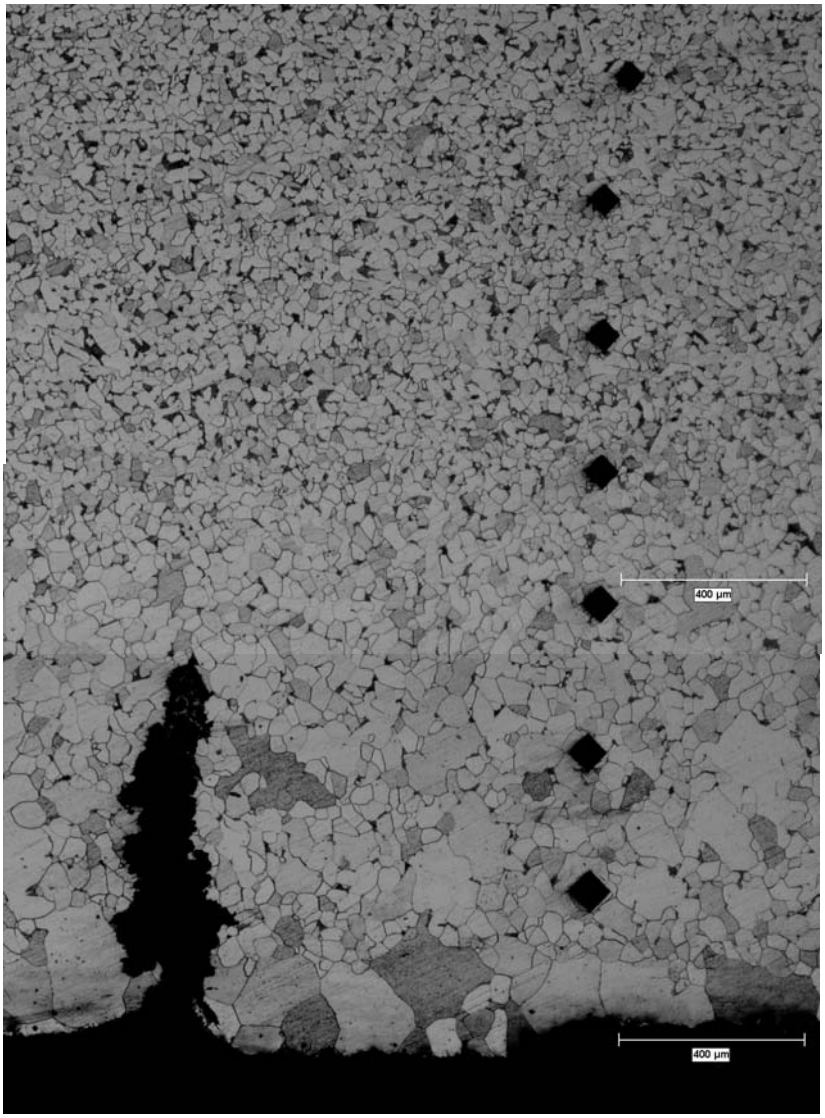

Figure 3.2.15. Micrographs showing microhardness indents in the areas of grain growth and de-carburized layer as well as normal carbon steel tube structure. Notice that the indent size decreases away from the tube surface.

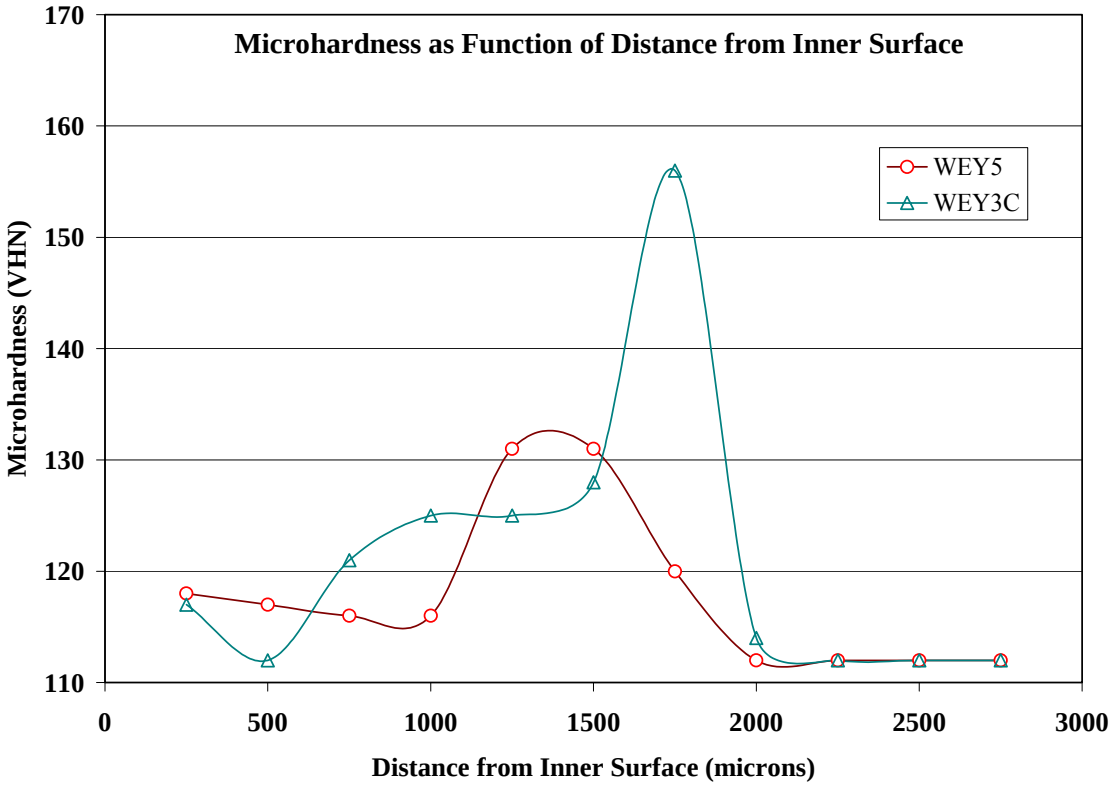

Figure 3.2.16. Microhardness data for tubes from one particular recovery boiler showing vickers hardness number as a function of distance away from the inner tube surface. There is clear indication of softer layer at the inner as well as outer surface of the tube whereas the hardness is higher in the middle.

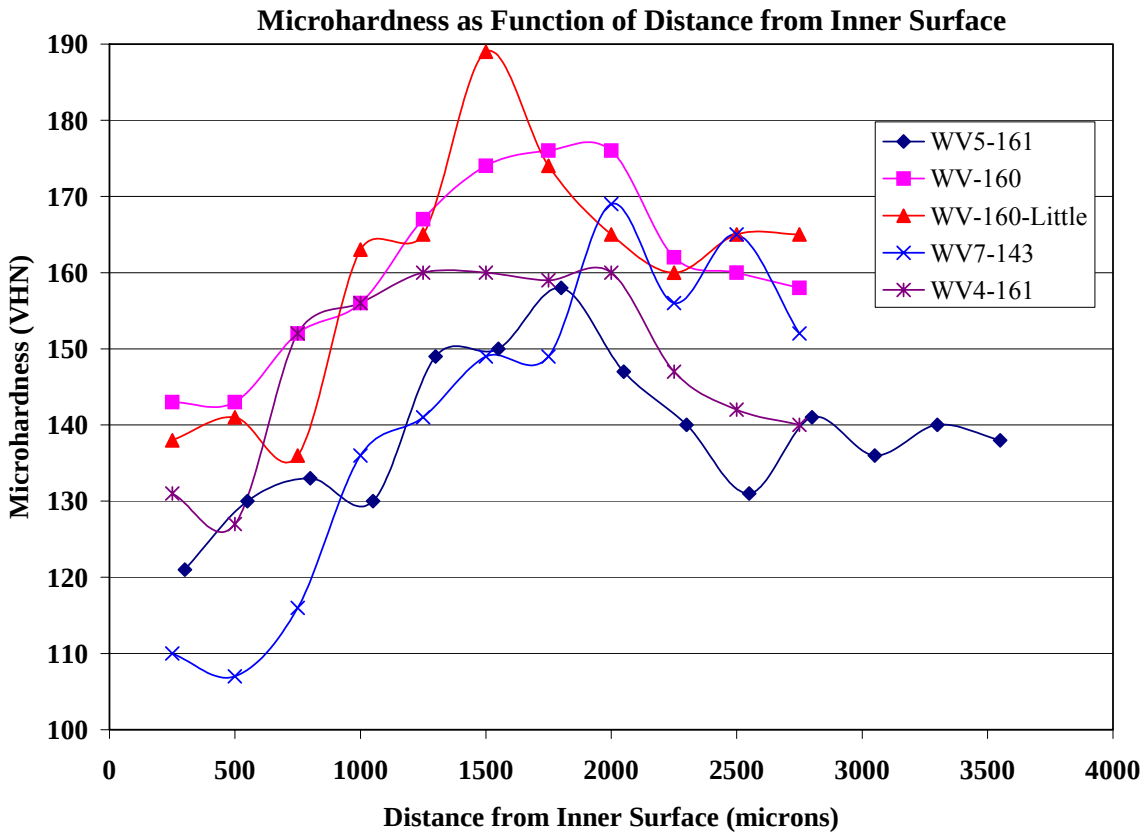

Figure 3.2.17. Microhardness data for a set of tubes from a recovery boiler showing Vickers hardness number as a function of distance away from the inner tube surface. There is clear indication of softer layer at the inner as well as outer surface of the tube whereas the hardness is higher in the middle.

The main aim for this task of the project was to examine some failed waterwall tubes with known SAC cracks and identify any microstructural features that are associated with these failures. We were looking for any microstructural changes in the carbon steel, close to the SAC failure area, that may have facilitated the initiation of SAC cracks in waterwall tubes. Rational behind this effort was that local changes in microstructure can occur during tube manufacture processes, due to improper welding of attachments, or during boiler operations due to local overheating for a long time period, and may make this material more susceptible to SAC initiation.

Eight more failed tubes from three different recovery boilers were received at the Corrosion Laboratory of Georgia Tech. These tubes were sectioned using a similar method as described earlier to reveal SAC affected inner surfaces of waterwall tubes. All tubes received had attachment welds on them. We focused our failure analysis in the areas under attachment welds. These tubes were examined for any waterside deposits associated with SAC cracks. Tubes had thin layer of corrosion products on the inner surface which may or may not have developed after these tubes were removed from the boiler. We did not detect any deposits associated with the crack areas in any of the tubes examined from this batch of tubes. A typical tube after initial cuts is shown in Figure 3.2.18.

Inner surface of tubes was cleaned to reveal SAC cracks. Small tube sections with SAC cracks were selected and mounted in cold-set epoxy. The specimens were polished to 0.25 micron diamond finish and were examined using optical microscope for the general shape and size of SAC cracks on each mounted specimen. Some tubes sections away from the SAC attack were also mounted and examined to compare the microstructure in the two areas (i.e. with and without SAC cracks). Polished carbon steel tube surfaces were etched using 5% Nital at room temperature. Etched waterwall tube microstructure was examined using an optical microscope.

Specimens with SAC cracks were also used to measure the microhardness (in VHN) profile of carbon steel along the tube thickness in the areas with SAC and away from this area. Load selection for microhardness measurements was done to get indent size which was about 5-8 times bigger than the average grain diameters. This was done to quantify the average value of the material properties in local areas along the tube thickness in areas affected with SAC.

Figures 3.2.19 to 3.2.21 show inner surface of cleaned tubes with longitudinal SAC cracks. Cracks in the examined tubes were longitudinal in tubes with longitudinal attachment welds as well as circumferential attachment welds. In some tubes, pitting attack could be noticed near SAC cracks. These pits were 20 to 250 microns in diameter at the tube surface and were filled with corrosion products.

Etched specimens revealed crack path and grain structure for the carbon steel tubes. Figures 3.2.22 to 3.2.28 show SAC cracks and grain structure for different boiler failed tubes. Corrosion attack did not follow grain boundaries. Boiler tube in Figure 3.2.22 shows a very small decarburized layer near the inner surface (3-4 grain thick). In general the cracks were not sharp as in typical stress corrosion cracks but were with blunt tips and bulbous regions. This indicates that these cracks must have grown through discontinuous mechanism.

Significant differences in the grain size near the inner surface and the middle of the tube section were found in some of the failed tubes. Large decarburized grains were typically found at the inner surface compared to center of wall. There were far fewer pearlitic grains near the surface indicating decarburization of this layer, shown in Figures 3.2.22 to 3.2.24. Large grain layer was not continuous in all the sections examined. In some cases, this layer was very localized and the thickness, even in the same section, varied significantly. A large number of cracks in Tubes # 5 and #3 stopped at the interface where small grained structure started. Lower mechanical strength of large grained (also decarburized) inner layer may be one of the reasons for crack initiation and growth till the high strength layer. This suggests that the cracks may either stop to grow or may require higher stresses and/or environmental conditions to grow further into the fine-grained structure. However, it is important to notice that not all tube sections with cracks showed differences in grain size. Tube #3 showed that even in the same tube there were areas with large grains and small grained structure at the surface, as shown in Figures 3.2.25 and 3.2.28.

Figures 3.2.26 and 3.2.27 show a typical SAC "pit". These pits were found in the same general area with SAC cracks. It is possible that the pitting attack may have role in crack initiation in boiler water environment under given stress conditions.

3.2.6.1 Microhardness of carbon steel tube sections in SAC affected areas

A few mounted specimens with SAC were used to map microhardness of carbon steel along tube thickness. Figures 3.2.29 to 3.2.33 show indentation sites and microhardness value in vickers hardness number (VHN). Higher number represents a harder material or one with higher yield strength. Tube #1 exhibited lower hardness value for the large grained layer close to the SAC crack whereas the tube had higher hardness through out the remaining thickness of the tube. In tubes sections where the grains were not very different throughout the section, we did not see much difference in the hardness value, as is expected. Figure 3.2.33 shows a very clear role of the large grained microstructure on cracking. In Tube #5 the large grained layer was not even sized along the tube surface. It is clear in Figure 3.2.33 that the cracks were longer where the light colored, large grained, layer was thickest. In the right

side corner of this specimen, there was very small difference in the grain size along thickness of tube. This observation suggests that the conditions that produced a layer with large grain size in the carbon steel tube were not evenly experienced along the entire inner circumference of the tube in this region.

Figures 3.2.34 to 3.2.28 show other sections of boiler tubes which do not show any obvious signs of changes in the microstructure of carbon steel at the inner steel surface. SAC cracks were also found in these tubes as is visible in Figure 3.2.36. This indicates that decarburized layer is not essential for SAC but may facilitate early initiation and growth of SAC.

Figure 3.2.18. Photograph showing a waterwall tube sectioned to reveal SAC cracks under the attachment weld on the cold-side of the tube.

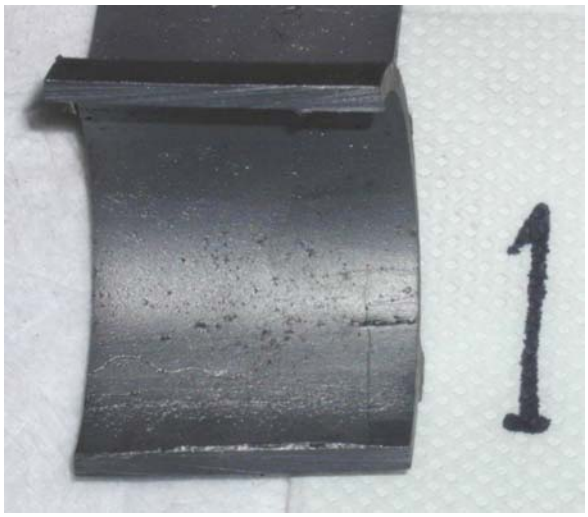

Figure 3.2.19. Section of tube # 1 showing SAC crack on the inner surface of a carbon steel tube. The affected area was under the attachment weld.

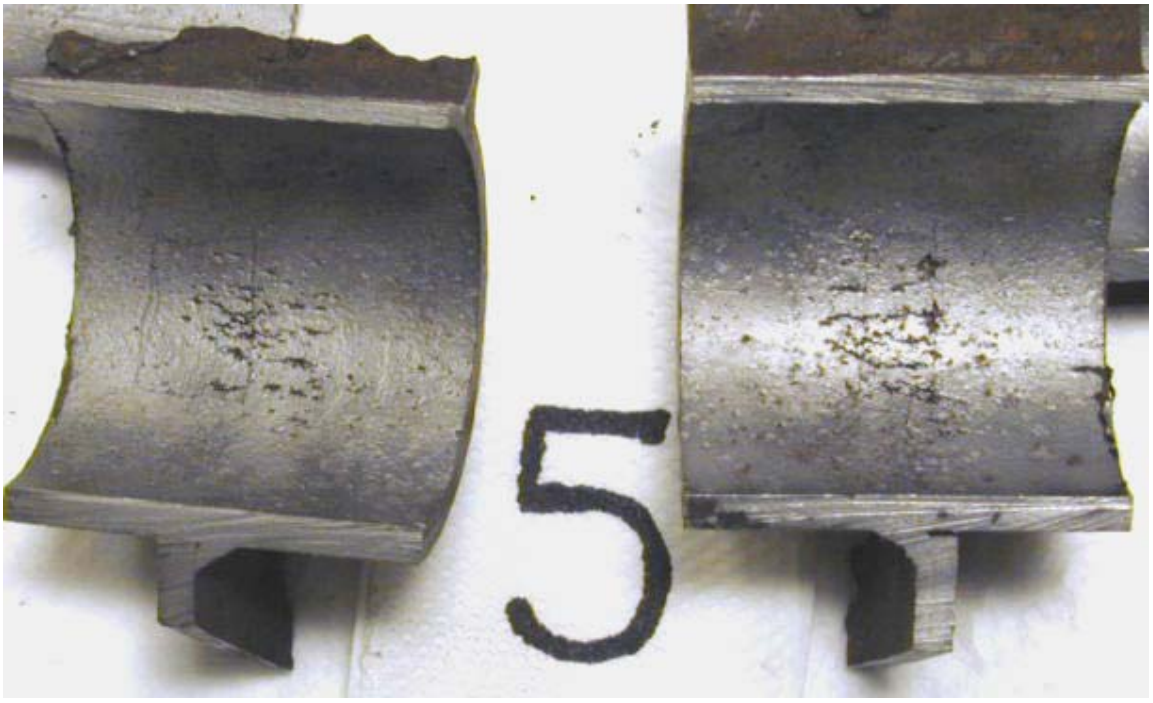

Figure 3.2.20. Section of two adjacent tubes # 5 showing SAC crack on their inner surface under the circumferential attachment weld. Notice that both adjacent tubes had SAC attack under the attachment weld at the same location.

(a)

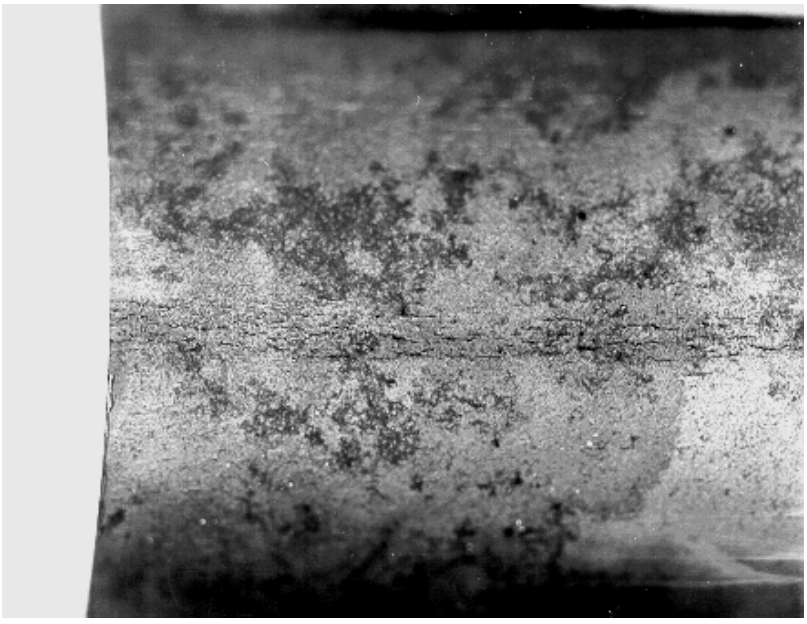

(b)

Figures 3.2.21. Section of tube-A showing longitudinal SAC cracks on their inner surface under the longitudinal attachment weld.

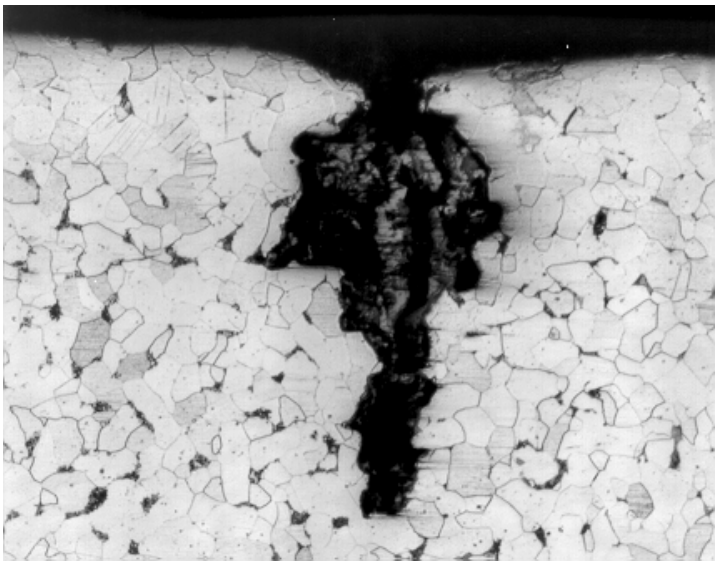

Figures 3.2.22. Micrograph of an etched section of tube-A showing a SAC crack on the inner surface under the longitudinal attachment weld.

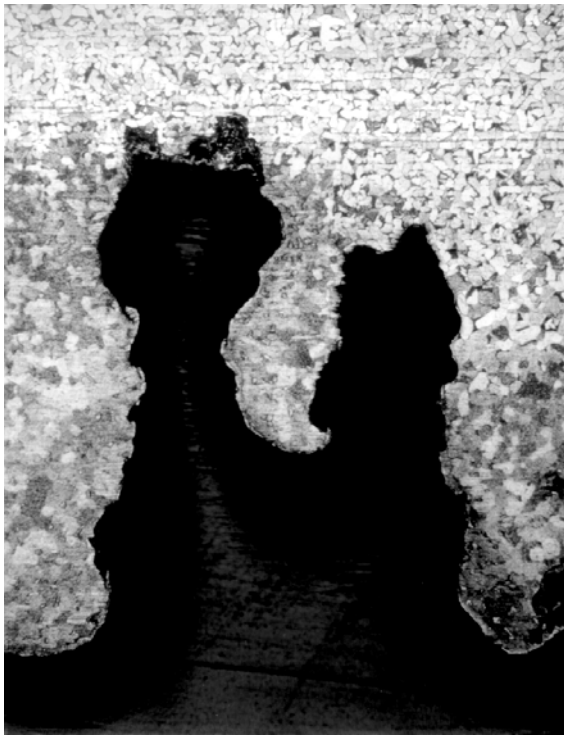

Figures 3.2.23. Micrograph of an etched section of tube #5 showing a SAC crack on the inner surface under the longitudinal attachment weld.

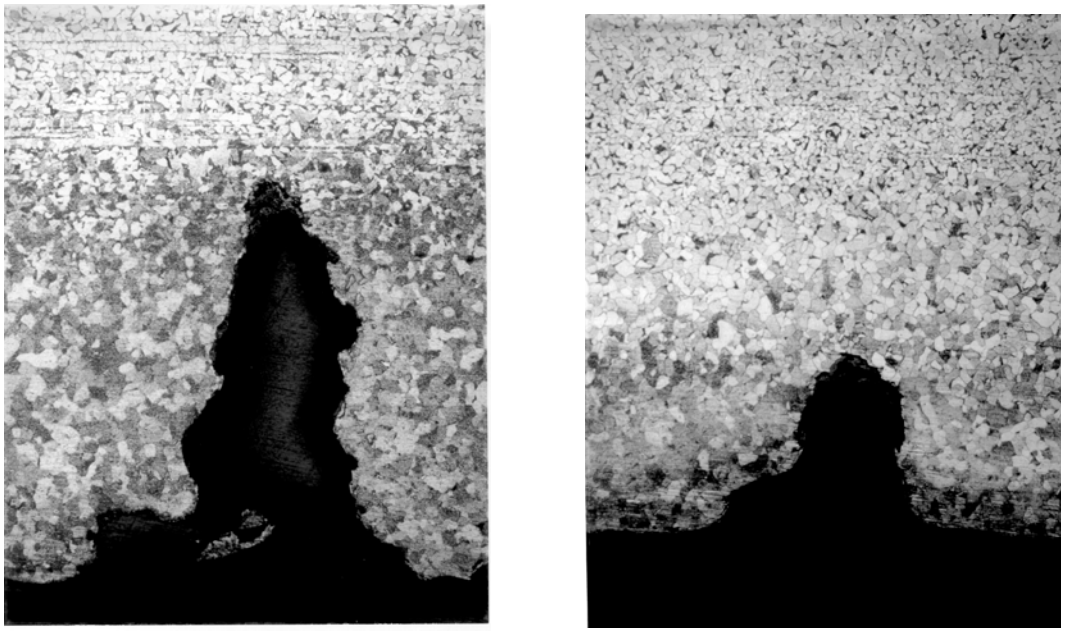

Figures 3.2.24. Micrographs of an etched section of tube #5 showing a SAC crack on the inner surface under the longitudinal attachment weld.

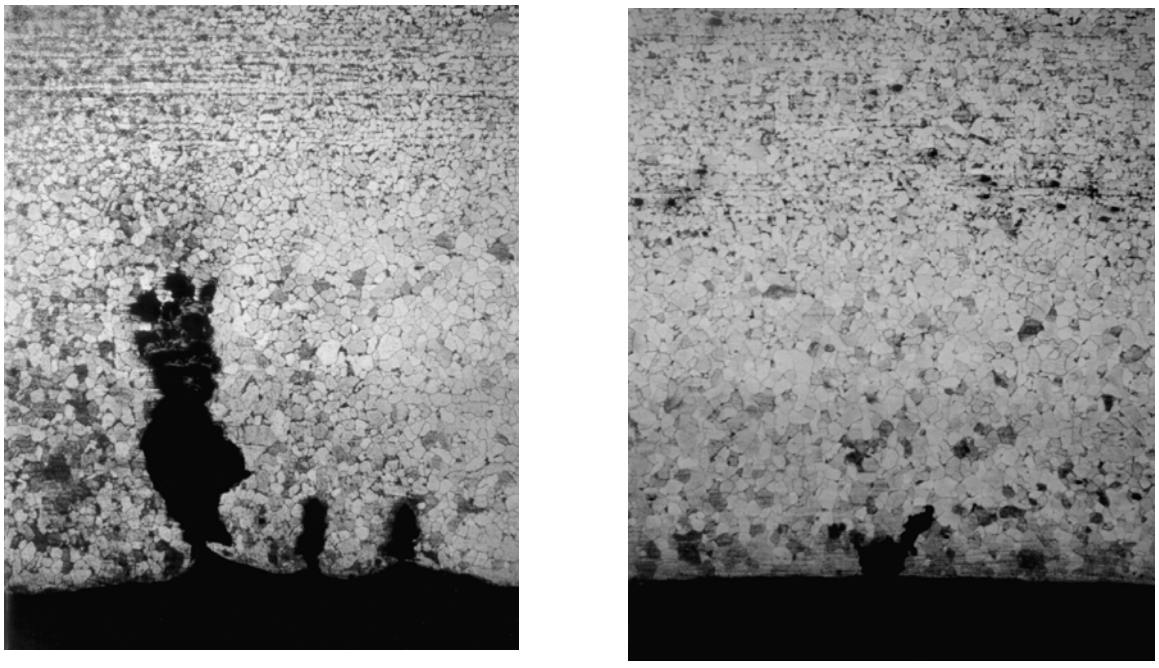

Figures 3.2.25. Micrograph of an etched section of tube #3 showing a SAC crack on the inner surface under the longitudinal attachment weld.

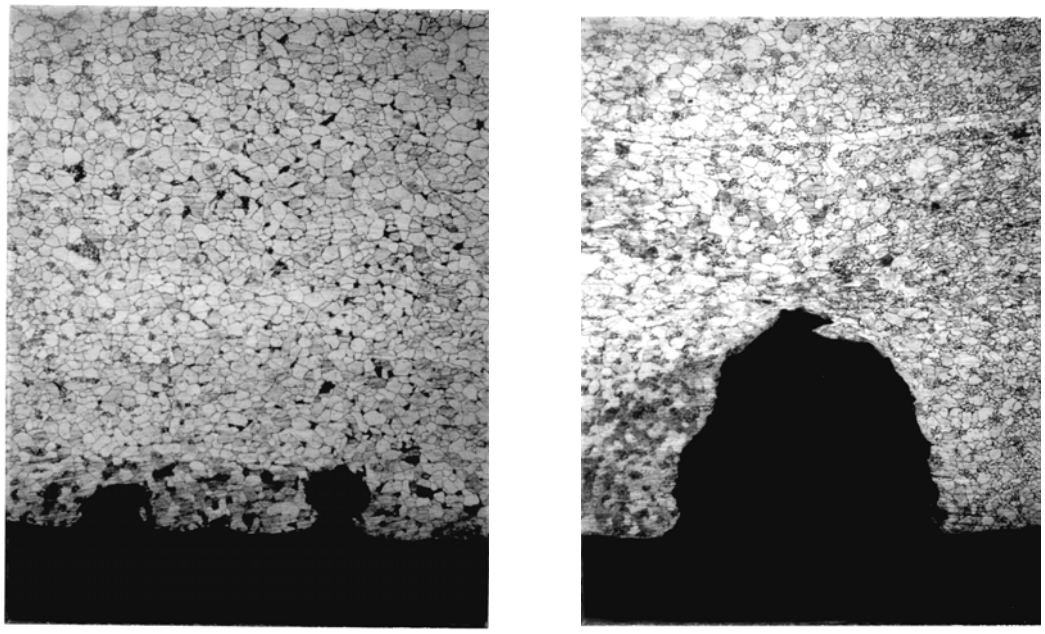

Figures 3.2.26. Micrographs showing an etched section of tube #1 with SAC "pits" on the inner tube surface. Pits were near cracks under a longitudinal weld attachment.

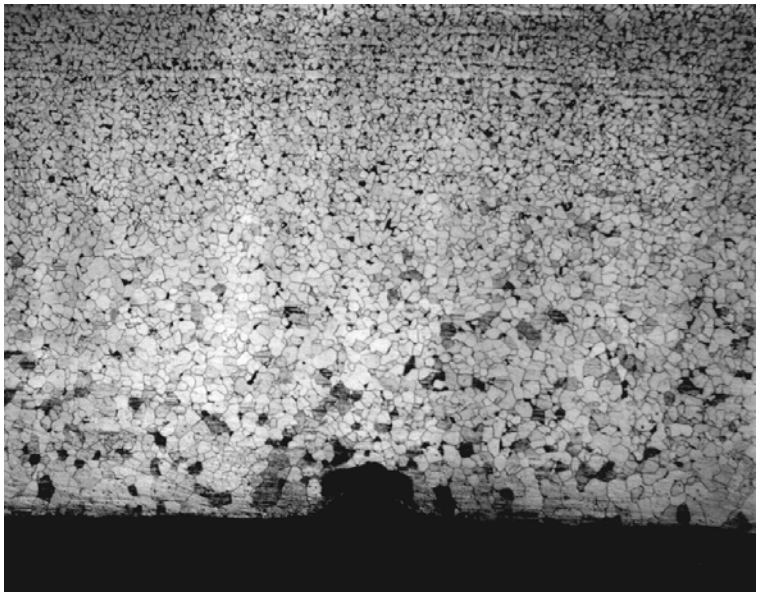

Figures 3.2.27. Micrograph of an etched section of tube #2 showing a SAC "pit" on the inner surface under the longitudinal attachment weld. Notice the differences in grain size through tube thickness.

Figures 3.2.28. Micrograph of an etched section of tube #3 showing a SAC crack on the inner surface under the longitudinal attachment weld.

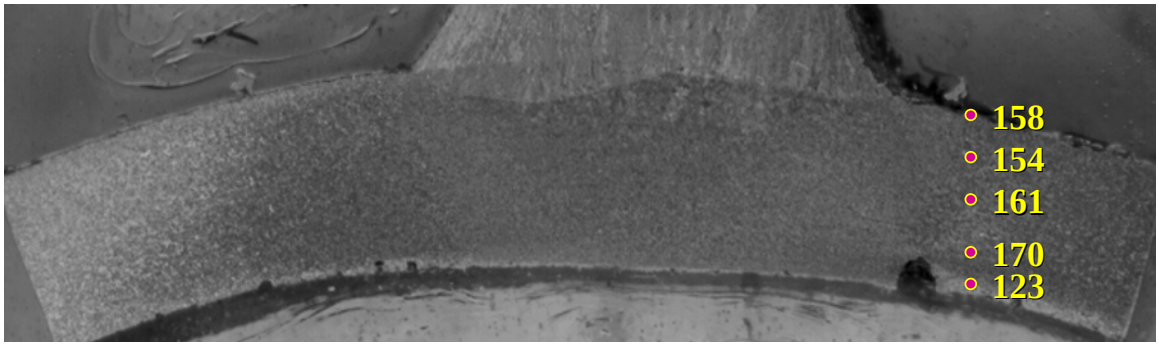

Figures 3.2.29. Microhardness *(in VHN)* of carbon steel tubes in different areas of Tube #1

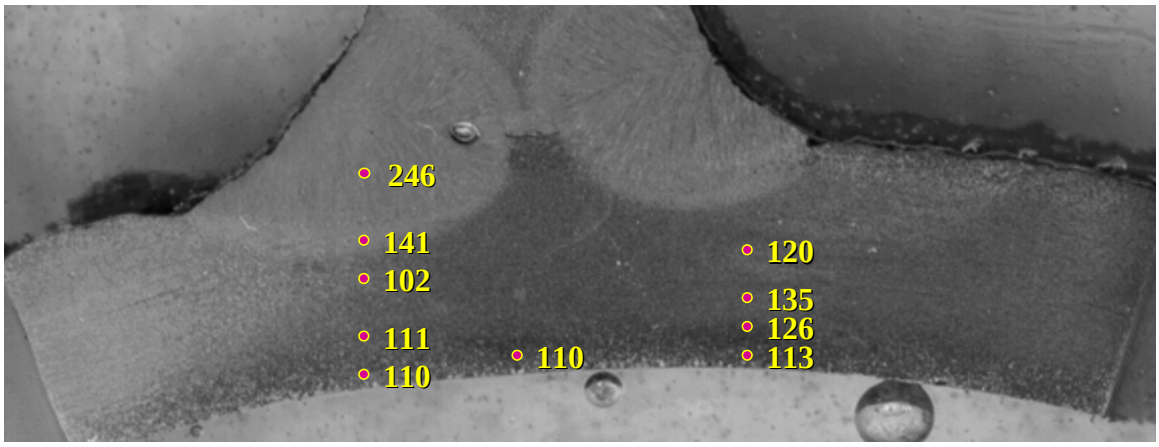

Figures 3.2.30. Microhardness *(in VHN)* of carbon steel tubes in different areas of Tube #2

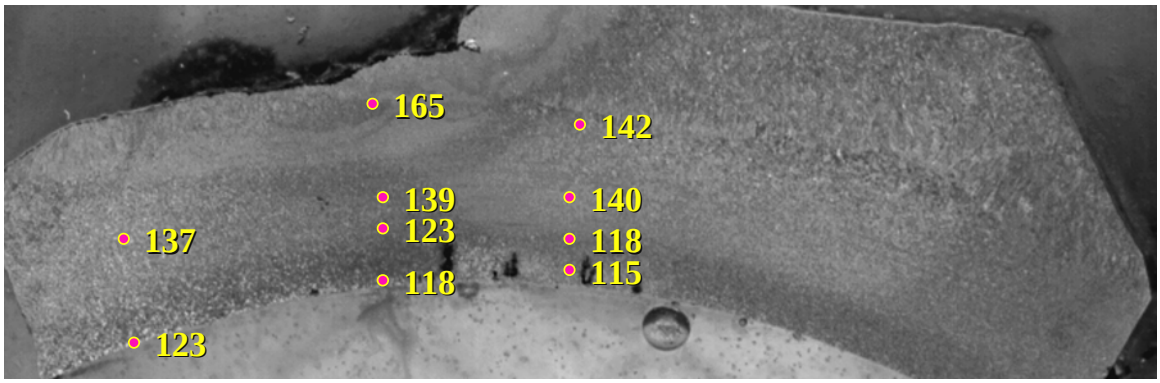

Figures 3.2.31. Microhardness *(in VHN)* of carbon steel tubes in different areas of Tube #3

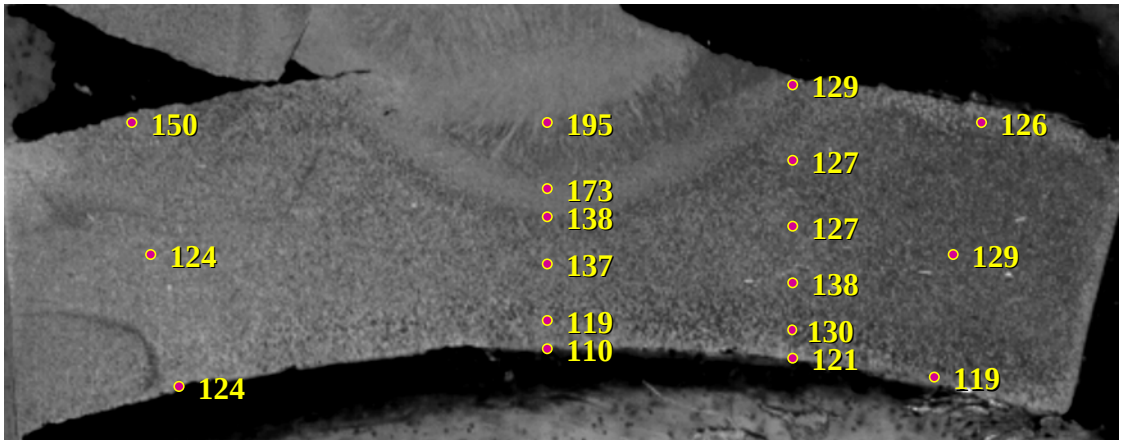

Figures 3.2.32. Microhardness *(in VHN)* of carbon steel tubes in different areas of Tube #4

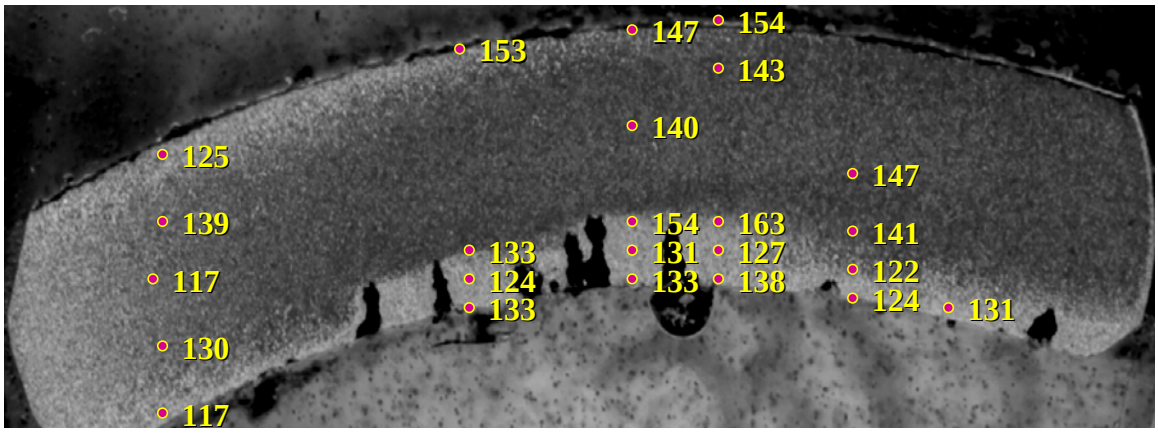

Figures 3.2.33. Microhardness *(in VHN)* of carbon steel tubes in different areas of Tube #5

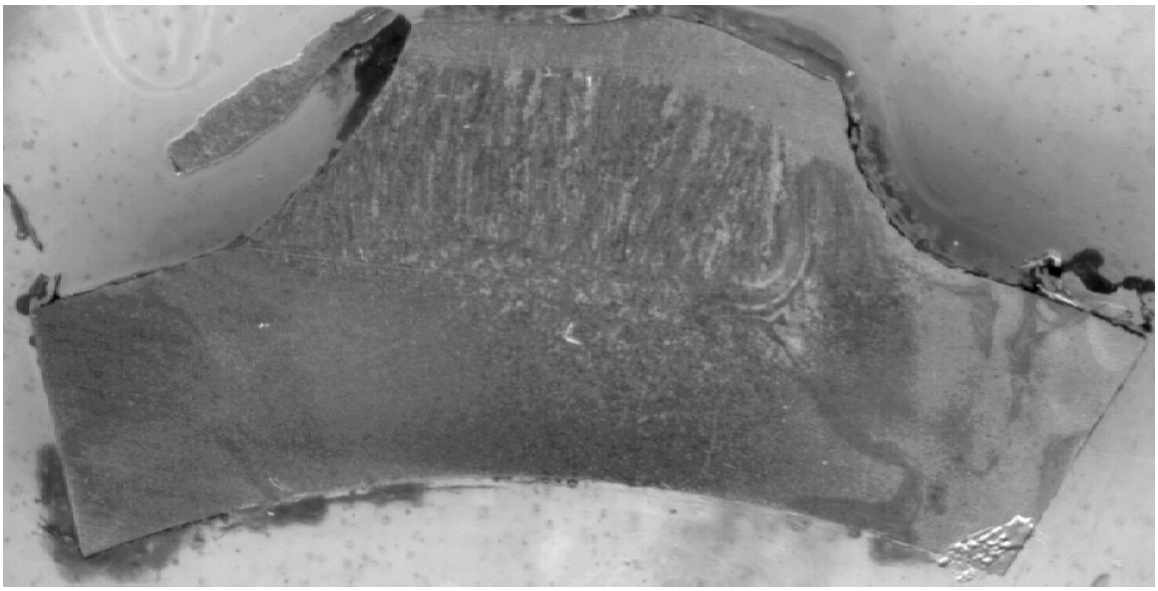

Figures 3.2.34. Section of carbon steel waterwall tube #6

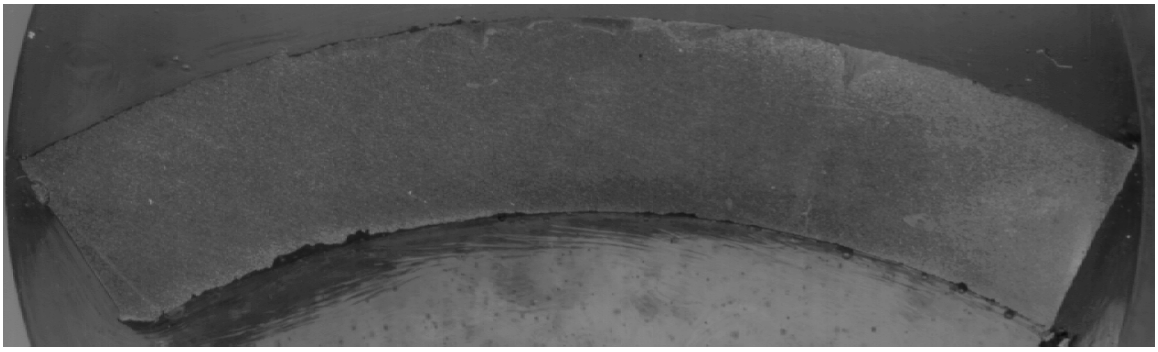

Figures 3.2.35. Section of carbon steel waterwall tube #7-1

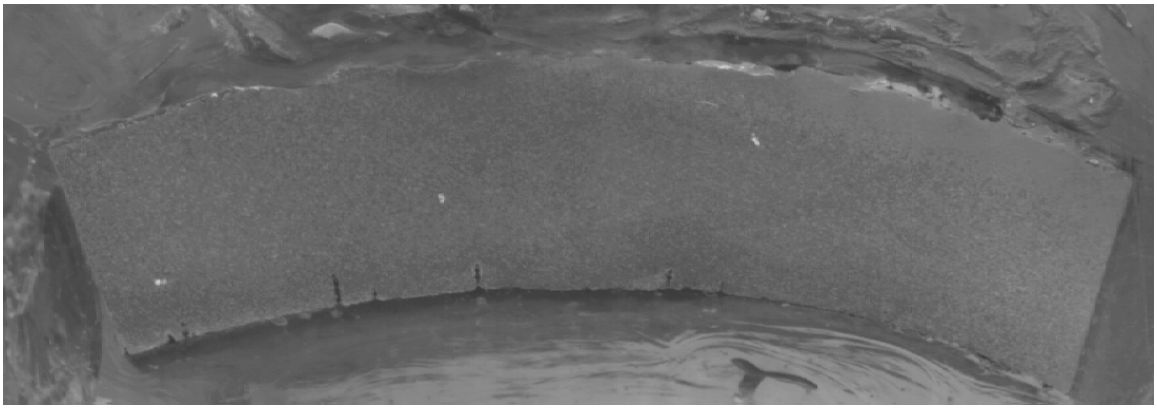

Figures 3.2.36. Section of carbon steel waterwall tube #7-2

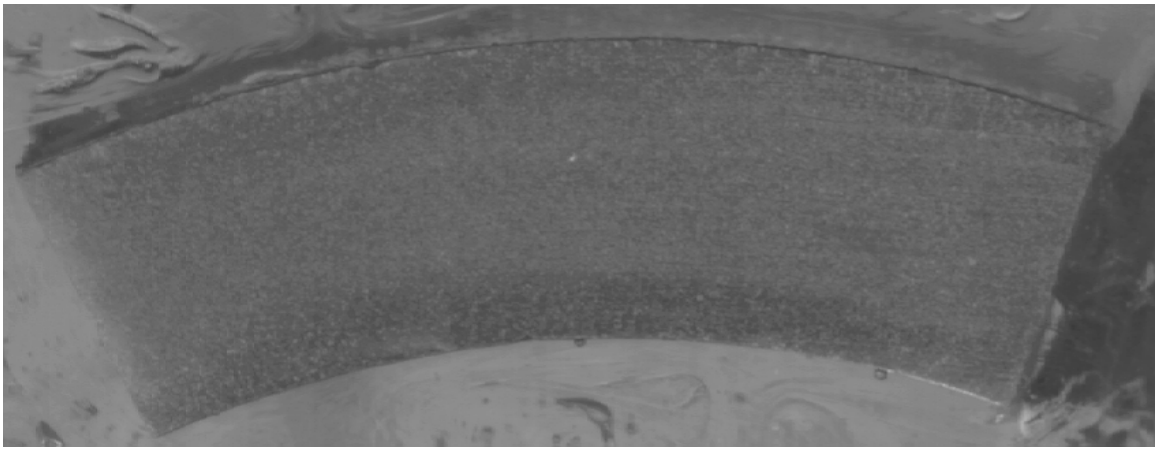

Figures 3.2.37. Section of carbon steel waterwall tube #7-3

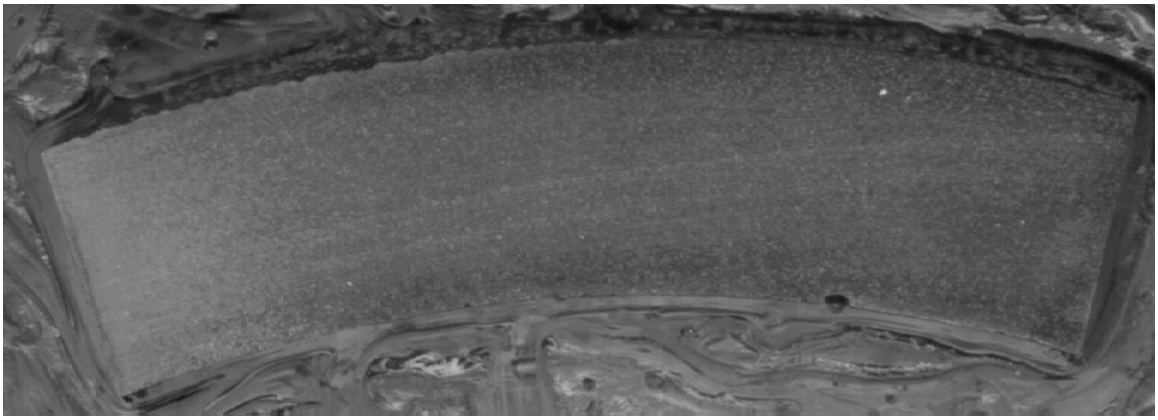

Figures 3.2.38. Section of carbon steel waterwall tube #8

3.2.7 Conclusions from Material Characterization Task

1. In selected tubes, SAC cracks were found on the inner surface of the waterwall tubes where some attachments were welded on the cold side of the tube.
2. Cracks in all tubes examined were in the longitudinal direction, irrespective of the weld attachment direction.
3. Cracks were generally blunt and had bulbous growth indicating discontinuous growth.
4. Cracks did not follow grain boundaries.
5. In a number of tubes, large grains were associated with SAC attack. In these tubes, the maximum length of crack was roughly equal to the thickness of the large grained layer.
6. Large grained layer was in both outer and inner surfaces of some tubes whereas in other tubes they were only found on the inner surface.
7. In some sections of the tube, large grained layer on the inner surface did not have even thickness and was also discontinuous in some regions.
8. Observations from eight failed tubes from three different boilers have shown that further investigation is required to understand the conditions (Heat treatment) under which these microstructural changes are possible during the tube manufacture, during attachment welding, or during boiler operations.

3.3 INSTRUMENTATION OF BOILER FOR STRAIN AND TEMPERATURE MONITORING

The recovery boiler at the Weyerhaeuser mill at Georgia was offered to the project for instrumentation of boiler tubes with thermocouples and strain gages. The purpose of this effort was to assess the frequency and magnitude of temperature and strain changes near an attachment weld during boiler operation in light of what is known about SAC mechanisms.

This particular boiler, in service for over twenty years, is not known to have experienced SAC problems during its service history. However, this boiler was selected for strain gage installation because the main aim was to measure extent of stresses in boiler tubes near attachment weld and tubes Mill personnel suggested that perhaps the most likely location for SAC in the boiler might be adjacent to the manway, at which point both longitudinal and horizontal scallop-type attachment welds intersect in close proximity to the restraint associated with the manway welds. Figure 3.3.1 shows the manway, which was located on the 7th floor of the boiler (about 35 m above the floor) and Figure 3.3.2 shows gages being installed just below the attachment that forms the lower boundary of the manway box.

Fig. 3.3.1. Manway opening into the boiler. The strain gages and thermocouples were installed at the lower right corner of the opening.

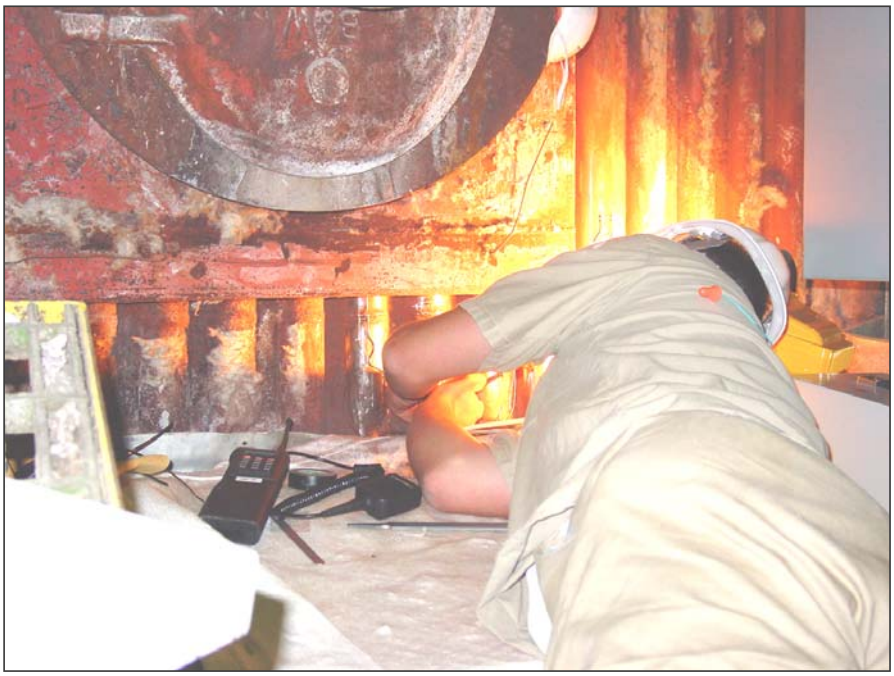

Fig. 3.3.2. Technician Adam Willoughby of ORNL attaching thermocouples and strain gages to the boiler tubes just below the manway box.

The temperature-compensated strain gages were Kyowa model KHC-10-120-G8-11. These gages were of the half-bridge capsule type, rated to 550ºC, and spot-weldable. The manufacturer supplied a calibration chart (gage factors and apparent strain as a function of temperature) for each individual gage. Gages applied to the tubes in the circumferential (curved) orientation were shaped to the appropriate radius by the manufacturer prior to calibration.

Prior to spot welding, the external tube surface was prepared with a combination of power wire brushing and other standard hand tools to the cleanliness condition prescribed by the manufacturer. Strict spot welding guidelines from the manufacturer, including power requirements and the position/order of the spot welds along the strip, were also maintained for each gage installation.

Thermocouples were type-K elements sheathed in 3 mm (1/8 in.) stainless steel strapped to the tube surface. Signals from the thermocouples and strain gages were routed to standard data modules and collected/stored with a standard personal computer for downloading

remotely. Strain and temperature data were collected every 30 seconds for about 55 weeks, representing a full year of operation between annual shut-downs as well as the initial restart period following each shut-down. [Due to a power failure, there was an approximately two-week period during which no data was collected.]

Figure 3.3.4 is a schematic of the gage installation. Longitudinal (flat) gages were installed as close as practical to the scallop weld forming the bottom of the manway box on both the tube crown (gage #1) and about 30º off the tube crown (gage #2) and at similar location centered about 18 cm from the scallop weld (gages #3, #4). Longitudinal gages were also placed at other locations relatively close (gage #17) and more remote (gage #18, #19) to the longitudinal weld forming the side of the manway box. Circumferential (curved) gages were generally centered on the tube crowns and located about 1.5 cm (closest practical approach), 2.5 cm, and 15 cm from the scallop weld forming the bottom of the manway on two different tubes (gages #8 - #10 and #11 - #13) as well as at similar positions slightly off the tube crown (gages #5 - #7) and on a tube without a nearby scallop or longitudinal weld (gages #14 - #16). Thermocouples were located on the external surface of the tubes (TC #1-3, 5-7) at a variety of locations intended to assess temperatures at variable distance from the bottom/sides of the manway box as well as one location (TC #4) that was on the manway sidewall as opposed to directly on the external surface of the boiler tube. Figures 3.3.5 - 3.3.7 show the strain gage and thermocouple installation locations.

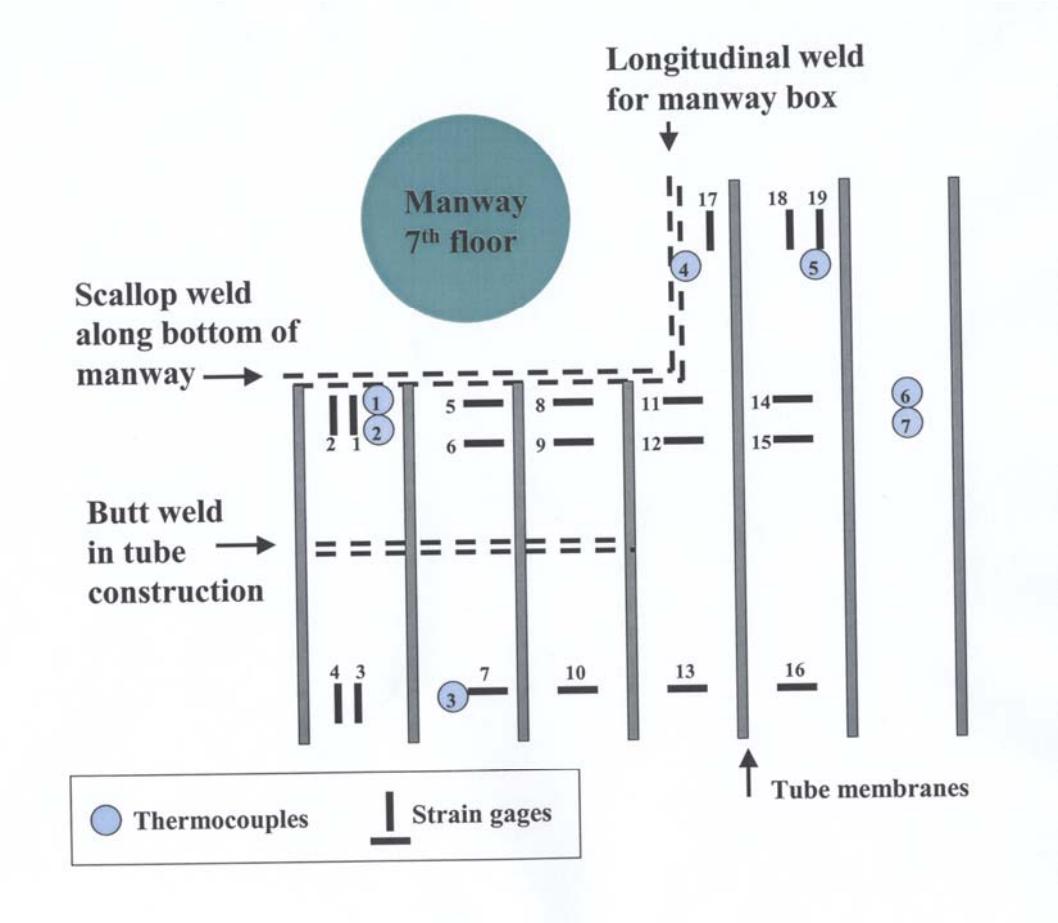

Fig. 3.3.3. Schematic diagram of the location of the strain gages and thermocouples around the manway box.

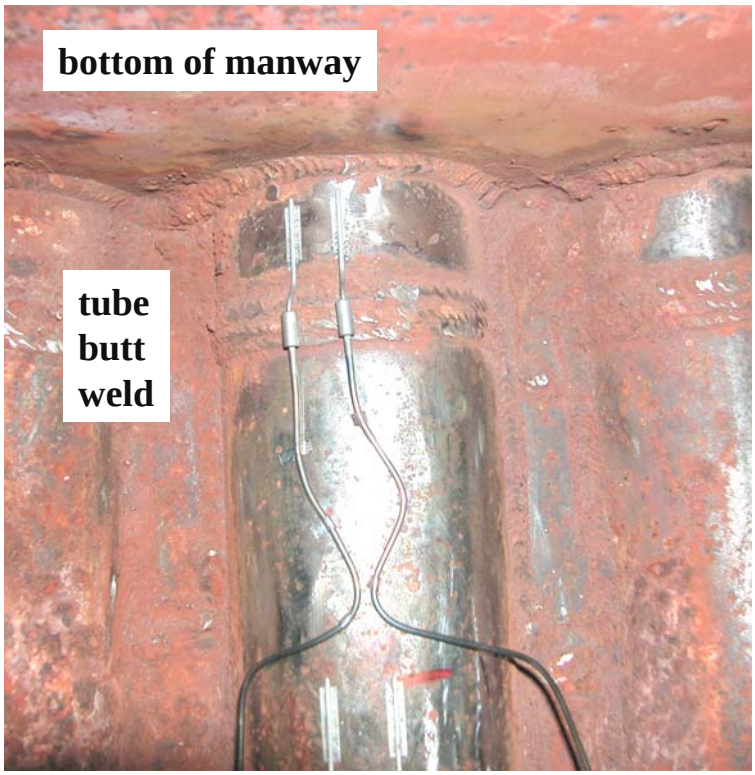

Fig. 3.3.4. Longitudinal strain gages attached to a cleaned tube close to the scallop weld that forms the bottom of the manway box (near top of photo) and similar gages about 20 cm from the bottom of the manway.

Fig. 3.3.5. Strain gages #1 and #2 along side thermocouples 1 and 2 near the bottom of the manway box.

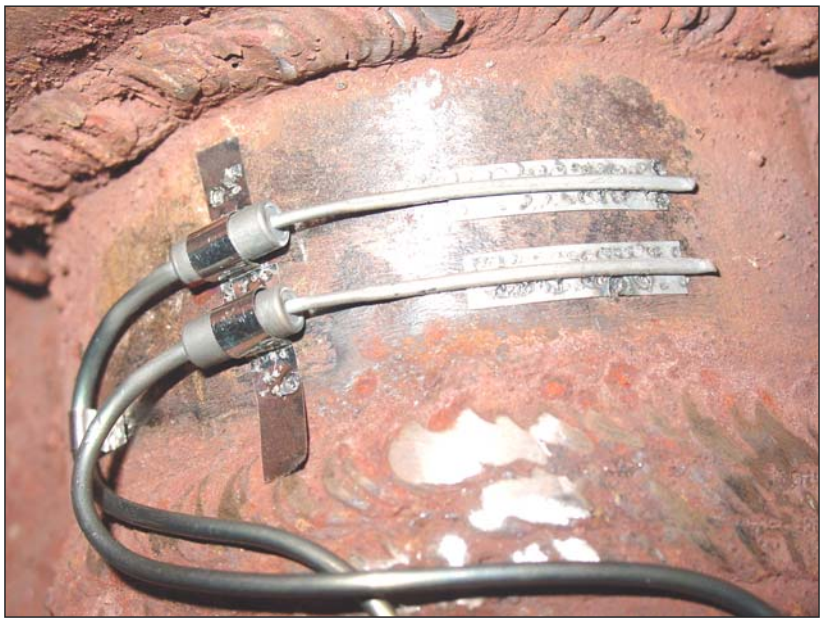

Fig. 3.3.6. Close-up view of circumferential strain gages attached between the bottom of the manway box and the tube butt weld.

3.4.1 Interpretation of Strain Gage Results

Over the entire data gathering period, thermocouples (TCs) #1, #2, #3, #6, and #7 all indicated approximately the same temperature (within 2-3ºC) during all phases of boiler operation, including the temperature decreases associated with modest upsets and even shut-downs. During normal operation, each of these TCs indicated a maximum nominal skin temperature of about 289-292ºC, while the boiler operators suggested a nominal water temperature of about 305ºC inside the boiler tubes. It is not surprising that the external TCs recorded a temperature somewhat less than that of the internal coolant, as the TCs – even beneath the boiler wall insulation – were not directly in contact with the external tube surface.

TC #4, mounted on the manway box wall rather than directly on a tube surface, routinely registered a temperature 10-15ºC below the other TCs during nominal operation, but the difference diminished somewhat during modest upsets and shut-downs. TC #5 failed early in the experiment. Analysis of the TC data suggests that the average temperature on the external surface of the boiler tubes is represented very well by the values from TC #1, so in

the data plots below which include temperature, values from TC #1 have been used.

Seventeen of the strain gages performed well throughout the period of data collection. Gage #7 (6 months) and gage #5 (8 months) failed during the experiment, but it is not clear why either gage stopped operating.

In the strain data that is reported below, the primary interest is to compare relative strain among gage positions on the boiler tubes. All portions of the boiler that are heated experience thermal strains associated with thermal expansion/contraction (and the difference in expansion coefficient between substrate and oxide) associated with normal operation cycles as well as ESPs. However, SAC is not observed throughout boilers – only immediately adjacent to attachment welds of various types. This implies that, over and above nominal thermal strains, there are mechanical stresses/strains associated with the attachment welds that contribute a critical distinguishing characteristic to the performance of the usually protective oxide in these regions. As a result, utilizing temperature-compensated strain gages to assess the differences in mechanical strains as a function of position relative to attachment welds is potentially useful to the study of SAC. It is recognized that temperature-compensated strain gages require various gage factors and modest corrections for apparent strain at different temperatures to generate precise data comparisons. However, as these correction factors are essentially identical among the gages employed (each gage has its own calibration data sheet) and that the relative difference among mechanical strains as a function of position is of primary interest, these additional factors have not been directly incorporated into the data plots or the discussion that follows. Further, it is important to recognize that the strain gages do not incorporate information about the state of stress existing in the tubes prior to attachment of the gages, only the change(s) that occur after the gages are attached, and information about the residual stress/strain in the tubes prior to attachment of the gages is not available.

It is also recognized that the relatively long length for the strain gages perhaps corresponds to results that incorporate an "averaging" effect for local strains along the entire gage length. This is perhaps most significant for the curved strain gages monitoring hoop stress, as experience suggests that the maximum hoop strain associated with the occurrence of SAC must be located very near the tube crown, else longitudinally-oriented SAC would be found at positions other than positions within a few degrees of the tube crown. Shorter gages would potentially improve the assessment of local strains, but such gages were not readily available at the time the boiler was made available for instrumentation.

In the strain data reported here, a positive value refers to a tensile strain at the location/orientation of the recording strain gage. Although some modeling work has been

attempted and a qualitative agreement between measured and calculated strains shown, the precise (quantitative) relationship between external surface strain measurements and internal strain values at suspect SAC locations is not yet clear. As a result, only relative strain changes among gage positions are considered here.

3.4.2 Startups and Shutdowns

Considering the initial pressurization of the boiler tubes along with significant changes in temperature (and development of temperature gradients), start-up of the boiler is considered an aggressive stress/strain event that perhaps contributes to the initiation and propagation of SAC. Figure 3.3.7 is a set of data representing the initial start-up of the boiler after the strain gages and TCs had been installed. In the start-up process, the temperature recorded by the TCs changes from near ambient to over 250ºC in only 3-4 hours. Following some equipment "shakedown" that caused the water temperature to be somewhat irregular over the subsequent ~30 hours, the boiler approached steady state operation.

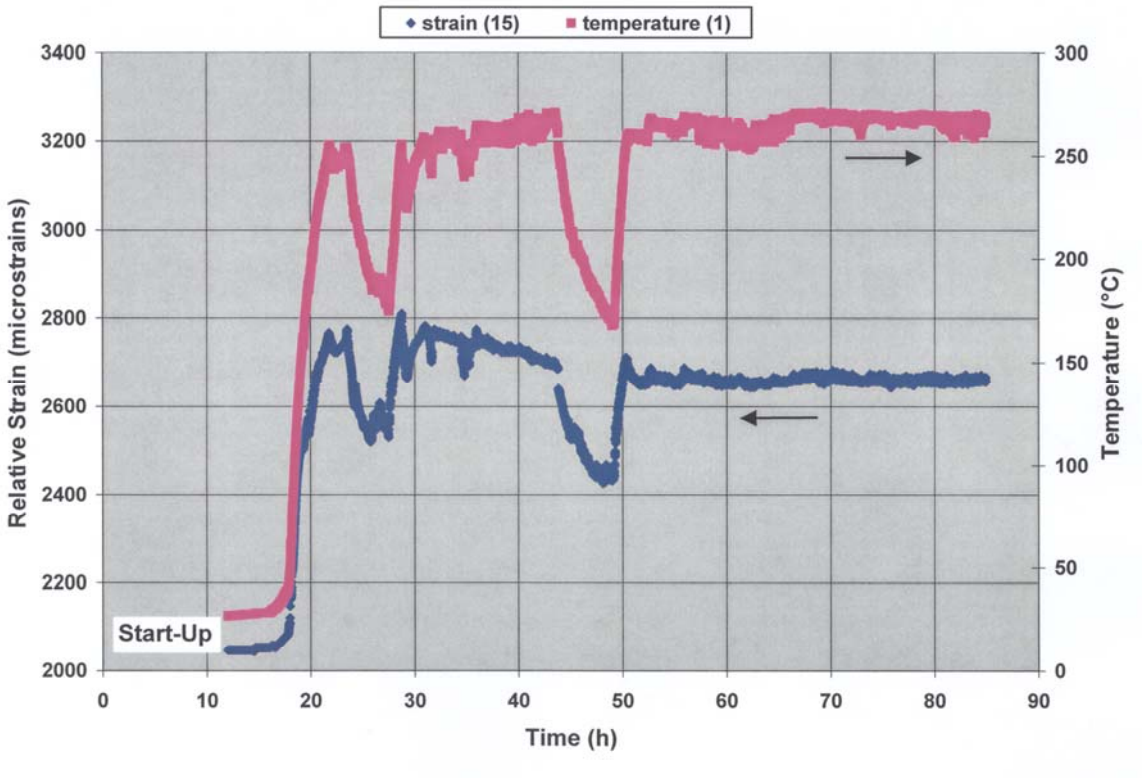

Fig. 3.3.7. Strain (gage #15) and temperature (TC #1) profiles representing the initial boiler start-up following installation of the gages.

Among all the strain gages available, data for gage #15 is plotted in Figure 3.3.7 because this gage exhibited the largest net strain change in response to the start-up conditions. In this case, the maximum strain occurred coincident with the end of the initial upset associated with the shakedown procedure (at about 42 h on the time axis). For some gages, the maximum strain was coincident with the end of the second shakedown upset (at about 50 hours in Figure 3.3.7), but none of the other gages exhibited a greater net change in strain than that for gage #15.

Over the course of the year in which data was gathered, the boiler experienced two emergency shutdown procedures (ESPs). ESPs typically occur when an off-normal safety measurement is detected; for example, an abnormal pressure or temperature in the coolant system that might indicate a leak of coolant into the boiler. Whatever the initiator, the goal of the ESP is to cease boiler operation as quickly and safely as possible. Due to the sudden change in boiler load – both stopping the operation and the subsequent restart – these events have long been suspected of representing a very aggressive strain on the boiler, which perhaps could exacerbate SAC tendency.

Figure 3.3.8 shows a representative strain and temperature profile for one of the ESP events at the mill. In this case, strain gage #15 does not represent the largest strain change for the event, but the strain profiles for all of the gages are qualitatively identical during the ESPs, and reference to gage #15 permits ready comparison with other data in this document.

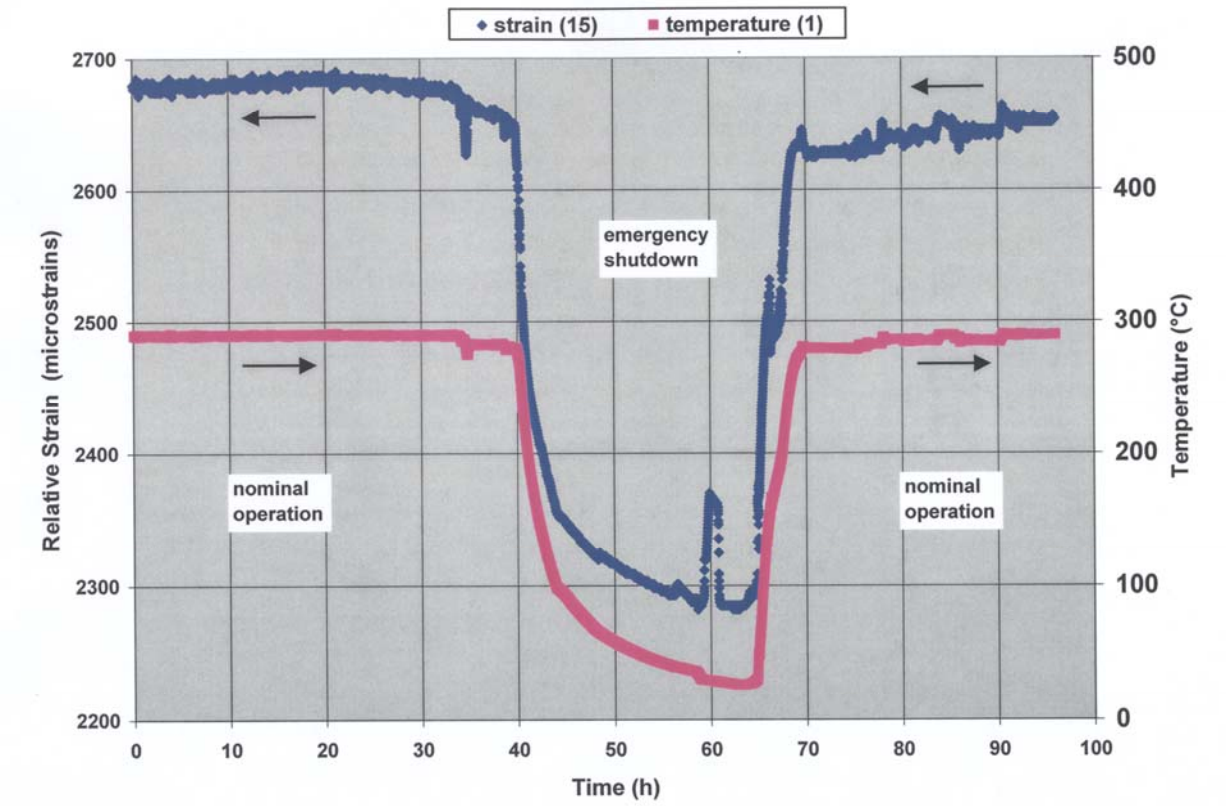

Fig. 3.3.8. Strain (gage #15) and temperature (TC #1) profiles representing the emergency shutdown and restart conditions in the boiler.

In Figure 3.3.8, the ESP begins at about 40 h into the time frame depicted, with restart of the boiler beginning about 24 h later. The brief strain excursion that occurs shortly before restart – at about 60 h in the graph – represents a cold (no corresponding temperature increase) pressure test at the operating pressure of the boiler. This result indicates that the mechanical strains associated with the temperature changes of boiler operation are substantially larger in magnitude that the mechanical strains associated with pressurization of the tubes.

Table 1 summarizes the strain change data for the initial start-up of the boiler, the shutdown/restart for each of the two ESPs, and the final restart at the end of the data collection period. These are, by far, the largest tensile strain changes experienced by the strain gages during the field experiment.

Table 3.3.1. Summary of shutdown and restart strains for four major events.

- - - - - - - - Strain change (microstrains) for event - - - - - - - -				
Strain Gage #	Initial start-up of boiler	first ESP	second ESP	Final restart of boiler
1	617 ●	651 ●	650 ●	683 ●
2	374	392 ●	384 ●	397 ●
3	223 ○	208	188 ○	166 ○
4	291	188 ○	168 ○	140 ○
5	512 ●	344 ●	---	---
6	634 ●	333 ●	344 ●	376 ●
7	358	314 ●	---	---
8	416	310	326 ●	350 ●
9	158 ○	163 ○	181 ○	183
10	144 ○	121 ○	134 ○	159 ○
11	422 ●	229	275	277
12	261	105 ○	133 ○	143 ○
13	445 ●	231	273	294
14	315	271	297 ●	320 ●
15	771 ●	318 ●	384 ●	636 ●
16	306	206 ○	226	254
17	224 ○	229	211	152 ○
18	202 ○	230	227	167
19	119 ○	109 ○	104 ○	92 ○
● = one of six largest values for the event ○ = one of six smallest values for the event				

One important trend is the recurring pattern suggesting the gages subject to the largest strains during the shutdown/restart activities. Table 1 indicates that strain gages #1, #2, #6, and #15 exhibited one of the largest six strain changes for at least three out of four events, and #5, #8, and #14 were among the highest strains in two out of four major events. Gages #3, #4, #9, #10, #12, and #19 routinely exhibited the lowest strain changes during these major events.

Several results summarized by Table 1 deserve comment. For example, the largest strain change recorded in the vicinity of the manway during the year-long experiment was 771 microstrains, occurring during the initial restart event, with an average strain change for the event among all the measurement locations less than half of that value. The magnitude of

strain change sufficient to fracture the magnetite film as a potential initiation step for SAC is not known for the conditions in these boiler tubes, as specific conditions of oxide growth and its total thickness are important factors, but literature values for the fracture of magnetite have been reported [11-13] at strains as low as 1-8 x 10^{-4} (100-800 microstrains).

Given that the preponderance of experience with SAC indicates that proximity to an attachment weld is critical, it was expected that the largest strains would be associated with gages relatively close to the attachment weld. Note, however, that for the major shutdown/restart events, the largest of the recorded hoop strain changes recorded in Table 1 occur for gages slightly removed (refer to Figure 3.3.3) from the attachment weld location. The gage exhibiting the greatest magnitude of strain change is generally the longitudinally-oriented gage on the tube crown close to the attachment weld (#1). As noted previously, however, the averaging that may occur over the gage length for the curved hoop strain devices may influence this result, as well as the fact that the hoop strain gages could not be placed particularly close to the attachment weld. Predictably, the gages with the lowest stain change in response to these major events are located somewhat remote to the attachment weld.

Among the longitudinal gages, gage #1 (tube crown, close to attachment weld) routinely exhibits a strain response about three times that of gage #3 or #18 (each also on the tube crown, but remote to the attachment weld). In addition, gage #1 routinely exhibits a strain response 65-70% greater than the adjacent gage (#2) only a few degrees off of the tube crown. Similar patterns among the hoop strain gages are not as apparent, except to note that gages relatively close to the transverse attachment weld generally exhibit a greater strain change during these major "upsets" than the gages more remote to the attachment.

3.4.3 Process Upsets

In the data shown in Figure 3.3.8, the boiler tube temperature leading up to the ESP is essentially constant/uniform and varies only 2-3ºC. Correspondingly, the boiler tube surfaces represented by the strain gages experience essentially no change in stress/strain during these "calm" periods. There is, however, one brief temperature excursion of about 11-12ºC that occurred 4-5 h prior to the ESP, which has a small relatively modest strain change associated with it. These small temperature/strain excursions represent some type of modest process upset and occurred periodically during the year of data gathering.

Exclusive of the two ESPs and the restarts following each annual shutdown, the TCs recorded a total of 41 events (in 55 weeks) with a temperature excursion from steady state of 10ºC or more. Of these, the temperature excursion was 30ºC or more (maximum of 95ºC)

only eight times. Periods of up to 26 days were observed between temperature excursions in excess of 10ºC.

Figure 3.3.9 is a representative example of the characteristics of the modest (in terms of temperature/strain excursion) process upsets. In this particular case, the size of the temperature excursion is relatively large (about 60ºC) and has a very typical total duration of 5-6 h. Note that the strain values do not precisely track temperature during the modest upset in that, during the reheating phase, the strain value seems to "overshoot" the nominal value expected from the relative strain value before and after the upset. While this behavior was typical among the modest upset conditions observed, the total strain change during these modest upsets was only a small fraction of the strain changes observed during shutdown/restart conditions. For example, the largest strain changes for the excursion shown in Figure 3.3.9 were observed for gage #1 (255 microstrains) and #11 (214 microstrains). These values are less than one-third of the maximum strain changes observed during the shutdown/restart events for the same gages.

Among the eight process upsets with a temperature excursion of 30-95ºC, gages #11 and #15 (eight times each) and gages #1 (seven times) and #2 (six times) routinely exhibited one of the six greatest relative strain changes, and no other gage was represented on this list more than twice. Similarly, gages #17 and #19 always exhibit the smallest relative strain changes in response to temperature excursions, with other gages apparently randomly on the list. Ith the exception of gage #11, the gages indicating the greatest response to the modest process upsets are among those exhibiting the greatest change during the shutdown/restart events, but the relative magnitudes would be ranked in a consistently different order. The reason for this behavior is not clear, except to note that the physical state of the boiler may not be precisely the same in each upset situation and thus the strain at each location may vary slightly as a function of the cause of the upset.

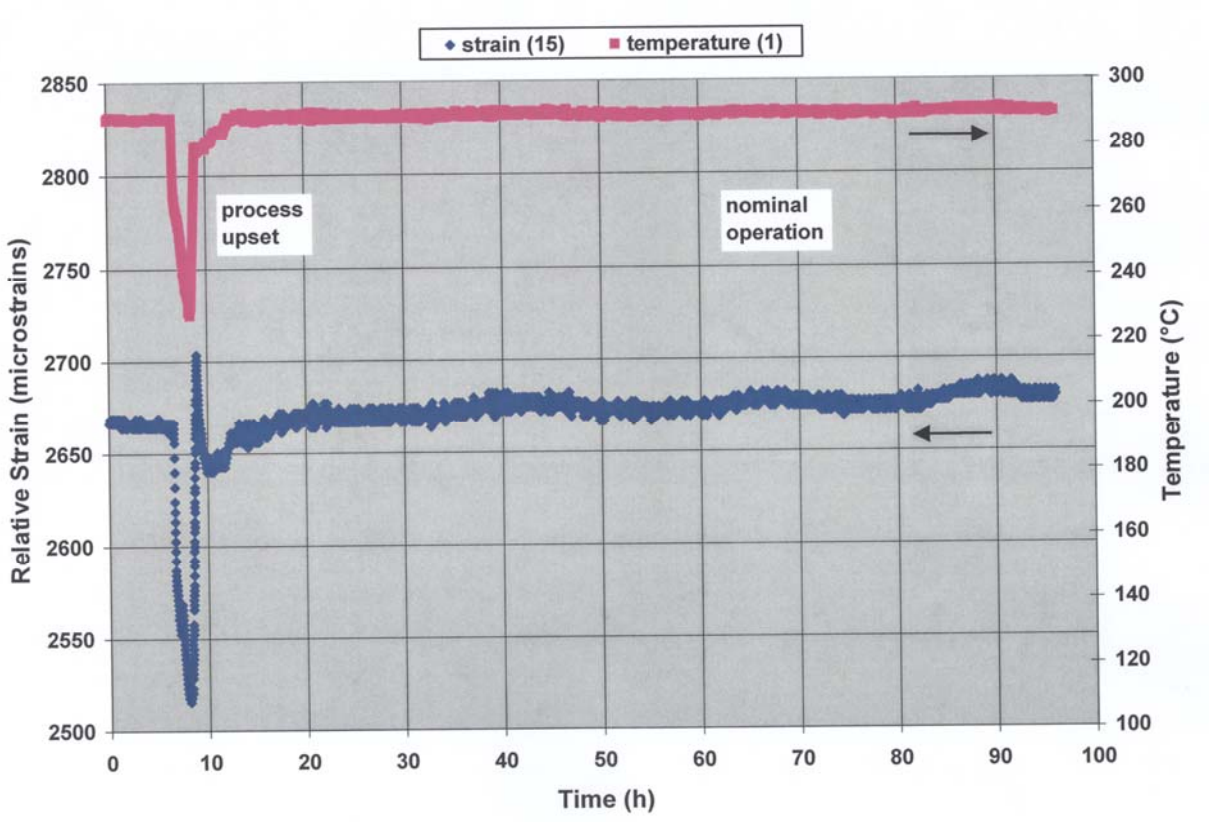

Fig. 3.3.9. Strain (gage #15) and temperature (TC #1) profiles representing a relatively modest process upset with a temperature change of about 60ºC.

It is difficult to fully interpret the strain gage results, particularly in the face of the inability to examine the boiler tubes in the area of the manway for SAC indications. Ultimately, this particular boiler experiences relatively few events in which the mechanical component of local strain (temperature compensation largely removes the purely thermal component) is substantially distinguished from the nominal minor variations. Without additional information, which would include physical examination of the boiler tubes which were instrumented, it is not possible to predict the significance of the magnitude of the mechanical strains recorded during this experiment. However, it seems likely that the relatively modest strains – recorded over 55 weeks of operation – and the low frequency of strain excursions indicate this boiler is not likely to be susceptible to SAC in the manway area, at least for the time period incorporated in this experiment.

3.4 FINITE ELEMENT MODELING

Finite element modeling has been used to carry out thermal and mechanical analyses of tube wall panels containing attachment welds to investigate the effect of the attachment weld on the stress distribution – and thus the potential contribution to SAC – in the panels. The finite element modeling work was carried out using the commercial software package ABAQUS [21]. The basic approach involves developing a finite element mesh to discretize the geometry under consideration, and applying suitable initial and boundary conditions to solve for the temperature or stress distribution. For the tube wall panels, the first task undertaken was to develop a two-dimensional (2-D) model to analyze the welding of a tube and membrane to form the wall panel. The stress distribution obtained from the 2-D analysis was mapped to a three-dimensional (3-D) model for the wall panel containing the attachment weld. The 3-D model involved analysis of the welding operation to join the attachment plate to the wall panel, followed by analysis of two normal cycles of boiler operation. For both the 2-D simulations of welding to make the panels and the 3-D simulations of welding followed by normal operating cycles, the thermal and mechanical analyses were carried out separately in a sequentially coupled manner. The thermal analysis was first performed to determine the temperature distribution, and the resulting temperature field was then used as input to the mechanical analysis to compute the stress distribution.

Assuming symmetry, the 2-D mesh was developed using 4-node linear quadrilateral elements for one half of the tube and the adjacent membrane. The welding process was assumed to be completed in four steps, corresponding respectively to application of the top weld, cooling to room temperature, application of the bottom weld, and cooling to room temperature. The elements in the mesh corresponding to the bottom weld were removed from the model during the first two steps, to remove any constraint effects due to the presence of these elements. The temperature distribution from the thermal analysis was used in the subsequent mechanical analysis to compute the stresses due to the panel fabrication. The results of the mechanical analysis were used to generate initial stress values for the 3-D model.

A 3-D finite element model was developed for the thermal and mechanical analyses of the tube wall panel containing the attachment weld. The tubes, membranes, and the attachment plate were discretized using quadrilateral shell elements, and the welds were discretized using triangular prism elements. Assuming symmetry conditions, one quarter of the tube wall panel containing the attachment weld was considered for the model used to examine the change in stresses under normal operation of the recovery boiler. For the thermal analysis, the panel initially at room temperature was taken through two operating cycles, each of which consisted of steps corresponding to heating to normal operating conditions followed by cooling to room temperature. Each step was analyzed assuming steady state conditions.

Under normal operating conditions, uniform heat flux was prescribed on the fireside (top) surface of the panel, and the flux value (200-300 kW/m^2) was chosen such that a temperature of about 340 °C was obtained at the crown of the tube on the fireside surface. The inside surfaces of the tubes were assumed to be in contact with pressurized water at 305 °C, and the cold side of the panel was assumed to be in contact with air at 100 °C, resulting in convective and radiant heat losses at these surfaces. The thermal analysis provided temperature distribution values, which were then used in the mechanical analysis. During normal operation, load due to pressurized water flowing in the tubes was applied as internal pressure of 8.62 MPa (1.25 ksi) on the inside surface of the tubes.

The results of the simulations (detailed extensively in Ref. 22 and 23, only summary information presented here) showed that the stress distribution in a tube is significantly altered by the presence of the attachment weld when compared to a tube that does not have an attachment weld. The constraint from the attachment weld prevents the free expansion of the tubes in that particular section of the wall panel. Figure 3.4.1 displays an example of this effect, and shows the distortion of the tubes containing the attachment weld relative to the tubes without the weld. The modeling results also suggest that the effect of the weld on the stress/strain distribution is confined to a short section of the tube – about 2-3 cm on either side of the weld – along the axial direction, with the greatest effect observed directly under the weld. This result is consistent with observations of SAC on samples of tubes removed from recovery boilers, in which SAC indications (refer to Figure 3.2.3) are limited to locations immediately adjacent to the attachment weld.

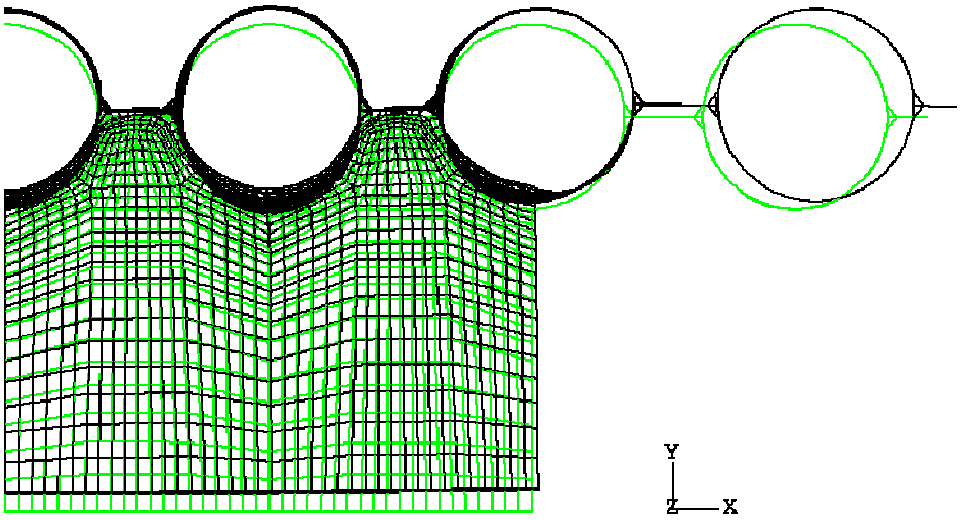

Figure 3.4.1. Initial mesh (green) and deformed mesh (black) for the tube wall panel showing the constraining effect of the attachment plate on the free expansion of the tubes under normal operating conditions. Displacements have been magnified by a factor of 10 for clarity.

As mentioned earlier, examination of a large number of samples has shown that the SAC indications that form on the waterside surface of carbon steel tubes are predominantly oriented parallel to the tube axial direction, suggesting that the component of stress in the circumferential or hoop direction plays a dominant role in the formation and propagation of these stress-assisted corrosion paths. Therefore, in examining the results of the simulations, special emphasis was given to the variation in hoop stress at the waterside surface on the cold side of the panel at the crown of the tube. Results were examined for a tube without any attachment weld and for a tube with an attachment weld at two locations—just under the weld and at a considerable distance away from the weld where the stress showed no variation in the axial direction.

Figures 3.4.2 to 3.4.4 compare the results of hoop stress calculations for a series of conditions for an SA210 carbon steel boiler tube panel. The calculations consider stresses associated with consecutive normal operating cycles – that is, an increase in temperature from ambient to the operating value and then a return to ambient at shutdown. The time axis in these examples is arbitrary and may be viewed simply as a sequence of steps. The change

in temperature and stress between any two steps is assumed to be instantaneous, although it is shown to vary in a linear fashion for convenience. For the cases described here, the condition of no initial fabrication stresses within the panel (clearly a hypothetical condition only – included to demonstrate the significance of residual fabrication stresses as a consequence of the themal/mechanical loading during operation) is compared with the case of residual stresses within the tubes/membranes resulting from panel fabrication (and calculated using the 2-D model [22]). For simplicity, stresses associated with the attachment weld itself have not been included in the analysis here (more on this later).

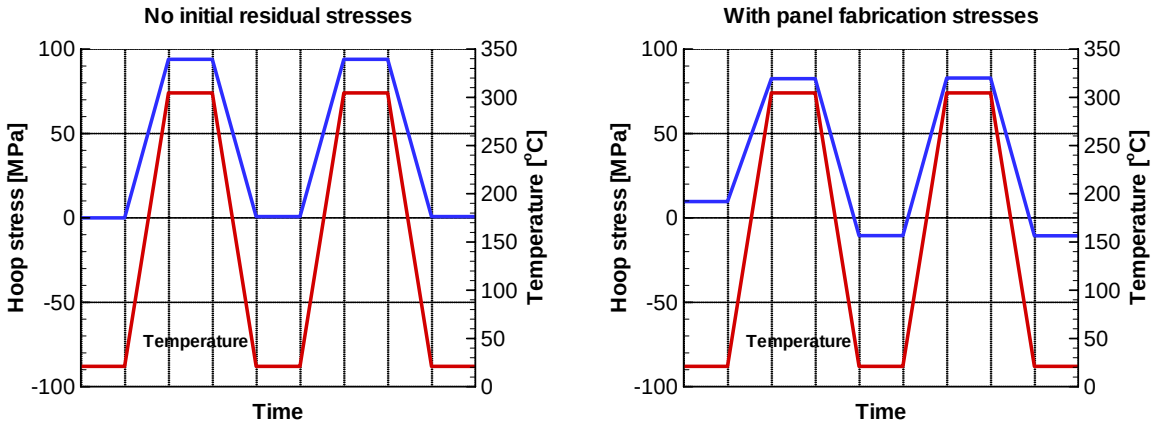

Figure 3.4.2. Variation of hoop stress with temperature for a carbon steel tube without an attachment weld at the waterside surface on the cold side of the wall panel during two normal operating cycles.

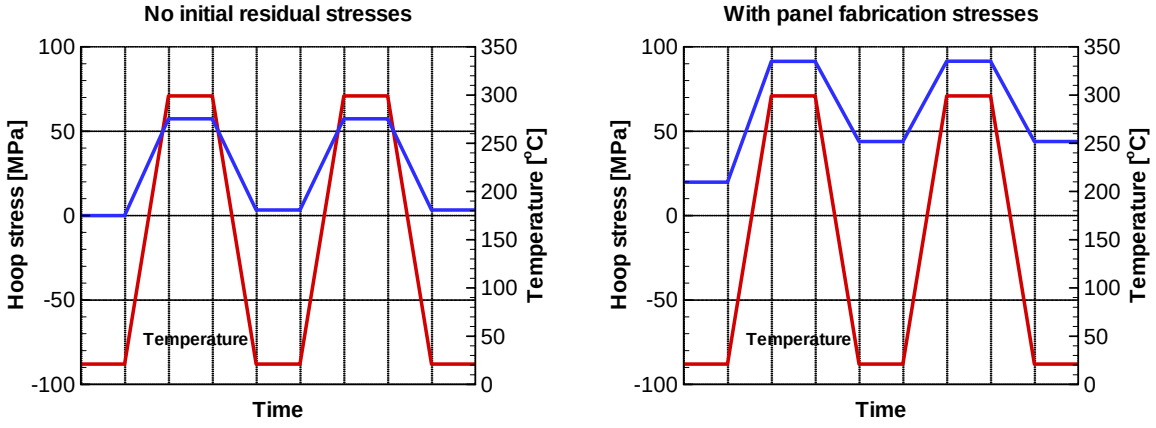

Figure 3.4.3. Variation of hoop stress with temperature for a carbon steel tube with an attachment weld at the waterside surface just under the weld during two normal operating cycles.

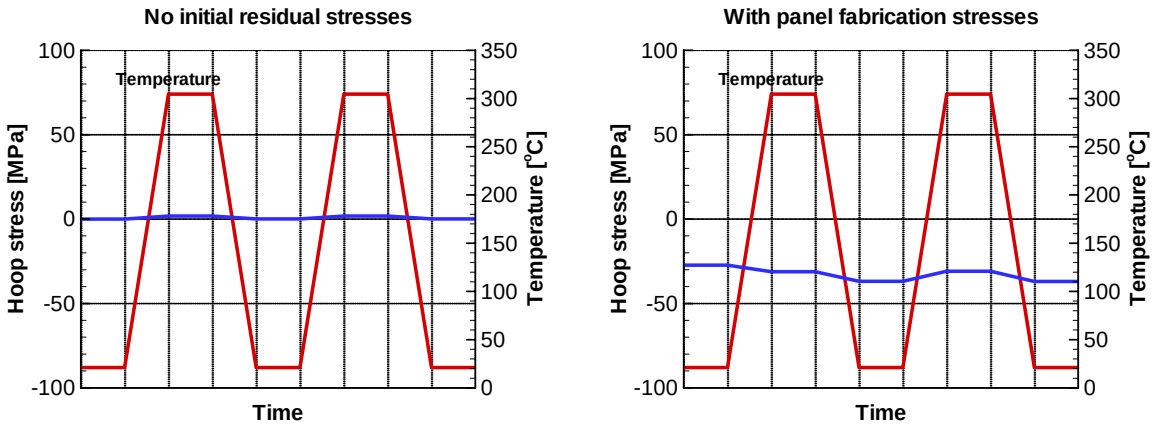

Figure 3.4.4. Variation of hoop stress with temperature for a carbon steel tube with an attachment weld at the waterside surface at some distance away from the weld during two normal operating cycles.

As shown in Figure 3.4.2, for the case with no initial stresses, the hoop stress becomes highly tensile at operating temperature, but returns to zero value upon shutdown. When stresses due to welding of the tube and membrane are included in the model, the hoop stress is slightly tensile initially, and becomes more tensile at operating temperature. Upon shutdown after the first cycle, the hoop stress does not return to the initial value, but instead becomes slightly compressive, indicating that some amount of plastic deformation has taken place. A second cycle causes the hoop stress to again become tensile at operating temperature, but no additional plastic deformation occurs, and the stress returns to the compressive value it had at the end of the first cycle.

Variation of hoop stress at the waterside surface for a tube with an attachment plate weld at a location just under the weld is shown in Figure 3.4.3 for the cases without and with initial panel fabrication stresses. For the case with no initial stresses, the hoop stress becomes tensile upon heating to operating temperature, although the magnitude is smaller than for the tube without the attachment weld. Upon cooling to room temperature at the end of the first operating cycle, the stress is very slightly tensile, indicating a small amount of plastic

deformation. When initial stresses are considered, the hoop stress initially is slightly tensile, and becomes more tensile upon heating the panel to operating temperature. Upon shutdown at the end of the first cycle, the hoop stress remains tensile but the magnitude is higher than the initial value. A second operating cycle causes the hoop stress to become more tensile at operating temperature and return to the value at the end of the first cycle. The two main differences from the earlier case (refer to Figure 3.2.2) for a tube with no attachment weld are, first, the stress after the first operating cycle returns to a compressive value for the earlier case while the stress remains tensile in this case, and second, although the increase in stress is higher, the magnitude of stress at operating temperature is lower for the earlier case.

Figure 3.4.4 shows the hoop stress variation on the waterside surface for a tube with an attachment plate weld, but at a location on the cold side of the tube some distance away from the weld. Independent of initial stress state, the hoop stress does not show significant change during an operating cycle. When stresses from joining of tube and membrane are included, the hoop stress is initially compressive, and remains compressive during the operating cycle.

The hoop stress at the waterside surface of the tube on the cold side of the panel in general becomes more tensile when the panel is subjected to operating conditions. However, there is a difference in the hoop stress after the first operating cycle for carbon steel tubes without and with an attachment plate weld. In the presence of an attachment weld, the hoop stress returns to a tensile value that is higher than the initial value, whereas for a tube without the attachment weld, the stress returns to a compressive value. At some distance away from the attachment weld, the stress in that tube remains compressive throughout the normal operating cycle. The presence of tensile circumferential stress when the tubes are cooled from operating temperature, when combined with poor water chemistry during shutdown, provides the conditions under which SAC can potentially initiate/propagate. Conversely, the presence of compressive hoop stresses in tubes without attachment welds, or remote to the attachment welds, is likely to inhibit SAC.

While the composite tube with a 304L stainless steel clad layer also in general shows tensile stress development upon heating to operating temperature, the hoop stress in this case is initially compressive (as compared to tensile hoop stress for a carbon steel tube) and returns to a compressive stress value (as compared to a tensile stress value for the carbon steel tube just under the attachment weld) after a normal operating cycle. [See Figure 3.4.5 and compare with Figure 3.4.3.] It is worth mentioning that the stress variation in the composite tubes is governed by the thermal expansion mismatch between the stainless and carbon steels, in addition to the thermal and mechanical loading. This difference in the hoop stress variation appears to provide an explanation for the presence of SAC indications in the carbon

steel tubes, and the absence of such indications in the composite tubes. However, this statement must be qualified by noting that the current analyses ignored the initial stresses due to the welding of the attachment plate to the wall panel, and including these stresses could lead to different results.

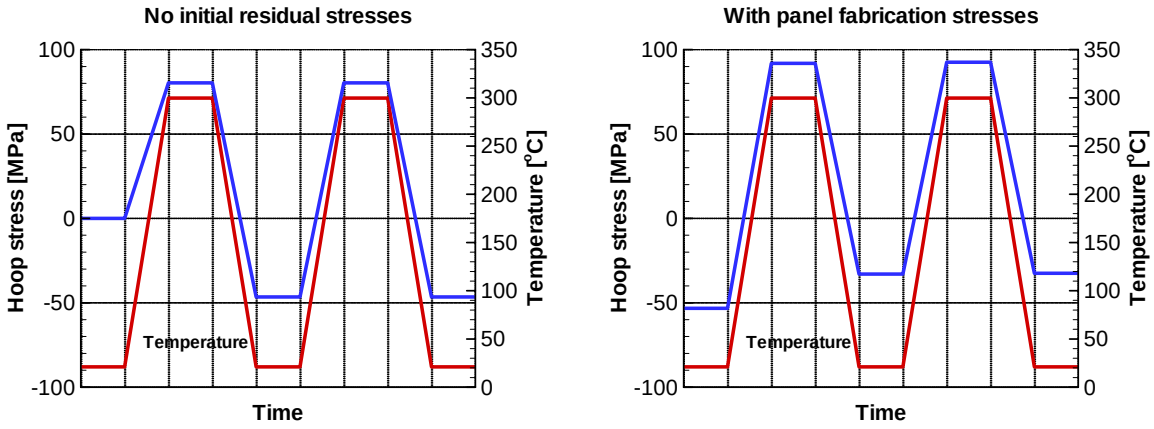

Figure 3.4.5. Variation of hoop stress with temperature for a composite tube with an attachment weld at the waterside surface just under the weld during two normal operating cycles.

During the early stages of the modeling work, only the initial stresses from 2-D welding analysis between the tube and membrane were included, and stresses due to the attachment weld were not considered in the analyses of the tube wall panels. The reason for this is that unlike the weld between the tube and membrane, which is applied along a straight line parallel to the tube axis, the welding of the attachment plate follows a more convoluted path along the circumference of tubes and across the membranes. Therefore, this welding process cannot be easily approximated using a simple 2-D model, and needs to be simulated considering the full 3-D geometry. An attempt was made to model the welding process using the 3-D model for the tube wall panel described above, but the analysis proved to be very time consuming and non-trivial. Therefore, as a first approximation, the effects of the attachment weld on the residual stresses were ignored in the initial analyses. It was found from both these initial simulation results, and also from observations of tube samples, that the effect of the attachment weld appears to be confined to a small section of the tube close to the weld. Based on this information, the 3-D model for the tube wall panel was slightly modified by limiting the length of the model in the axial direction, with greater refinement of the mesh close to the attachment weld. This model was then used to simulate the welding of the

attachment plate, and incorporate the stresses associated with the attachment weld in the analysis.

Results of hoop stress variation at the waterside surface are shown in Figures 3.4.6 to 3.4.8 for panels made of carbon steel and composite tubes at different locations. For the tube without an attachment weld (Figure 3.4.6) and for the tube with the attachment weld at a considerable distance away from the weld (Figure 3.4.7), the results are not very different from the earlier case where the stresses from the attachment weld were neglected. The overall trends are very similar with only some small differences in the magnitude of the stress values. The stress values are compressive during shutdown, and even the tensile stresses at operating temperature are of low magnitude. However, the results for the tube with the attachment weld at a location just under the weld (Figure 3.4.8) show greater differences from the earlier case. Due to the attachment weld, the initial stress in this case is highly tensile. For the carbon steel tube, upon heating to operating temperature, plastic deformation causes the stress to remain at yield, with a lower tensile stress value at the higher temperature. Subsequent cooling to room temperature causes the hoop stress to increase in magnitude. A second operating cycle causes the hoop stress to become less tensile at operating temperature and return to the more tensile value upon shutdown. Unlike the case of the tube with no attachment weld, the hoop stress in the presence of the attachment weld remains highly tensile throughout the operating cycle.

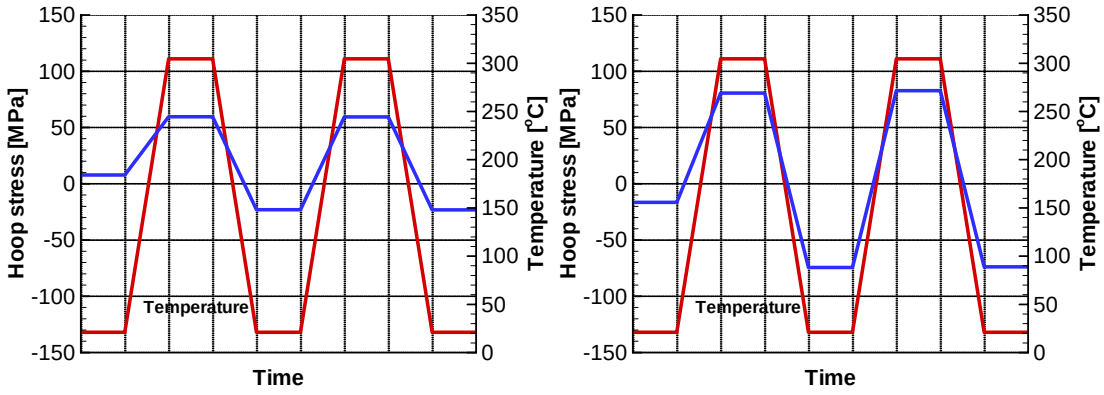

Figure 3.4.6. Variation of hoop stress with temperature for a carbon steel tube (left) and a composite tube (right) without an attachment weld at the waterside surface on the cold side of the wall panel during two normal operating cycles.

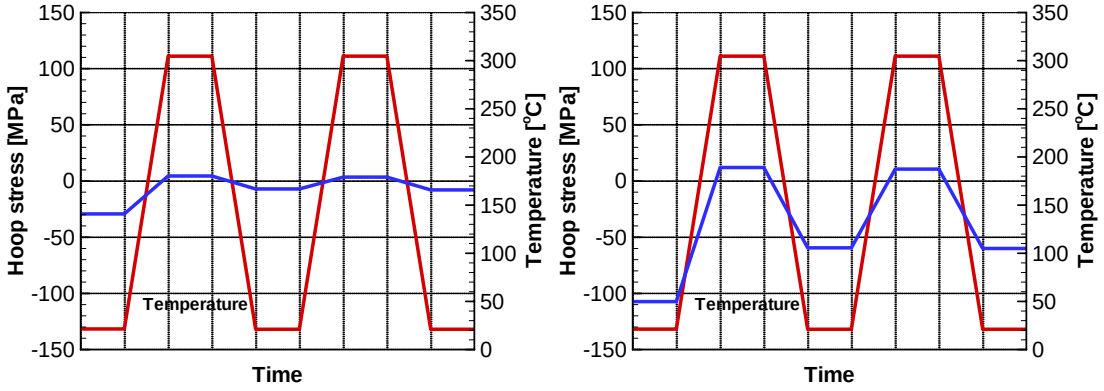

Figure 3.4.7. Variation of hoop stress with temperature for a carbon steel tube (left) and a composite tube (right) with an attachment weld at the waterside surface at considerable distance away from the weld during two normal operating cycles.

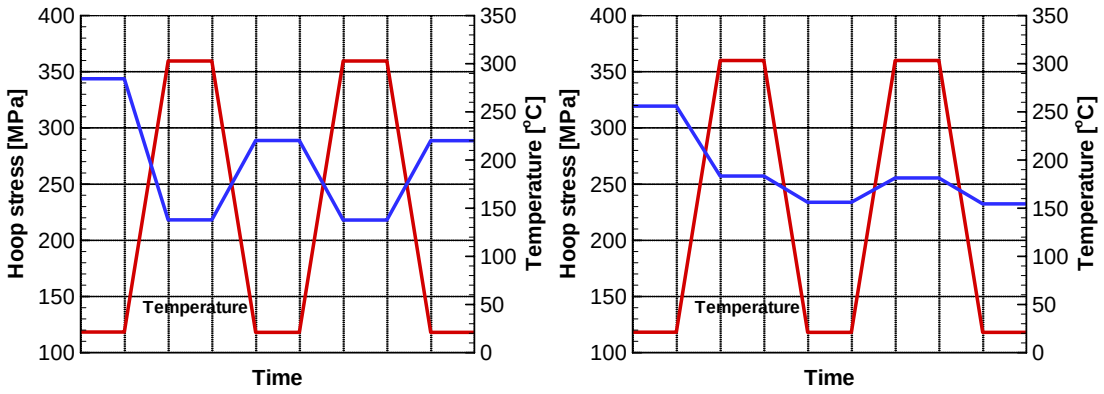

Figure 3.4.8. Variation of hoop stress with temperature for a carbon steel tube (left) and a composite tube (right) with an attachment weld at the waterside surface just under the weld during two normal operating cycles.

For the panel with the composite tube, the hoop stress is initially highly tensile due to the attachment weld. Heating to operating temperature causes the stress to remain tensile, although the magnitude is reduced due to the higher temperature. Cooling to room temperature causes further reduction in the magnitude, although the stress continues to remain tensile. A second operating cycle causes an increase in the stress upon heating, and a decrease in stress upon cooling. This is in contrast to the result for the carbon steel tube (shown in Figure 3.4.8 on the left), where heating to operating temperature causes a lower

stress and cooling to room temperature causes the stress to increase. Although the hoop stress for the composite tube just under the weld remains tensile throughout the operating cycle, the lower magnitude for the stress, especially during shutdown (when the water chemistry can be particularly aggressive towards the steel) might serve to explain the observation that 304L clad composite tubes do not seem to have the same susceptibility to SAC under attachment welds that is typically seen in carbon steel tubes. At the same time, it could also be argued that the composite tubes may not be completely immune from SAC, and the lower stress magnitude might only serve to delay the onset of SAC indications when compared with the carbon steel tubes. The presence of a tensile hoop stress in the composite tubes could be taken as an indicator that the potential for SAC exists, and more work is required to relate the magnitude of stress to the time taken for the initiation of SAC.

Some additional work was also performed to study the effect of changing the parameters used in the model for the application of the attachment weld, but these cases did not result in an appreciable difference in the trends generated by the modeling results. Similarly, modification of the properties of the inner layer of material (e.g., simulation of a thin decarburized zone) also did not influence the results within the present level of sophistication in the model.

3.4.1 Conclusions from Strain Measurements and FEM Simulations

An array of non-destructive techniques, including two ultrasonic wave methods, radiography, and borescope inspection, proved to be generally ineffective for locating SAC on boiler tubes removed from service. In part, this was due to inability to confirm the presence of SAC until destructive evaluation (metallography) had taken place, so specimens bearing SAC were not exposed with equal frequency to all inspection methods. Limitations of each method for field inspection were identified, and the reliable detection of SAC in an operating boiler remains problematic.

Wall penetrations of up to 30% of the wall thickness were found associated with SAC among the boiler tubes examined after removal from service. All SAC penetrations were located immediately adjacent to a scallop-type attachment weld and exhibited a significant accumulation of somewhat porous, mixed oxide filling/covering the SAC penetrations. Invariably, the SAC penetrations were transgranular and essentially straight (non-branching), with bulbous and/or rounded features, and filled with alternating layers (Fe_2O_3 and Fe_3O_4) of oxide, indicating changing corrosion conditions during the propagation of the SAC. A decarburized layer was observed on the ID surface of most of the boiler tubing which was somewhat softer than the bulk material and which may encourage the initiation of SAC due

to its lesser strength compared to the nominal steel.

Data from gages on tubes near/around a substantial scallop-type attachment weld in an operating boiler suggest that shutdown/restart events (4 in almost 13 months of data gathering at this mill) generate by far the most significant strains associated with operation. Proximity and orientation relative to the position of the attachment weld was a significant factor in strain response to operational events. Much more modest process upsets, involving a temperature drop/return of between 10 and 95ºC (41 in almost 13 months) were more numerous but much less threatening in terms of strain change associated with each. Although the failure criteria for the internal oxide on the tubes is not known, it seems likely that it is primarily the shutdown/restart events that lead to initiation and/or propagation of SAC.

The results of the initial modeling simulations showed that the stress distribution in a wall tube is significantly altered by the presence of an attachment weld. Without an attachment weld, or on portions of the wall tube removed from the attachment by more than about 2 cm, residual stresses (thermal/mechanical) tend to remain small and compressive on the tube ID at the end of each operating cycle. However, immediately adjacent to an attachment weld, residual stresses on the tube ID tend to increase and become tensile following an operating cycle. The location of the maximum tensile hoop stress in the model – confined to a distance within about 2 cm of the attachment weld – and the location of longitudinally-oriented SAC on boiler tubing are identical, lending credibility to the model results. The presence of a tensile hoop stress when the tubes are cooled from operating temperature, combined with potential water chemistry upsets during shutdown periods, provides conditions under which SAC can initiate and propagate.

The initial model results for co-extruded composite tubing (carbon steel with a outer layer of 304L stainless steel) suggest a much different stress distribution following an operation cycle. In contrast to the carbon steel tubes, the composite tubing tends to exhibit residual compressive hoop stress (or at least smaller tensile stresses) adjacent to attachment welds following an operation cycle, consistent with field observations that composite tubes do not seem as susceptible to SAC as carbon steel tubes. Attempts to modify the model to examine the effects of attachment weld variables and surface decarburization on stress distributions revealed inconclusive results, suggesting further model development as an area for future work.

3.4.2 References for Material Characterization and Finite Element Modeling

1. Electric Power Research Institute, EPRI-TR-100455, "Corrosion Fatigue Boiler Tube Failures in Waterwalls and Economizers – Volume 4: Summary Report and Guidelines for Corrosion Fatigue Evaluation," prepared by Ontario Hydro, Toronto, Canada, December 1993.
2. Sylvester, W. R., "Waterside Corrosion Fatigue Cracking – Is There a Single Cause and Solution?" ABB C-E Services TIS 8318, Combustion Engineering, Inc, Windsor, CT, 1987.
3. Sylvester, W. R. and Sidla, G., "Waterside Stress-Assisted Corrosion Cracking in Boilers," Pulp and Paper Canada, Vol. 91, No. 6 (1990) p.T248.
4. Schoch, W. and Spahn, H., "On the Role of Stress-Induced Corrosion and Corrosion Fatigue in Water-Wetted Boiler Components," in Corrosion Fatigue: Chemistry, Mechanics, and Microstructure, NACE, Houston, TX (1972) p.52.
5. Dooley, R. B., "A Vision for Reducing Boiler Tube Failures," Power Engineering, Vol. 96 (1992) p. 33.
6. Gabrielli, F., "An Overview of Water-Related Tube Failures in Industrial Boilers," Materials Performance, Vol. 27, No. 1 (1988) p.51.
7. Esmacher, M. J., "Stress-Enhanced Corrosion of Boiler Tubing," Materials Performance, Vol. 26, No. 5 (1987) p. 17.
8. Masterson, H. G., Castle, J. E., and Mann, G. M. W., "Waterside Corrosion of Power Station Boiler Tubes," Chemistry and Industry (1969) p. 1261.
9. Sharp, W. B. A., "An Overview of Stress-Assisted Corrosion in the Pulp and Paper Industry," National Association of Corrosion Engineers 2004 Annual Conference and Exhibition, March 28-April 1, 2004, New Orleans, LA, *Corrosion2004* Paper 04513.
10. Pawel, S. J., Willoughby, A. W., Longmire, H. F., and Singh, P. M., "An Experience with Detection and Assessment of SAC in a Recovery Boiler," National Association of Corrosion Engineers 2004 Annual Conference and Exhibition, March 28-April 1, 2004, New Orleans, LA, *Corrosion2004* Paper 04517.
11. Hancock, P. "Mechanical Considerations of the Growth and Breakdown of Surface Metal Oxide Films," Werk. und Korros., Vol. 21 (1970) p. 1002.
12. Hurst, R. C., Davies, M., and Hancock, P., "The Determination of the Fracture Strains of Growing Surface Oxides on Mild Steels at High Temperatures," Oxidation of Metals, Vol. 9, No. 2 (1975) p. 161.
13. Field, E. M., Stanley, R. C., Adams, A. M., and Holmes, D. R., "The Growth, Structure, and Breakdown of Magnetite Films on Mild Steel," Proc. 2nd Int. Cong. Metall. Corrosion, London, Butterworks (1963) p. 829.
14. Fujii, C. T. and Meussner, R. A., "The Mechanism of High Temperature Oxidation of Iron-Chromium Alloys in Water Vapor," J. Electrochem. Soc., Vol. 111 (1964) p. 1215.

15. Potter, E. C. and Mann, G. M. W., "Oxidation of Mild Steel in High Temperature Aqueous Systems," Proc. 1st Int. Cong. Metall. Corrosion, London, Butterworks (1961) p. 417.
16. Potter, E. C. and Mann, G. M. W., "Mechanism of Magnetite Growth on Low Carbon Steel in Steam and Aqueous Solutions up to 550°C," Proc. 2nd Int. Cong. Metall. Corrosion, London, Butterworks (1963) p. 872.
17. Eberle, F. and Anderson, C. H., "Scaling Behavior of Superheater Tube Alloys in ASME High Temperature Steam Research Tests at 1100-1500°F," Journal of Engineering for Power, Vol. 84, No. 3 (1982) p. 223.
18. Bonner, E. H., "Water Treatment for the Prevention of Water Side Corrosion in Boiler Plant," Power Works Engineering, Vol. 19, No. 1 (1979) p. 10.
19. Goldstein, P., "A Research Study on Internal Corrosion of High Pressure Boilers," Trans ASME, Vol. 91A (1969) p. 75.
20. Marsh, T. F., "The Morphology of Magnetite Growth on Mild Steel in Alkaline Solutions at 316°C," J. Electrochem. Soc., Vol. 113, No. 4 (1966) p. 313.
21. ABAQUS/Standard User's Manual, Version 6.2, Hibbitt, Karlsson & Sorensen, Inc., 2001.
22. Sarma, G. B., Pawel, S. J., and Singh, P. M., "Modeling of Recovery Boiler Tube Wall Panels to Investigate the Effect of Attachment Welds on Stress-Assisted Corrosion," Paper 53-4, Proceedings, 2005 TAPPI Engineering, Pulping, and Environmental Conference, August 28-31, 2005, Philadelphia, PA.
23. Sarma, G. B., Pawel, S. J., and Singh, P. M., "Modeling the Effect of Attachment Welds on Stress-Assisted Corrosion in Recovery Boiler Tubes," *Corrosion2006* Paper 06240 at the National Association of Corrosion Engineers 2006 Annual Conference and Exhibition, March 12-16, 2006, San Diego, CA.

3.5 EVALUATION OF ENVIRONMENTAL EFFECTS

3.5.1 Critical Parameters in Boiler Water Chemistry Affecting SAC

Failure of carbon steel boiler tubes from waterside have been reported in the utility boilers and industrial boilers for a long time [1, 2]. Main aim for this task was to evaluate the role of water chemistry, stresses, and temperature on crack initiation and growth. In the utility industry, waterside tube cracking, generally referred to as corrosion fatigue, has been recognized as a major cause for boiler downtime [1, 3]. Significant volume of work has been published to understand corrosion fatigue in carbon steel tubes [4-7].

Use of carbon steel for the service of high temperature water applications strongly depends upon the formation and stability of the protective magnetite film, Fe_3O_4, on the waterside surface of boiler tubes [8]. Chemical or mechanical disruption of the magnetite film may lead to the initiation of local corrosion or cracks. Rupture of the protective film by fatigue-generated strains may also depend upon the film composition and properties along with the magnitude of strain. Protective magnetite film on the tube surface is typically thin and compact, whereas the film associated with SAC, under attachment welds, is porous and non-protective [8].

Previous work on utility boiler environments has shown that the oxygen concentration has a significant effect on sharp corrosion fatigue cracks in carbon steels [2, 6-7, 14-15]. However, the effect of oxygen on SAC mechanism in industrial boilers, with lower temperature and pressure, is not very clear. For carbon steel boiler tubes, Dooley [2] reported that the corrosion fatigue is strongly influenced by water chemistry where the oxygen concentration is the major factor. Results from phosphate water-chemistry tests indicate a two-orders-of-magnitude increase in dissolved oxygen from 10 to 1000 $\mu g \cdot kg^{-1}$ may decrease the number of thermal cycles required to initiate corrosion fatigue cracks by one-order-of-magnitude (from 1000 to about 100)[2]. This type of increase is associated with the boiler startup, when oxygen may enter the water and the thermal strains are also the greatest. This study also shows that the stress range needed for initiation of corrosion fatigue depends upon the water chemistry variables, as the water chemistry deviates from the optimum values, the stress required to initiate corrosion fatigue decreases. This may explain the large variation on corrosion fatigue occurrence from one boiler to another or form one area in a boiler to another due to possibilities of variation in water chemistry as well as stress due to attachment welds or other sources [2].

A number of investigators have studied the mechanism of magnetite film growth on iron/carbon steel surface and resulting morphology [16-20]. Some investigators used strong

alkaline solutions to develop thicker oxides, but have reported that the morphology of the magnetite developed under these conditions was similar to the magnetite film formed on boiler tube surfaces under normal operating conditions. There is some discrepancy among the results from magnetite growth experiments reported [20], magnetite film grown under very similar conditions was reported to be either a thick and relatively porous [17-18] or it was reported to be thin, compact and protective [16].

Overall tube failure due to corrosion fatigue or stress assisted corrosion can be separated into two distinct stages; crack initiation and crack propagation. These stages may further depend upon the environmental factors like temperature and water chemistry as well as on the stress state of boiler tubes. Understanding of initiation and propagation stages is essential to predict the overall life of tubes under a given set of conditions. Relatively smaller amount of work has been dedicated to the understanding of corrosion fatigue crack initiation processes compared to the crack propagation processes [21].

The present project is aimed at developing an understanding of SAC mechanism in industrial boilers with special emphasis on the recovery boilers in the pulp and paper industry. This study is also aimed to examine if the sharp corrosion fatigue cracks in utility boilers are mechanistically related to the blunt bulbous SAC cracks in industrial boilers. A recirculation-loop autoclave facility was developed to simulate industrial boiler environments [13]. Slow strain rate rig with recirculation autoclave was used to investigate the mechanism of film growth and the effects of water chemistry and stress parameters on the overall SAC initiation.

Main variables that were controlled or tested in this work include temperature, stress, and dissolved oxygen. Next sections describe results from this work which have helped us understand SAC phenomenon and mechanisms for bulbous crack morphology.

3.5.2 Test Methods

The material used in this study was a carbon steel SA-210, typically used for industrial boiler tubes, with a composition of 0.21%C, 0.78%Mn, 0.017%S, 0.011%P, 0.22%Si, 0.03%Ni, 0.09%Cr, 0.01%Mo, and bal. Fe. Smooth tensile samples with 0.125” diameter and 0.5” gage length were machined out of SA-210 carbon steel tubes. The samples were machined with the tensile axis oriented along the pipe length. Slow strain rate tests (SSRT) were carried out in an autoclave with recirculation loop. Tensile samples were polished to a 2000-grit finish and cleaned with acetone before testing. Water chemistry parameters (i.e., dissolved oxygen, temperature, pH and conductivity, etc.) were individually monitored and controlled [13]. Initial strain rate of 2×10^{-6} s^{-1} was used for all tests in this study. Test temperatures ranged

from 110°C to 320°C. Dissolved oxygen in the pure water was controlled between 10ppb to 10ppm in different tests by, individual or combined use of, passing N_2 through the solution or additions of different amounts of Na_2SO_3. After each test, one half of the failed tensile sample was mounted and polished to quantify crack velocity, crack density, fracture strain, and percentage area reduction.

Fatigue tests were carried on 516 G70 carbon steel using compact tension (CT) specimens. CT samples were machined out of 0.5-inch-thick plates. 516 G70 plate material was used instead on SA-210 tubes as both materials have similar nominal composition, as shown in table 3.5.1. The CT specimens were polished to a 2000-grit finish and cleaned with acetone before testing. The fatigue crack growth tests were conducted on a servo-hydraulic closed-loop testing machine under sinusoidal cycles using displacement control at a frequency of 20 Hz and R-ratio of 0.3. The fatigue crack growth tests were performed only in lab air at room temperature (22 °C). Some CT specimens were given different heat treatments under inert atmosphere to vary their grain size and see its effect on the threshold stress intensity for crack growth for carbon steels. Crack growth was monitored using a long distance traveling microscope unit attached to the test rig. The precision of the traveling microscope units was 0.01 mm. Pre-cracked CT specimens were subjected to fatigue conditions to measure crack growth rate. Stress intensity values (K_1) were calculated from the load values and crack length at a given time. In this study, the various ASTM standards (E3, E7, E8, E112, E399, E647, E1820, E1823) were followed in processes of specimen preparation, experimental measurement, and subsequent analysis.

Nominal composition of steels tested in this study are listed in Table 3.5.1. Although there was some decrease but the data indicates that UTS and yield strength of this carbon steel did not change significantly from room temperature to 300°C.

Table 3.5.1 Nominal composition of carbon steels used in this study (in wt %)

	C	Mn	S	P	Si	Ni	Cr	Mo
SA210	0.27 max	0.93 max	0.058 max	0.048 max	0.10 min	0.03	0.09	0.01
516G70	0.27 max	0.79-1.3	0.04 max	0.035 max	0.13-0.45	0.01	0.02	0.03

A series of coupon exposure tests were also conducted to study the growth and morphology of the magnetite film on carbon steel surface under different conditions. Test coupons with dimension 0.5” x 1.0” x 0.1” were machined out of SA-210 tubes. Samples were polished to

2000-grit finish and cleaned with acetone before exposing them in the autoclave. Water chemistry was controlled for each test, as described earlier. In each test, the anode to cathode area ratio for the test coupon, exposed to the boiler water, was changed by either putting a coupon into an isolated ceramic holder or by electrically connecting the coupon to the surface of a large carbon steel fixture with stable magnetite film. After each exposure, the surface film was characterized using x-ray diffraction, atomic force microscopy (AFM) and scanning electron microscopy (SEM) techniques.

3.5.3 Effect of Temperature and Dissolved Oxygen

Slow strain rate tests were carried out in pure water, with or without water treatment to control oxygen. Typical stress strain curves from these tests are shown in Figure 3.5.1. Tests carried out without removal of oxygen (~2ppm of dissolved oxygen) showed environmentally induced cracks (EIC) whereas; tensile samples tested in water with dissolved oxygen controlled around 5ppb did not show any sign of EIC and had ductile failure, as is shown in Figure 3.5.2. However, in the presence of dissolved oxygen in the water, crack velocity as well as crack density on smooth tensile samples increased with an increase in the test temperature, as shown by results in Figure 3.5.3. As expected, material shows a decrease in ductility with an increase in cracking susceptibility. When the water was treated to control the dissolved oxygen in water, the percentage reduction in area for carbon steel did not change significantly with an increase in test temperatures from 250^{o}C to 320^{o}C, as is shown in Figure 3.5.4a. Under these conditions no signs of stress corrosion cracks were shown. However, carbon steel samples showed stress corrosion cracking in the presence of dissolved oxygen, and both % area reduction and fracture strain decreased when the test temperature was increased in the range of 110^{o}C to 320^{o}C. This decrease in ductility is an indirect indication of an increase in stress corrosion cracking susceptibility. A series of tests were carried out at 300^{o}C & 320^{o}C, where the oxygen level was controlled by use of nitrogen and chemical treatment to see the effect of dissolved oxygen on cracking susceptibility in pure water at high temperatures. Percentage reduction in area & fracture strain for the carbon steel decreased with an increase in the dissolved oxygen under boiler conditions, as shown in Figure 3.5.4b.

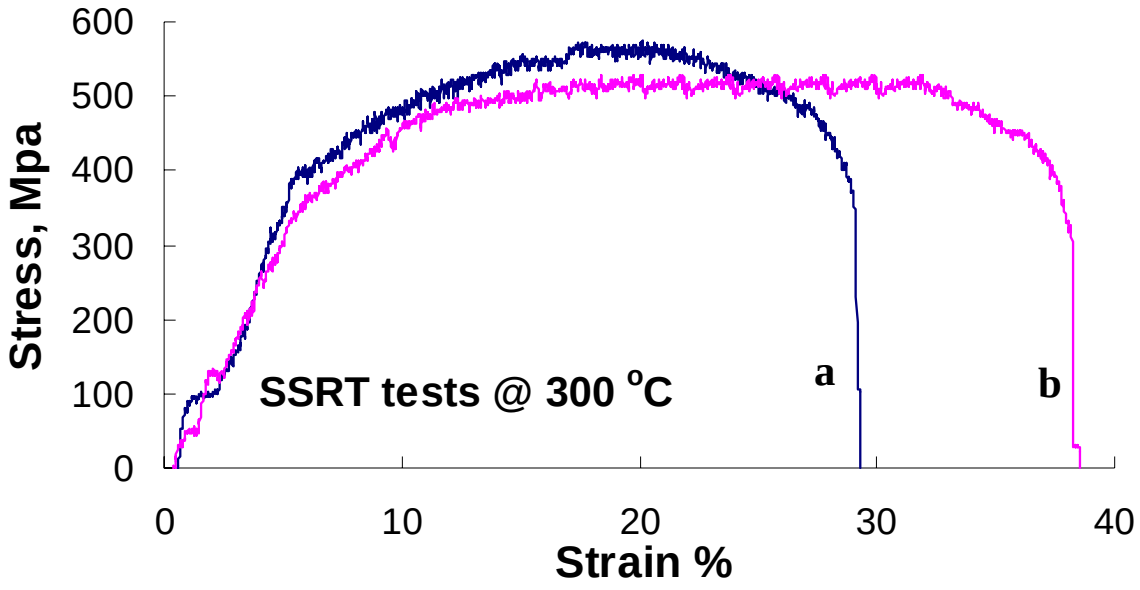

Figure 3.5.1 Stress strain curve for SA210 carbon steel samples tested at 300oC in water with (a) ~2ppm and (b) ~5ppb dissolved oxygen.

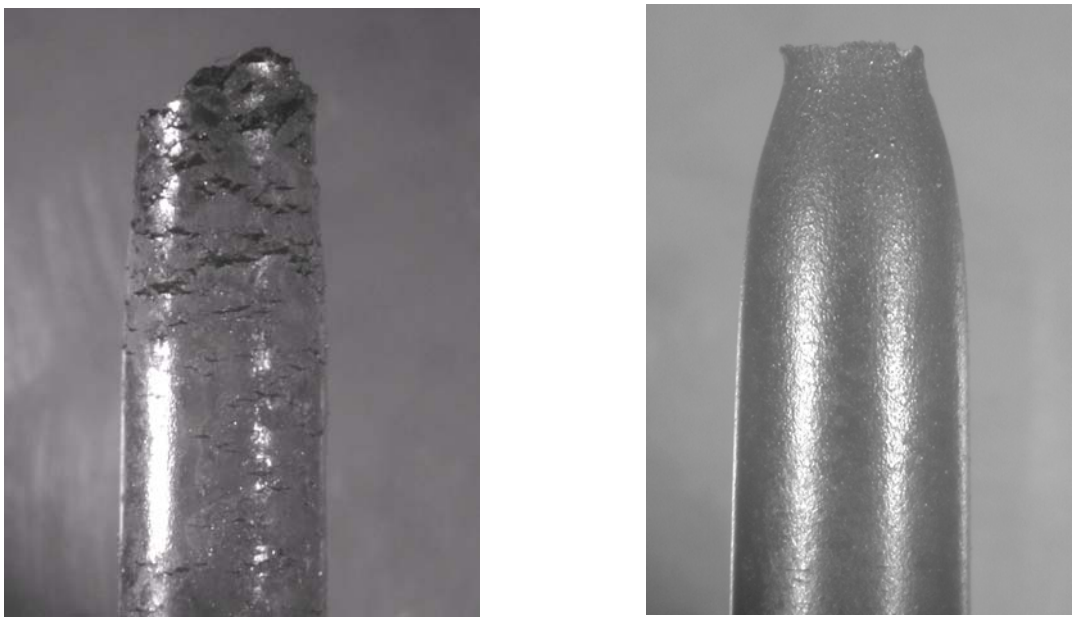

(a) (b)

Figure 3.5.2 SA210 carbon steel samples tested at 300oC in water with (a) ~2ppm and (b) ~5ppb dissolved oxygen.

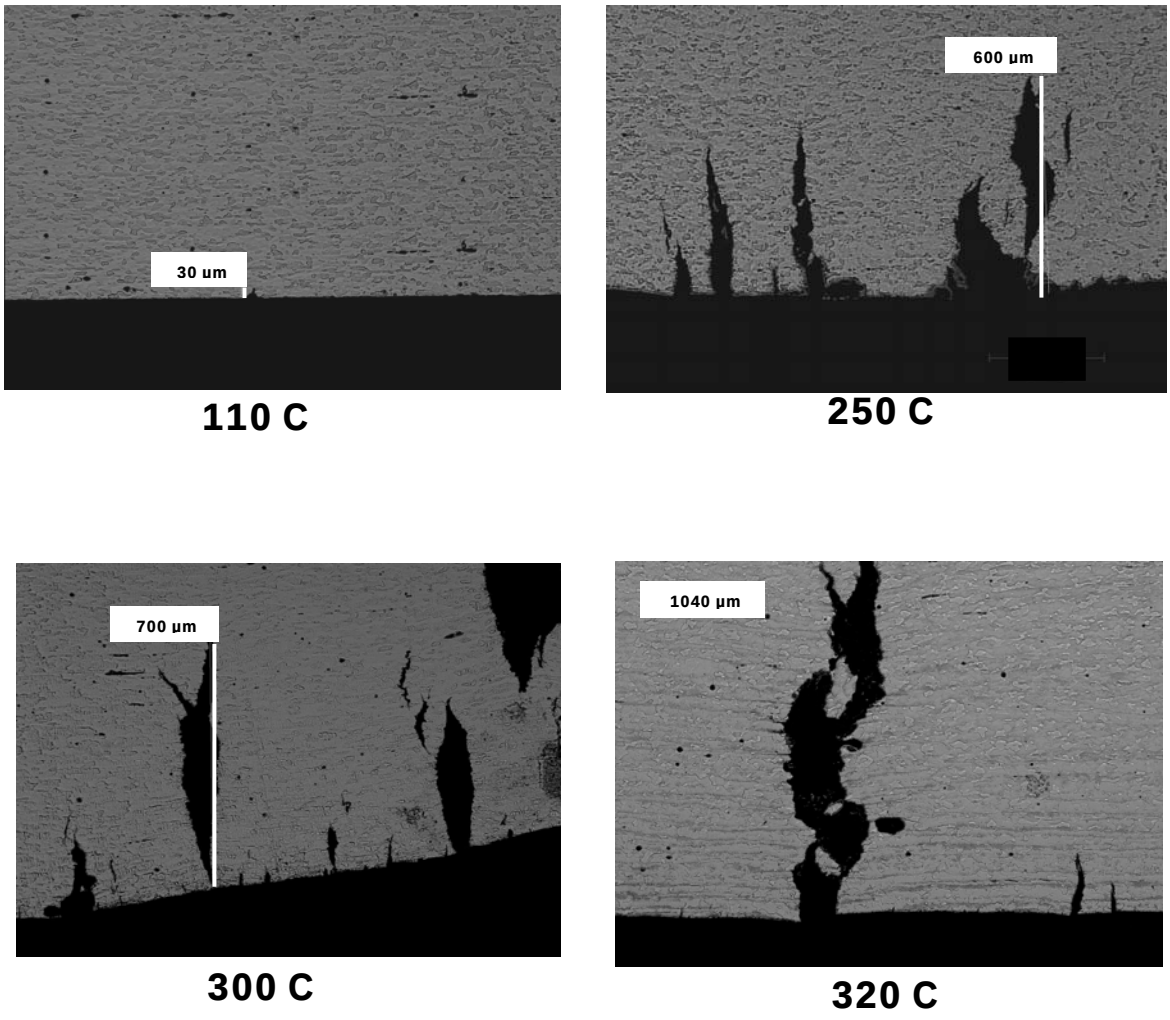

Figure 3.5.3 Effect of Test temperature on crack length for SA210 carbon steel samples tested by SSRT method in boiler water with ~2ppm dissolved oxygen.

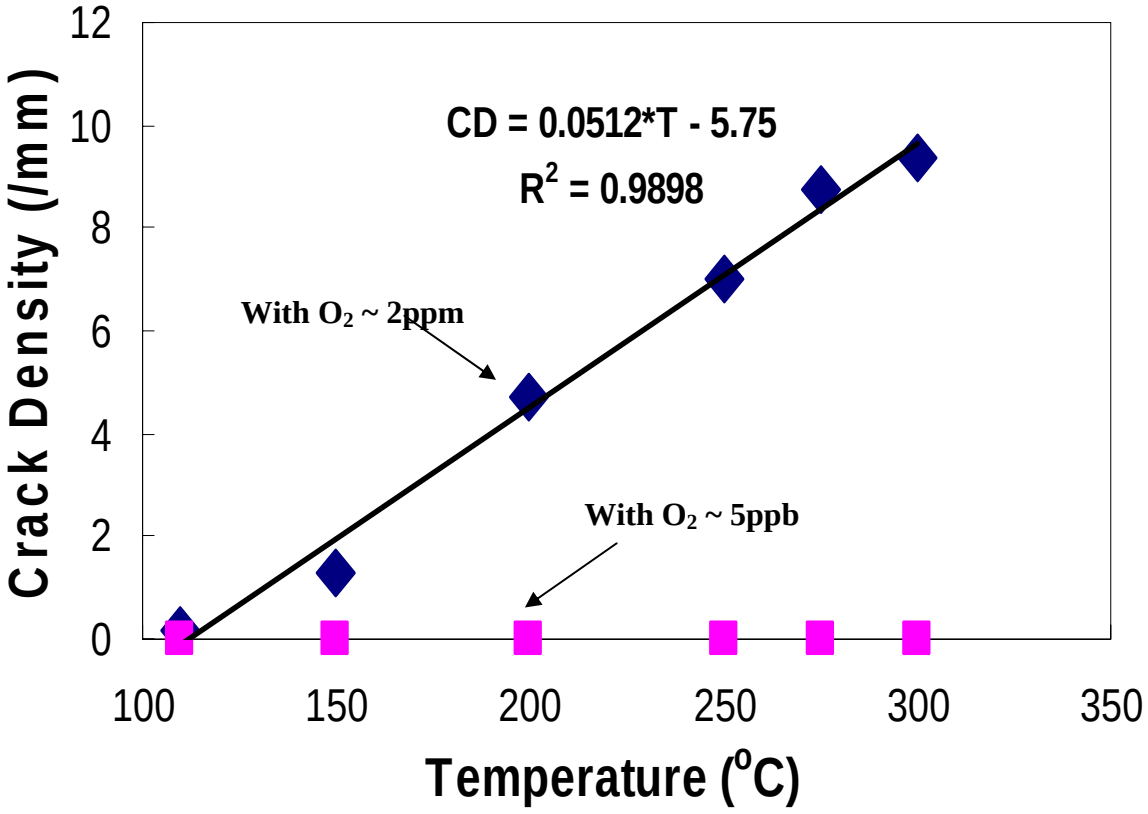

Figure 3.5.4. Effect of test temperature on crack velocity for SA-210 carbon steel samples tested in pure water without oxygen removal treatment

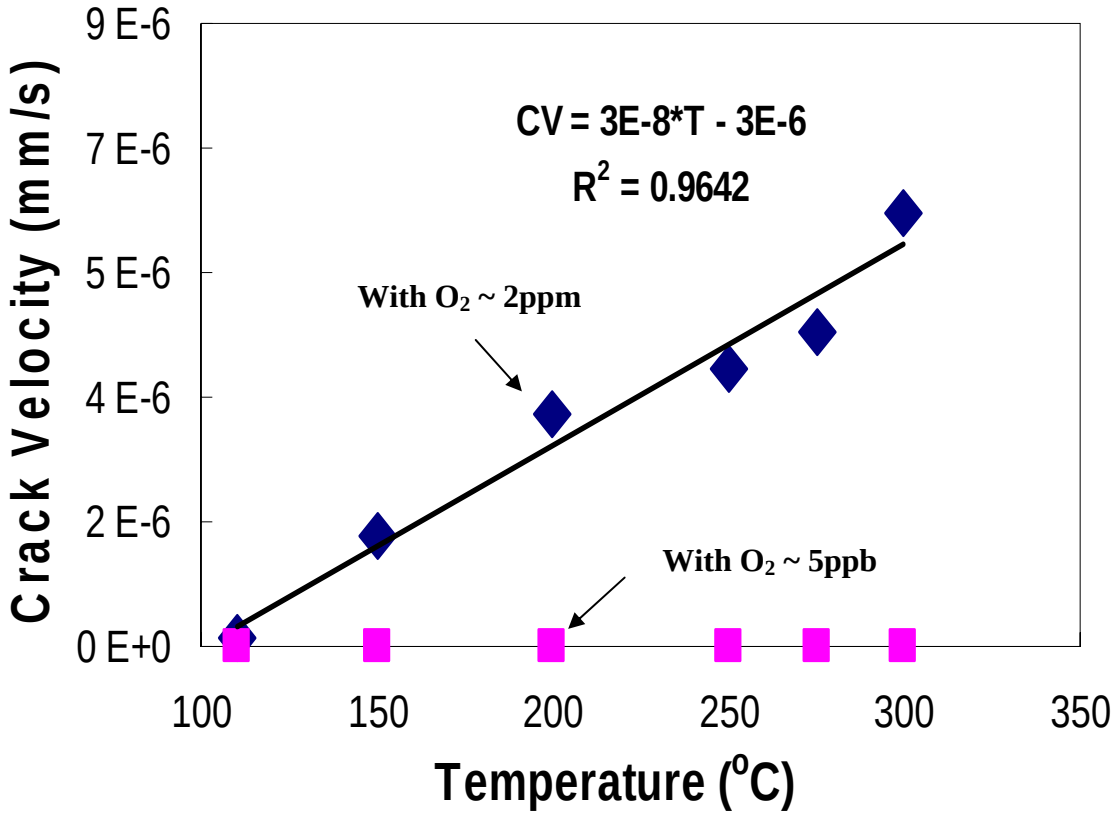

Figure 3.5.5. Effect of test temperature on crack density for SA-210 carbon steel samples tested in pure water without oxygen removal treatment

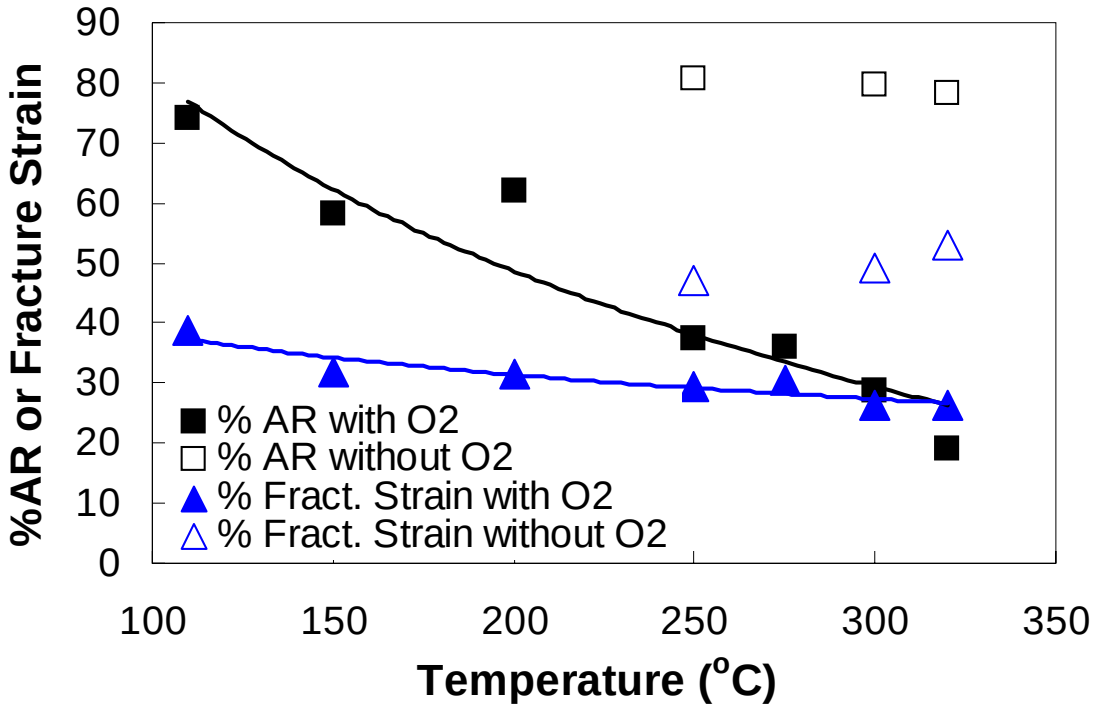

Figure 3.5.6. Effect of test temperature on the ductility of SA-210 samples tested by slow strain rate of $2x10^{-6}$ s^{-1} in pure water.

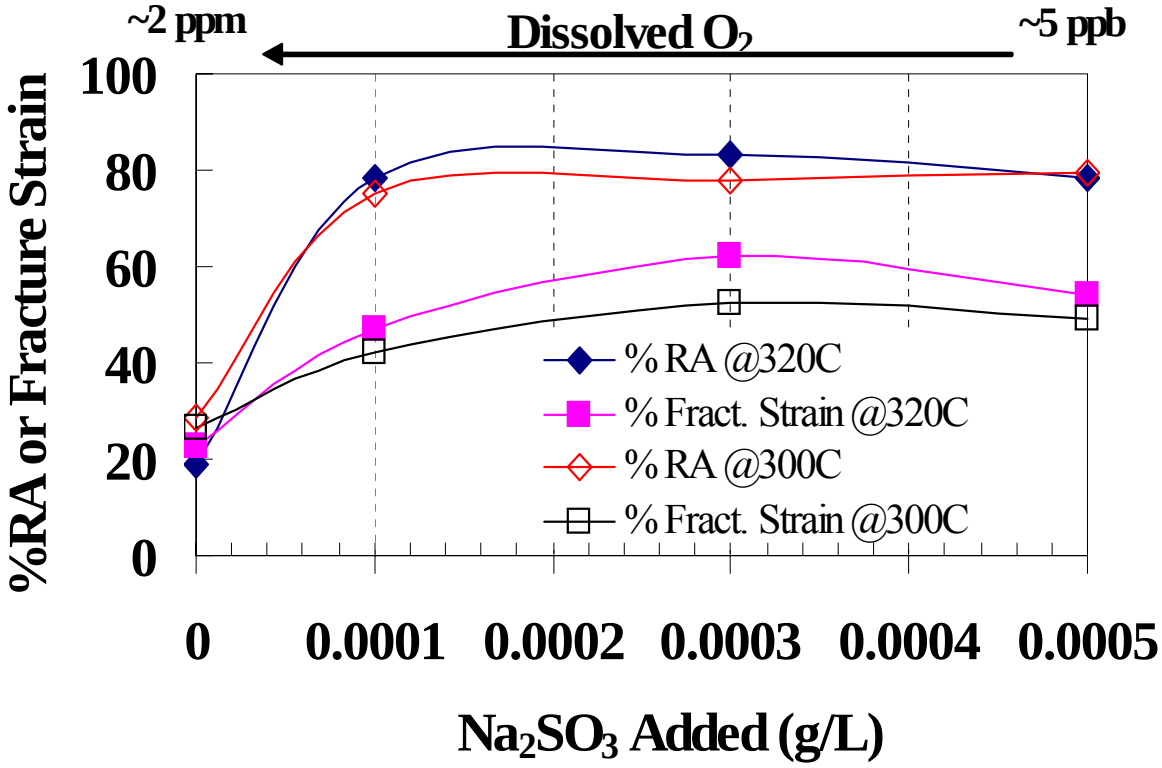

Figure 3.5.7. Effect of dissolved oxygen on the ductility of SA-210 samples tested by slow strain rate of $2x10^{-6}$ s^{-1} in pure water.

3.5.4 Effect of Stress State

Overall tube failure due to corrosion fatigue or stress assisted corrosion can be separated into two distinct stages; crack initiation and crack propagation. Understanding of initiation and propagation mechanisms of crack is essential to predict the overall life of tubes under a given set of conditions. Relatively smaller amount of work has been dedicated to the understanding of corrosion fatigue crack initiation processes compared to the crack propagation processes. Present study was aimed at developing an understanding of initiation and propagation of the bulbous SAC cracking mechanism in industrial boilers with special emphasis on the recovery boilers in the pulp and paper industry.

3.5.4.1 Effects of Cyclic Loading on SAC Cracking

To see the effect of low amplitude frequent fluctuating stresses on waterside cracking of carbon steel, slow strain rate tests with fluctuating stresses were carried out. There were two main questions we had in mind while designing these tests; first if the cracks will develop in water with 5ppb oxygen in presence of fluctuating stresses; second if the crack density and overall crack velocity will change with fluctuating stresses in water with 2ppm oxygen. SSRT test with cyclic loading (Frequency = 0.001 Hz, Amplitude = 80 Mpa, R = 0.85) were conducted in lab at 300^{o}C to compare with a monotonous SSRT test without cycling load superposed. The results from these tests are given in Table III. Both crack velocity as well as crack density on carbon steel samples under cyclic loading were found to be higher than for the ones tested under monotonous SSRT loading in oxygenated boiler water. Total test time or the time for the specimen to fracture was reduced due to the cyclic loading effects even the oxygen concentration in boiler water was reduced by chemistry treatment. These results indicate that even small amplitude fluctuating stresses can affect both crack initiation and propagation mechanisms at 300^{o}C in oxygenated water and thereby can reduce the time to failure.

Other cyclic loading that boiler tubes experience are related to boiler shutdown and startup. Although exact frequency may vary but the high amplitude cycles have very low frequency in boiler tubes. To see their effect of low frequency cycling on crack density and crack growth rate, two SSRT tests with cyclic loading (Frequency = 0.00004 Hz, Amplitude = 300 Mpa, R = 0.4) were conducted to check the effects of mean loading on SAC cracks. Test samples were loaded to the maximum stress values using normal slow strain rate (2 x 10^{-6} S^{-1}) and then the cycling was started. Tests were stopped after 67 hours and were examined for crack density and length. These tests were done with two different values of mean stress as shown in figure 3.5.5.d. Results from tests are also shown in table III. When the mean value of the cyclic loading increased from 280 Mpa to 380 Mpa, the crack velocity did not change

much but the number of cracks found in sectioned specimen had doubled, as shown in Figure 3.5.4.a and Figure 3.5.4.b.

Corrosion fatigue cracks were found to initiate on smooth carbon steel tensile samples under high amplitude, low frequency loading with mean stress of 280 Mpa. This indicates that the environment induced cracking can initiate below the yield strength (328 Mpa) of SA-210 under tested temperatures. This also indicates that such high amplitude cyclic loading, like during boiler shutdown and startup, can be detrimental to the boiler if water chemistry is favorable for cracking (with higher oxygen levels). However, at higher mean stress of 550 MPa and frequency, even with low amplitude, the crack density and growth rate was much higher than for the tests with low mean stress.

Low and high frequency corrosion fatigue tests showed that the crack density and crack growth rate is affected by the cyclic loading. These results also suggest that the strain rates may also have an impact on stress corrosion cracking of carbon steel in pure water system. A series of SSRT tests with three different strain rates (strain rate = 2×10^{-7} s^{-1}, 2×10^{-6} s^{-1} , 2×10^{-6} s^{-1}) were conducted in pure water at 300^{o}C. As is shown by the results in Figure 3.5.5.(a-c), no cracks were found on tensile samples under different constant strain rate loading when the oxygen concentration was controlled around 5 ppb level. However, in the presence of 2 ppm dissolved oxygen in the water, stress corrosion cracks appear on the surface of tensile samples. Crack density decreases as the strain rate goes up. With strain rate of 2×10^{-7} s^{-1}, crack density was about 16 cracks/mm compared to the roughly 1 crack /mm at strain rate of $6x10^{-6}$ s^{-1}. One important reason for this may be that exposure time increases with low strain rates. However, the trend is not the same for crack velocity. Crack velocity was found to be maximum at the $2x10^{-6}$ s^{-1}compared to the lower and higher strain rates tested. This may be due to competing mechanisms involved in overall stress corrosion cracking where the magnetite film breaking and passivation rates may dominate at high and low strain rates respectively. Whereas the two mechanisms seem to have optimum effect at a strain rate of $2x10^{-6}$ s^{-1} . When strain rate have high value (6×10^{-6} s^{-1}), there is less enough time for the passive film to form on the surface and the failure may be more due to mechanical effects than environmental effects. This may explain why the crack velocity & density are low on carbon steel samples tested at high strain rate of 6×10^{-6} s^{-1}, as shown in Figure 3.5.9 and Figure 3.5.10. Results in Figure 3.5.11, show percentage area reduction and fracture strain of the tested tensile samples increase with an increase of the strain rate, which also indicates a more ductile fracture for carbon steel at higher strain rate in 300 ^{o}C boiler water. Although more work is needed to understand the exact mechanism but limited results indicate that SAC crack initiation initiates due the local fracture on magnetite surface film as the first step.

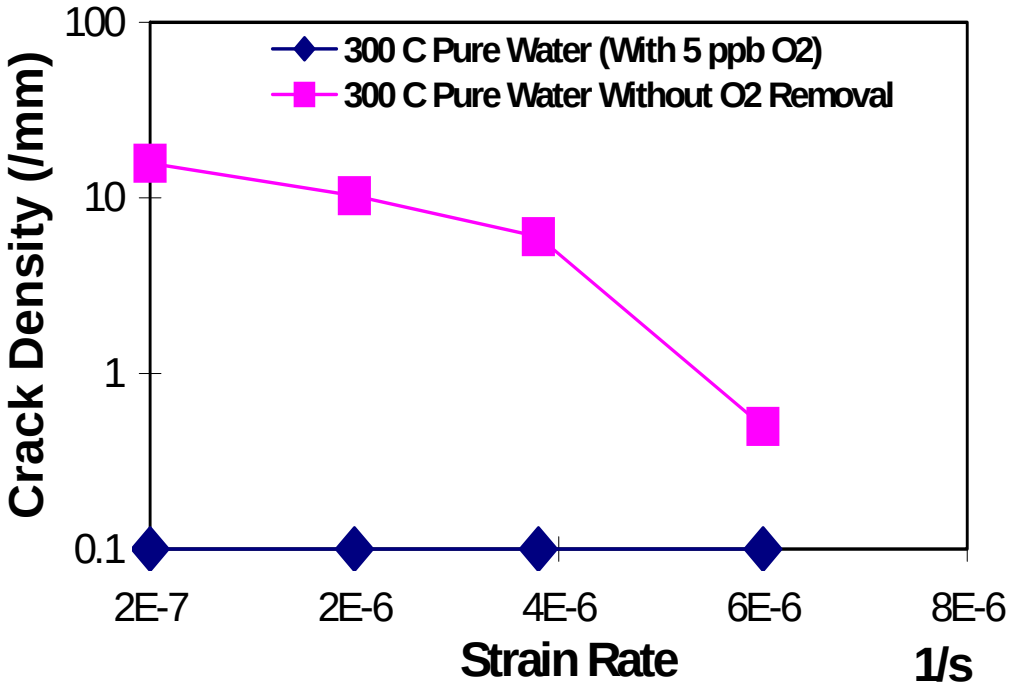

Figure 3.5.8 Effect of strain rate on crack density for SA-210 samples tested by SSRT at 300°C in boiler water.

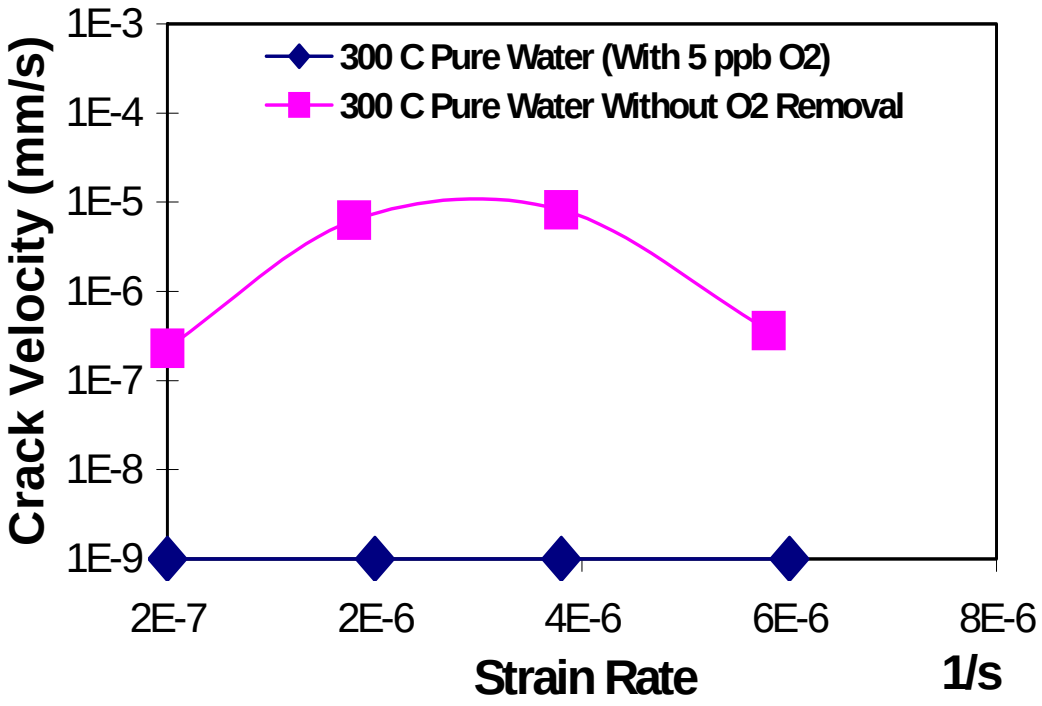

Figure 3.5.9 Effect of strain rate on crack velocity for SA-210 samples tested by SSRT at 300^{o}C in boiler water.

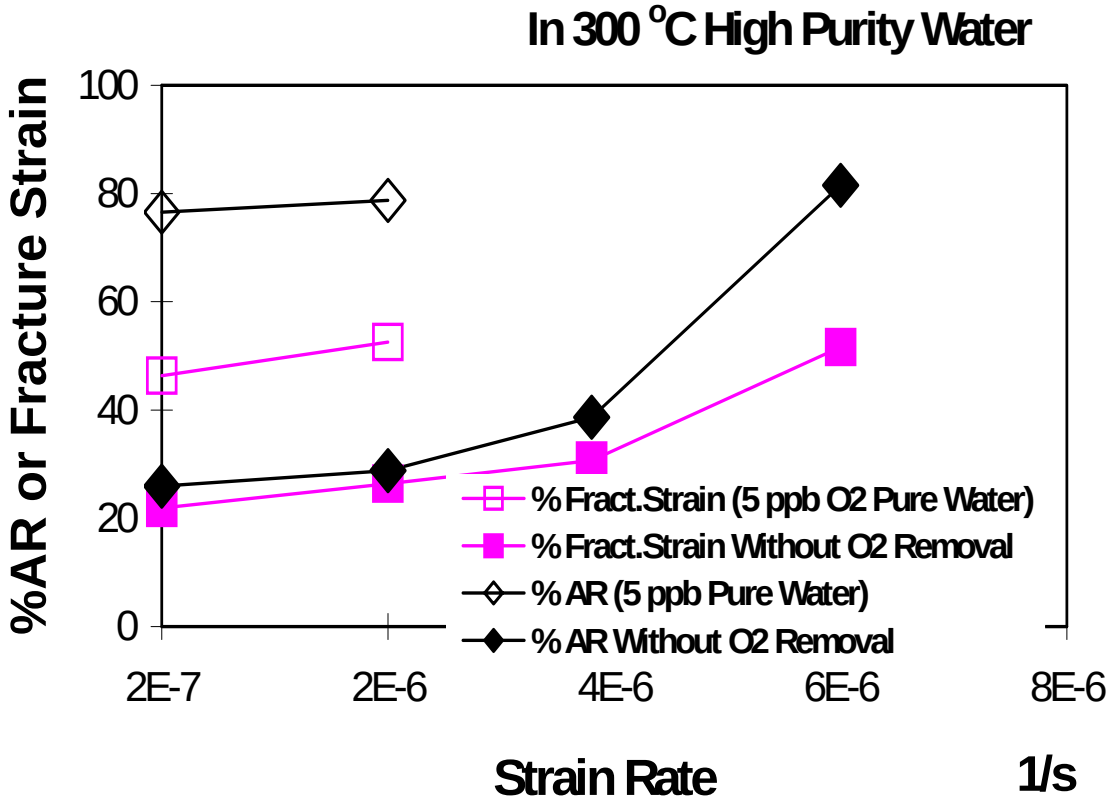

Figure 3.5.10. (a) Effect of strain rate on Fracture strain and % reduction in area (%AR) for SA-210 samples tested by SSRT at 300°C in boiler water.

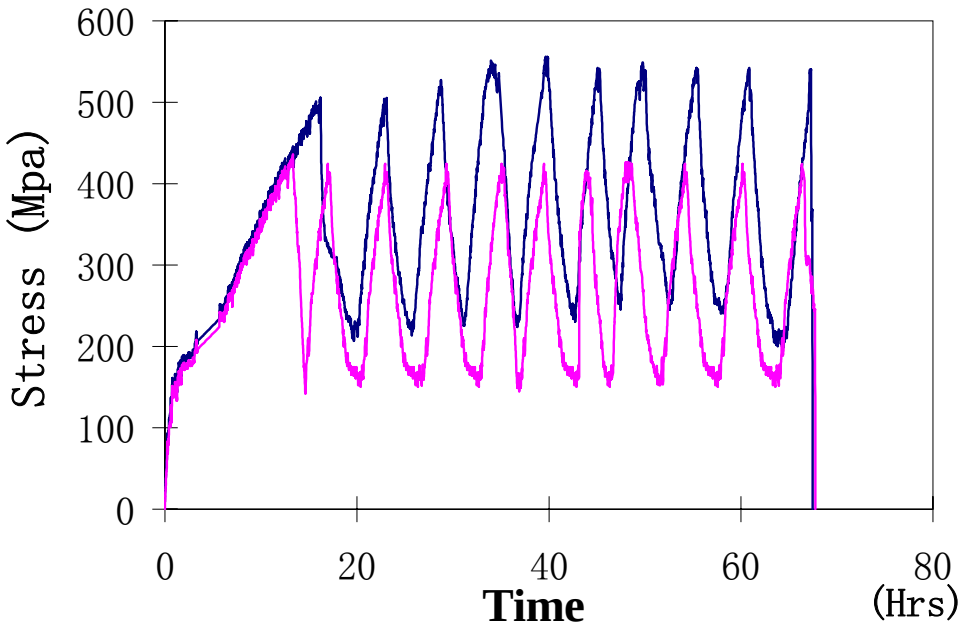

(a)

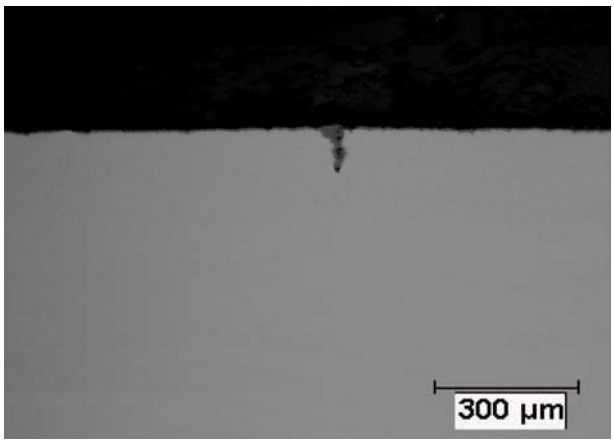

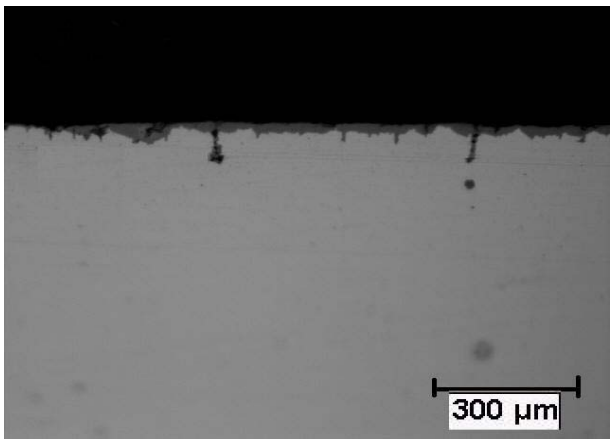

(ib) **(iib)**

Figure 3.5.11**.** (a) stress vs time curves for cyclic loading tests done at different mean stress values (b) Oxide filled SAC cracks on carbon steel samples tested in pure water, with about 2ppm dissolved oxygen at 300^{o}C, under cyclic loading with (ib) mean stress value 280 Mpa (iib) with mean stress value 380 Mpa. Notice that sample tested at higher mean value had higher crack density.

Table 3.5.2 Effect of Cyclic Loading Parameters on SAC Susceptibility of SA210-Carbon Steel in boiler water with ~2ppm dissolved oxygen.

Environment Description (Temp, O2 Level, etc)	Mean Stress (Mpa)	Amplitude (Mpa)	Frequency (HZ)	R-ratio	Crack density (/mm)	Crack velocity (mm/s)	Time to fracture (hrs)
300 oC Untreated Pure Water	UTS	Mono-SSRT	-	-	9.35	$6.24E^{-7}$	45.9
300 oC Untreated Pure Water	280	300	0.00004	0.4	1.36	$1.01E^{-7}$	Stopped at 67 hrs
300 oC Untreated Pure Water	380	300	0.00004	0.4	2.67	$0.95E^{-7}$	Stopped at 67 hrs

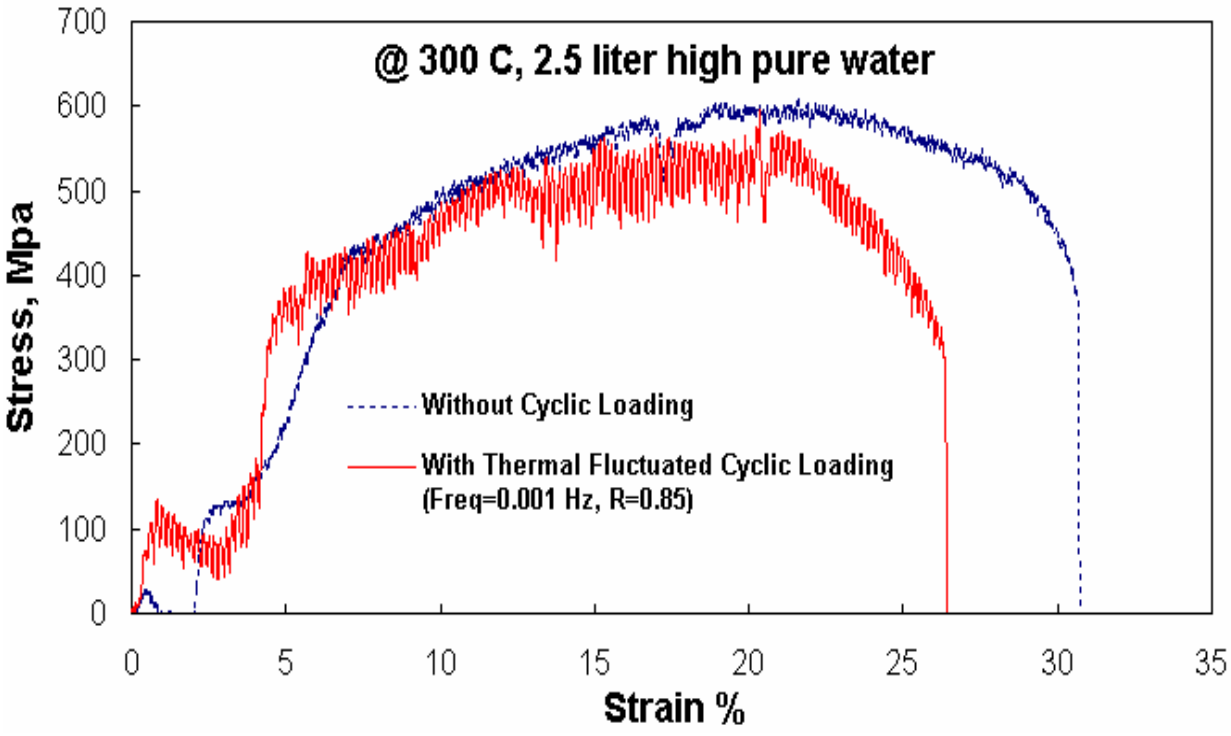

Figure 3.5.12 Stress Strain curves for samples tested with of without low frequency cycle imposed on the slow strain rate test.

Table 3.5.3 Effect of Cyclic Loading Parameters on SAC Susceptibility of SA210-Carbon Steel in boiler water with ~2ppm dissolved oxygen.

Environment Description (Temp, O_2 Level, etc)	Mean Stress (Mpa)	Amplitude (Mpa)	Frequency (HZ)	R-ratio	Crack density (/mm)	Crack velocity (mm/s)	Time to fracture (hrs)
300 ^oC Untreated Pure Water	UTS	monotonous SSRT	-	-	9.35	6.24E-7	45.9
300 ^oC Untreated Pure Water	UTS	80	0.001	0.85	11.19	6.27E-7	36.7

3.5.5 Effects of Microstructure on SAC Cracking

Metallurgical factors like grain size affect mechanical behavior and fatigue properties on carbon steels, however their effect on corrosion fatigue crack initiation and propagation in boiler water environments is not known. A limited amount of initial work was carried out to quantify the effect of grain size on threshold stress intensity factor for crack propagation. These tests were carried out in lab air to develop baseline data for effects of metallurgical parameters on fatigue behavior of carbon steel. The annealing temperature and times to heat treat CT samples are shown in table IV. Resulting grain size was measured by intercept method using image analysis software Clemex Vision PE/Lite. The microstructure and properties (grain size, hardness) after different heat-treatment are also listed in table IV. Image analysis data indicates that the ferrite/pearlite ratio in all heat treated samples was similar. After heat-treatment the CT specimens were polished to a 2000-grit finish and cleaned with acetone before put on fatigue testing on a MTS machine. Results in Figure 3.5.13 show that as the annealing time increased and the micro hardness decreased due to grain growth, the value of $\Delta K_{threshold}$ for crack propagation increased accordingly. From the Figure 3.5.13 a steady state crack growth rate region, linear zone of the curve can be described by Paris' Law Equation: $da/dN=A(\Delta K)^p$ As the hardness and grain size changed, the slopes of Paris region for different CT specimens did not show significant difference, which means the rate of crack propagation did not change much with the change of microstructure characteristics described in table IV. Although sufficient data is not available at this time but the corrosion fatigue crack initiation and growth behavior for carbon steel tubes in boiler water environment is also expected to change with grain size.

Table 3.5.4 **Heat treatments used to vary grain size of carbon steel**

Conditions	**Heat-treatments**	**Grain Size (μm)**	**Hardness (VHN)**
A	As Received	27.0	245
B	45 min. /1000 ^{o}C + air cooled to room temperature	28.5	211
C	90 min. /1000 ^{o}C + air cooled to room temperature	30.2	156
D	24 hours/1000 ^{o}C + + air cooled to room temperature	------	141
E	60 hours /1000 ^{o}C + air cooled to room temperature	53.1	140

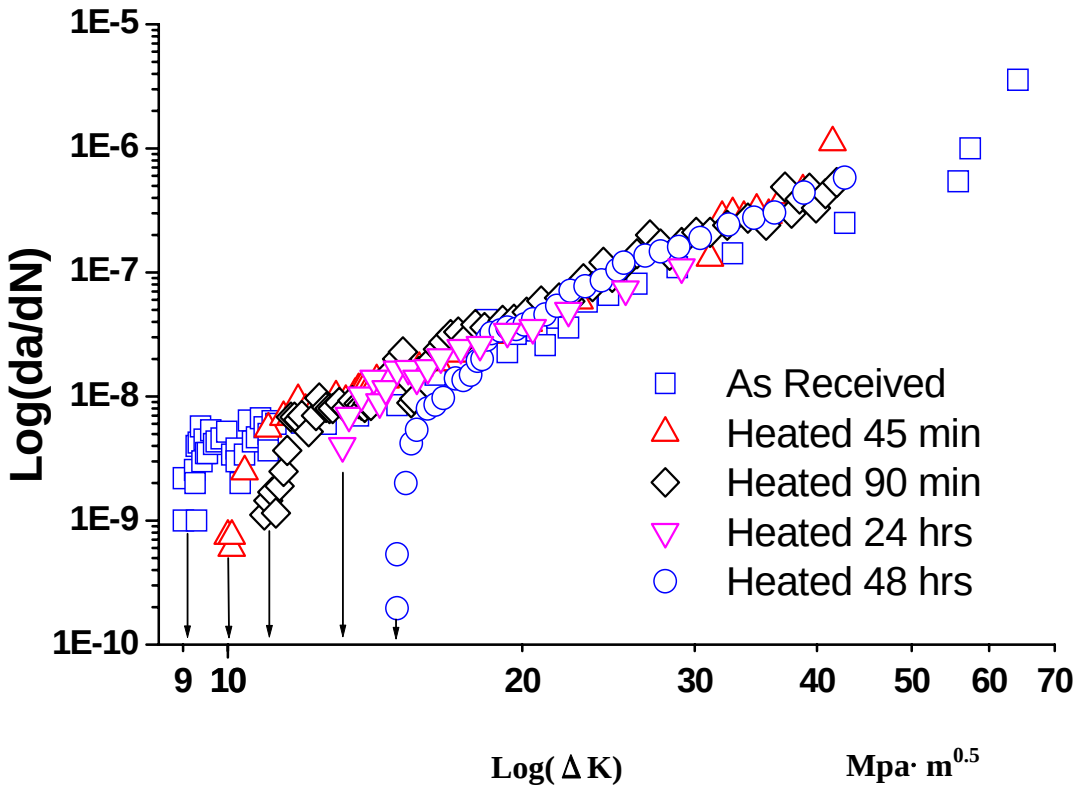

Figure 3.5.13**.** Effect of heat treatment (and resulting grain size) fatigue behavior of SA210 carbon steel

3.5.6 Magnetite Film and Morphology

Failure analyses of boiler tubes have shown that the protective magnetite film on the normal tube surface is thin and compact. Whereas in areas with SAC cracks, typically under weld attachments, the magnetite film is thick and porous. Strain concentration at attachment welds can damage the magnetite film repeatedly, especially during boiler shutdown and startup. Local damage of protective magnetite film can lead to exposure of the bare metal to boiler water. Bare carbon steel area will act as an anode whereas the surrounding tube surface with magnetite film will act as a large cathode. This may lead to high corrosion rates and easier corrosion fatigue or SAC crack initiation in these local areas.

Previous work on carbon steel in caustic solutions has shown that the morphology of magnetite film is dependent on relative area ratios of anode to cathode [16-18, 20]. Similar tests were performed in pure water to study the effect of relative areas of anode to cathode on magnetite morphology in boiler water environments. Samples being either electrically isolated or attached to a large cathode (anode to cathode area ratio 1:200) were exposed to pure water at 320^{o}C for 100 hours. After the test, surface film was characterized by x-ray diffraction and the magnetite film was detected for both types of samples. Film was also characterized for its surface morphology by using atomic force microscope. Results indicated a significant difference in the surface morphology of film for the two samples, as shown in Figure 3.5.14. Electrically isolated sample had a thin, irregularly grained, compact magnetite film on the surface, as shown in Figure 3.5.14a. Whereas the sample attached to a large cathode had a rough and porous magnetite film, with tetrahedral crystals on the surface, as shown in Figure 3.5.14b. These results were very similar to the films grown in caustic solutions by Potter and Mann [17-18], Bloom [16], and Marsh [20]. Film on the isolated coupon may provide greater protectiveness and therefore significantly thinner than the film on a sample attached to a large cathode. SEM characterization of magnetite film surface showed that pits formed more frequently on electrically isolated coupons. This is similar to the results by Bloom [16] who also reported that thinner and non-porous film may eventually form pits on the surface due to local film rupture/damage.

These results explain why the magnetite film on normal boiler tubes is different from the film in areas with SAC, where the film may be repeatedly damaged due to strain concentration. Once the film is locally disrupted, the remaining intact magnetite on the sample may act as a cathodic surface and the bare metal in the damaged areas will actively corrode to form a porous, non-protective thick magnetite film, as is also reported by Potter and Mann [17-18]. Figures 3.5.15 to 3.5.21show AFM micrograph as well as 3-D topography of the same area scanned. It can be seen that the unexposed surface in Figures 3.5.20 and 3.5.21 had a very smooth surface with average roughness of around 7-10 nm in the selected areas. However, for SA210 carbon steel exposed to boiler water at 320^{o}C for 72 hours, in contact with the autoclave surface acting as a large cathode, showed an average surface roughness between 70 to 95 nm on samples depending upon the area selected, with tetrahedral crystals on the surface, as is shown in Figures 3.5.15 to 3.5.19.

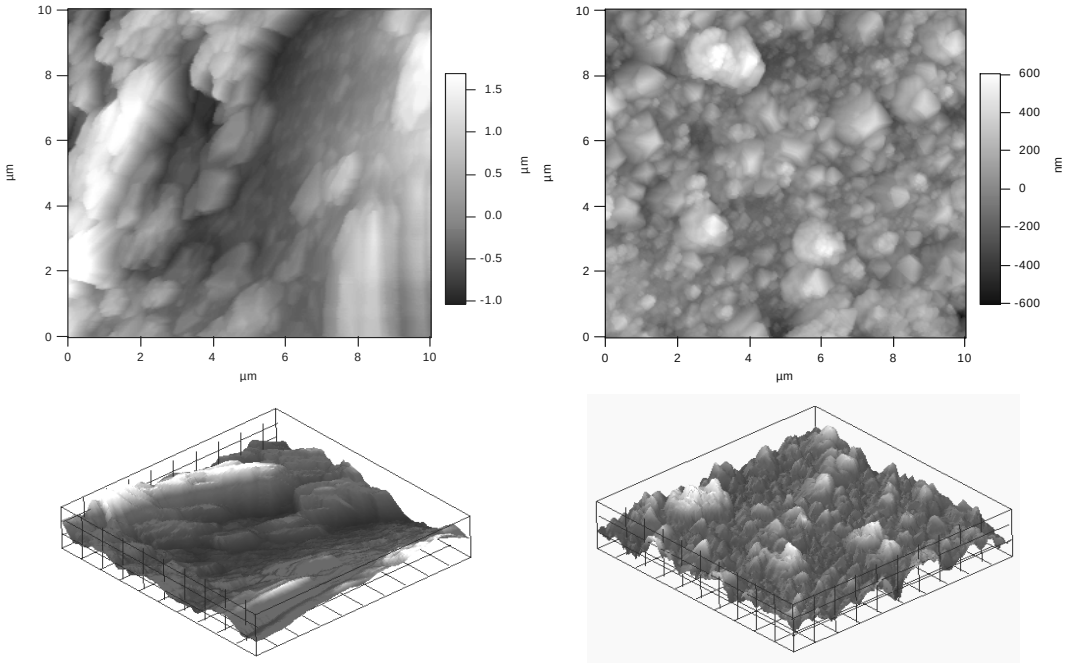

(a) (b)

Figure 3.5.14 (a) Magnetite film on the surface of an electrically isolated carbon steel coupon (*Anode/Cathode area ratio =1)* (b) Surface of a test coupon in-contact with a large cathode *(Anode/Cathode area ratio =200)* showing tetrahedral crystals

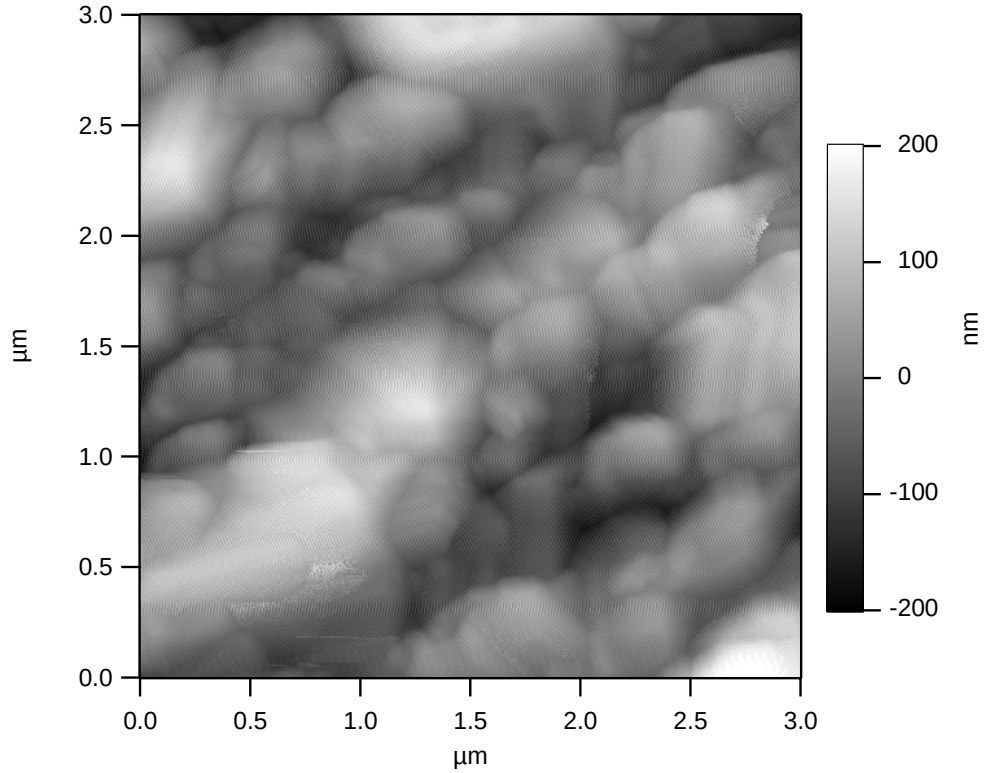

Figure 3.5.15 AFM scan for SA210 sample exposed for 72hr at 320^{o}C-Chpw. (AFM scan away from hole). Roughness = 70 nm.

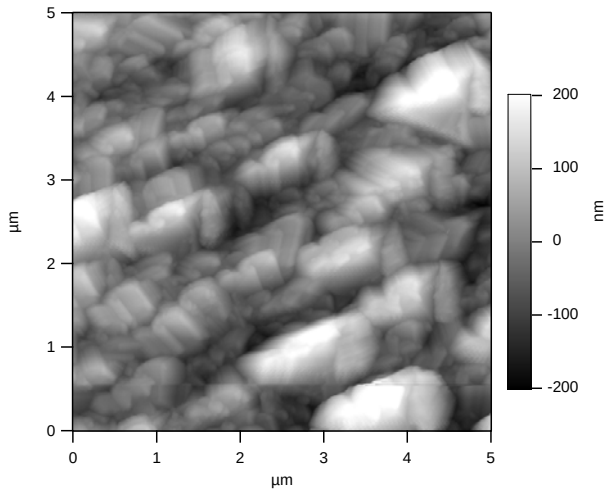

(A)

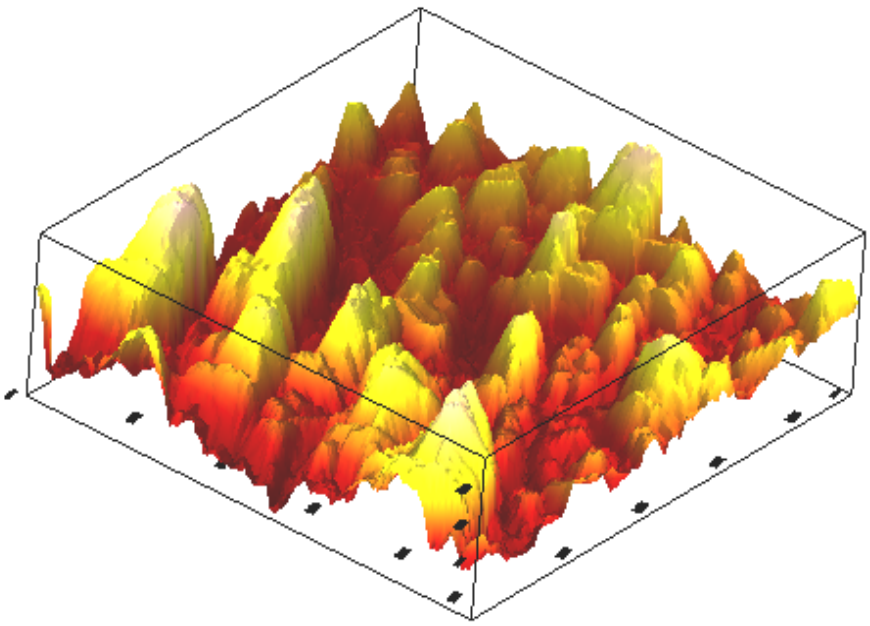

(B)

Figure 3.5.16 (A) SA210 sample exposed to water at 320°C. 5 micron topography scan away from hole. Roughness = 80 nm. (B) 3-D image of topography of 5 micron scan shown above.

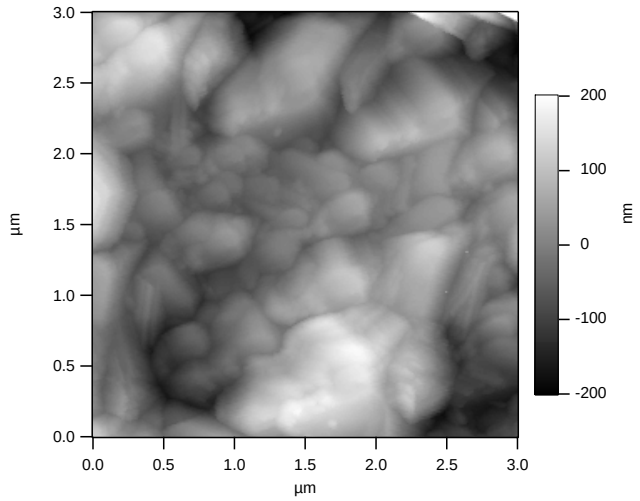

(A)

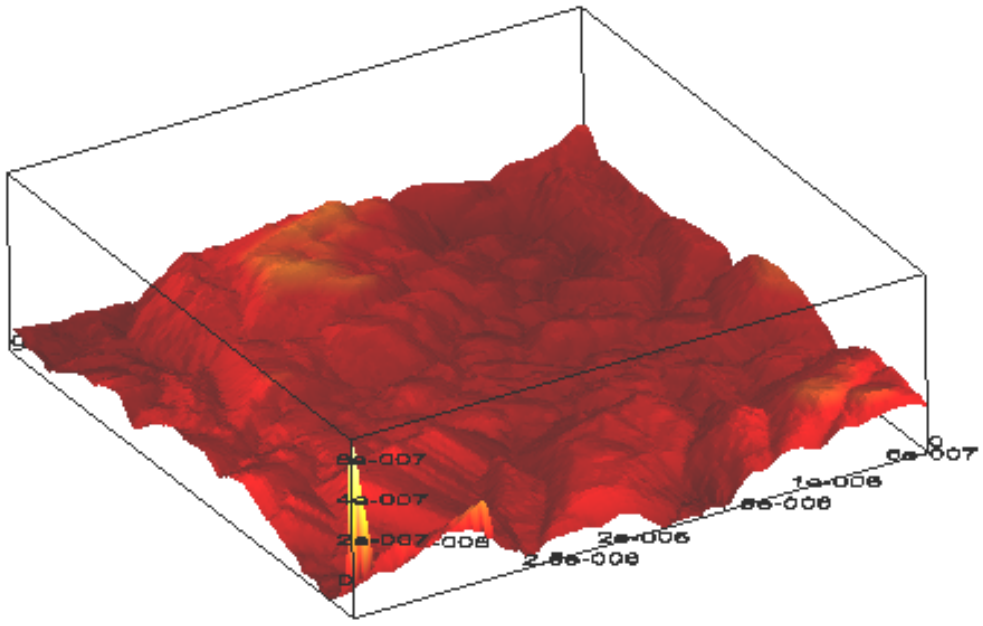

(B)

Figure 3.5.17 (A) SA210 sample exposed to water at 320°C. 5 micron topography scan away from hole. Roughness = 70 nm. (B) 3-D image of topography of 3 micron scan shown above.

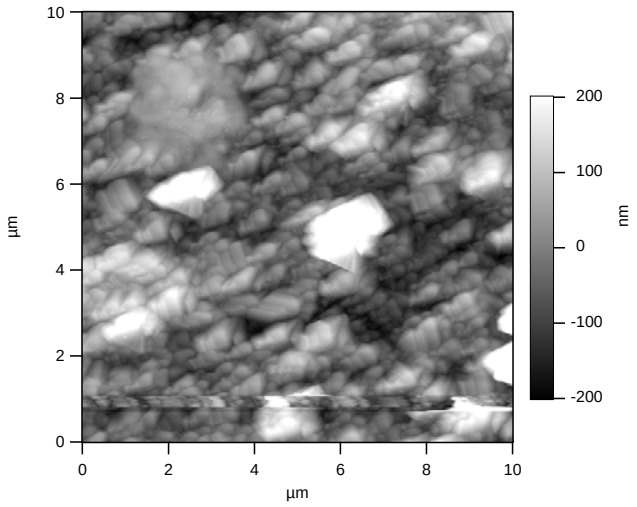

(A)

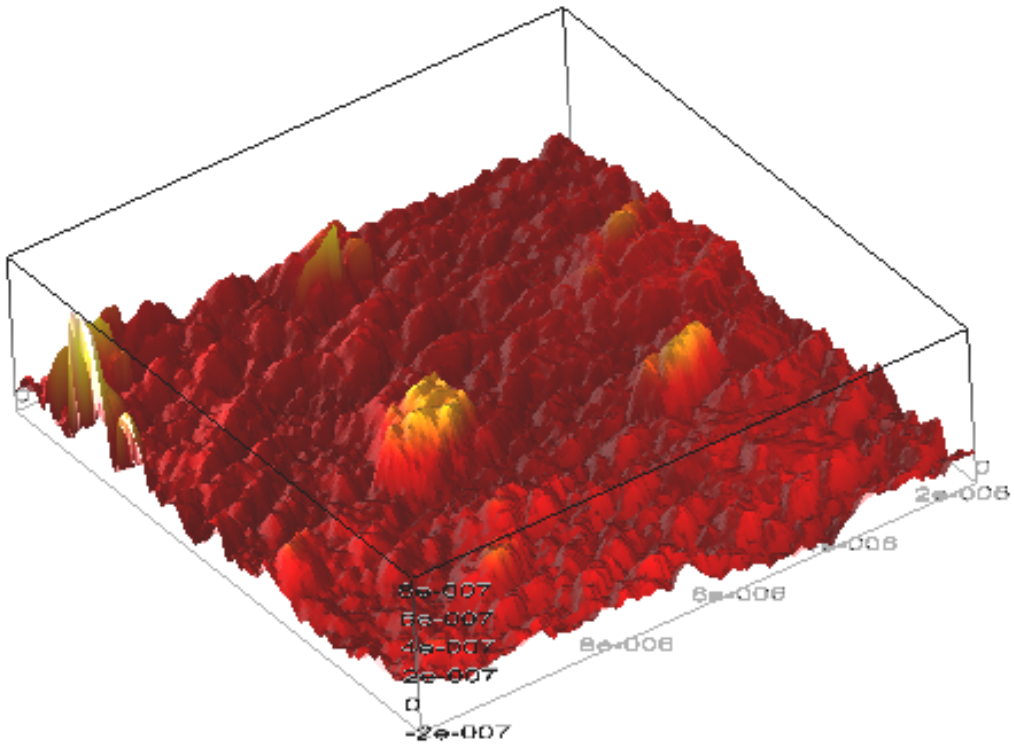

(B)

Figure 3.5.18 (A) SA210 sample exposed to water at 320oC. 10 micron topography scan away from hole. Roughness = 93 nm. (B) 3-D image of topography of 10 micron scan shown above.

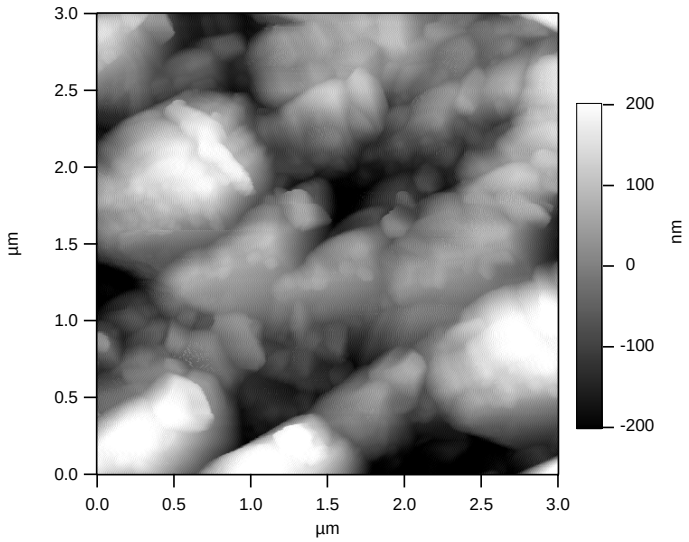

(A)

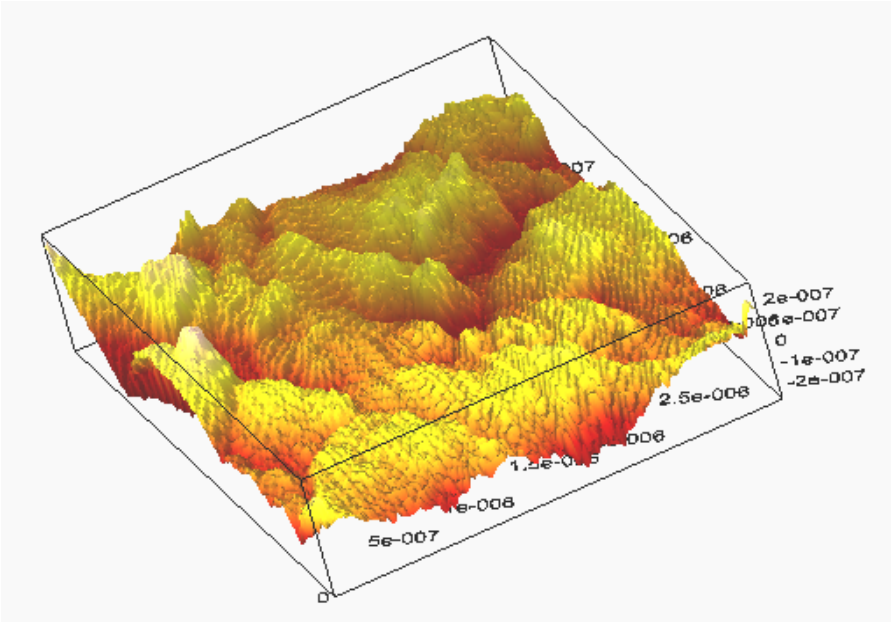

(B)

Figure 3.5.19 (A) SA210 sample exposed to water at 320oC. 3 micron topography scan away from hole. Roughness = 100 nm. (B) 3-D image of topography of 10 micron scan shown above.

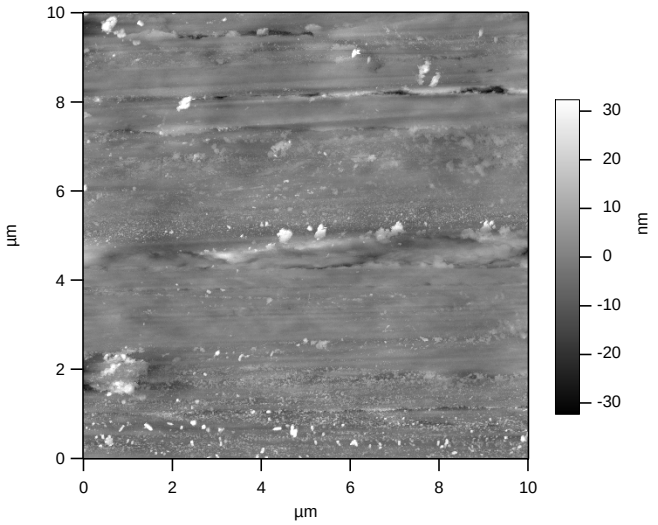

(A)

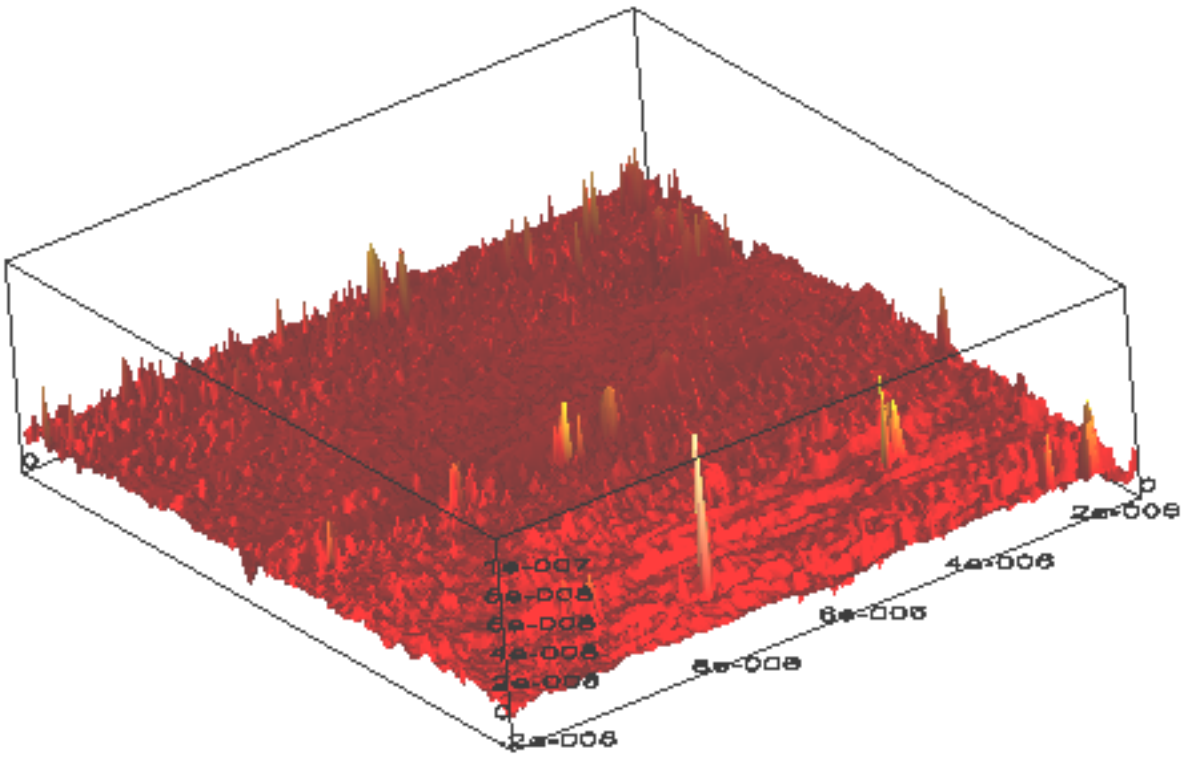

(B)

Figure 3.5.20 (A) Unexposed SA210 sample. 10 micron topography scan away from hole. Roughness = 7 nm. (B) 3-D image of topography of 10 micron scan shown above.

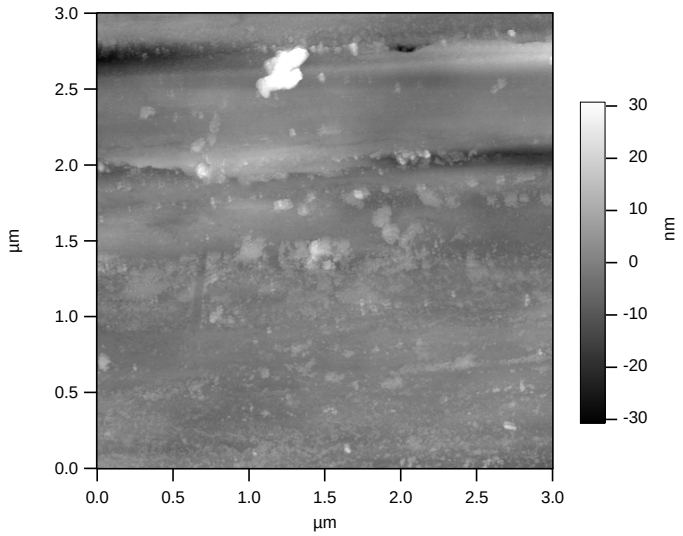

(A)

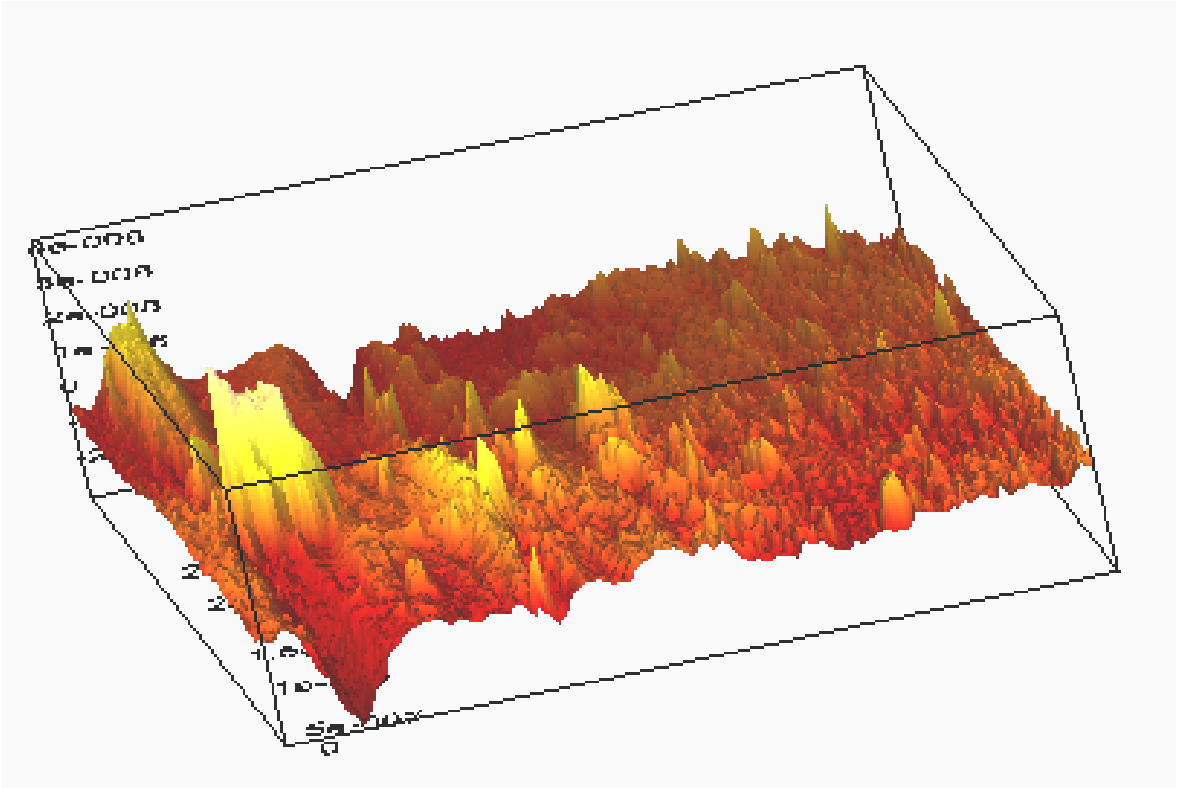

(B)

Figure 3.5.21 (A) Unexposed SA210 sample. 3 micron topography scan away from hole. Roughness = 5 nm. (B) 3-D image of topography of 3 micron scan shown above.

3.5.7 Mechanism of Stress Assisted Corrosion "Bulbous" Crack Growth

Carbon steel cracks under slow strain rate tests in pure water at high temperatures were typically transgranular with sharp crack tips. However, the field SAC cracks in industrial boilers were typically bulbous and blunt, as is shown in Figure 3.5.23. Interrupted tests were carried out to simulate the effect of boiler shutdown conditions on crack growth and morphology. Representative results are shown in Figure 3.5.24. It can be seen that relatively short interruptions (10 hours) in SSRT tests, where the temperature was lowered to 80^{o}C and water was aerated for 10 minutes with oxygen, flowing at 1.0 L/min, produced active corrosion around the sharp crack tips. Numbers of bulbous growths correspond to number of interruptions. Sharp stress corrosion cracks continued from the blunt tip on subsequent application of test conditions. This elucidates how the sharp corrosion fatigue cracks and the stress assisted corrosion (SAC) cracks with bulbous features in different types of boilers may have the same growth mechanism but different shape due to different boiler operation history.

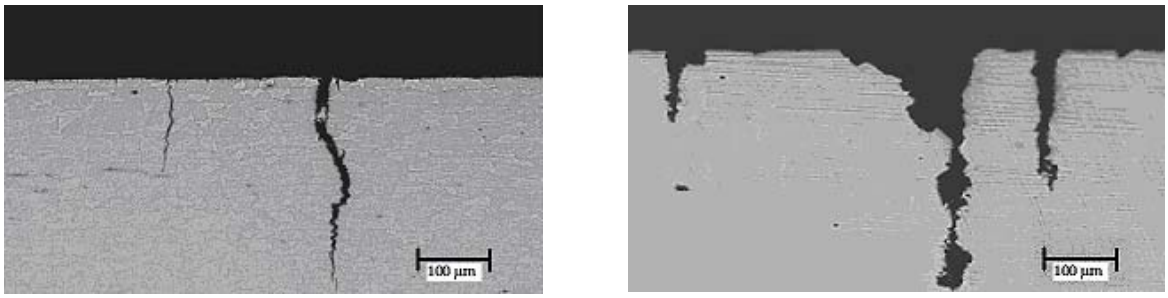

(a) (b)

Figure 3.5.22 Cracks from SSRT tests done in pure water at 300^{o}C (a) sharp crack from test without interruption. (b) Crack from test with interruptions to simulate boiler shutdown.

3.5.7.1 SAC Initiation and Propagation Mechanism

The morphology of a magnetite film is dependent on relative area ratios of anode to cathode. Our previous work on carbon steel in boiler water [13] at 3 20^{o}C and published work on carbon steel in concentrated caustic solutions [16-18, 20] have shown that the areas with comparable cathode to anode areas develop compact and protective magnetite films, as shown by AFM micrograph in Figure 3.5.14 (a). Whereas the carbon steel samples attached to a large cathode (area ratio 1:200) and exposed to pure water at 3 20^{o}C had a rough and porous magnetite film, with tetrahedral crystals on the surface, as shown in Figure 3.5.14 (b).

On new carbon steel tubes or on thoroughly acid cleaned tube surface, a compact and protective magnetite film will develop on the entire surface. During start up or shut down, the magnetite film can be damaged locally near weld attachments leading to bare metal surface. The bare metal, exposed due to magnetite film damage, will act as an anode whereas the

surrounding tube surface with magnetite film will act as a large cathode. Under these conditions a non-protective porous magnetite with tetrahedral surface crystals will be formed, as shown in Figure 5(b). The porous film may further lead to high local corrosion rates and easier corrosion fatigue or SAC crack initiation in these areas during startup or shut down. Every time the film is damaged locally, the process repeats itself as boiler water may come in contact with the bare metal. However, if the water chemistry is corrected, further initiation and propagation of SAC pits or cracks may be stopped. Initiation of SAC cracks, which may start from these local pits, is shown in the schematic in Figure 3.5.23.

During boiler shutdown if oxygen enters the boiler water system, this may produce typical SAC morphology for cracks. In the presence of oxygen the crack tips corrode preferentially and may lead to the formation of bulbous crack morphology, as shown schematically in Figure 3.5.23.

The mechanism above for SAC initiation and propagation was tested in the laboratory by carrying out some interrupted slow strain rate tests (ISSRT) in our boiler simulation autoclave. The loading curve of ISSRT test is shown in Figure 3.5.25. Stress strain curve and resulting sharp crack for an equivalent test without any interruption is shown in Figure 3.5.24. The boiler temperature and other working conditions were applied during loading part of the test (i.e., 0-15 hrs, 30-45 hrs); during shutdown the stress was lowered to 30% yield stress and oxygen was introduced into autoclave, (i.e., 15-30 hrs, 45-60 hrs). Tests were interrupted at different stages of these tests and the samples were sectioned to understand the mechanism.

Results show that small pits initiate during first loading, as shown in Figure 3.5.23. Cracks propagate during second loading mostly from the initial pits. Crack tips were attacked in cases where oxygen was introduced in autoclave during shutdown. In cases where cracks were initiated but oxygen was not introduced during shutdown, cracks did not show any sign of crack blunting. The crack shapes of simulated SAC during different stages are exactly the same as we derived in our proposed SAC mechanism as shown in Figure 3.5.25.

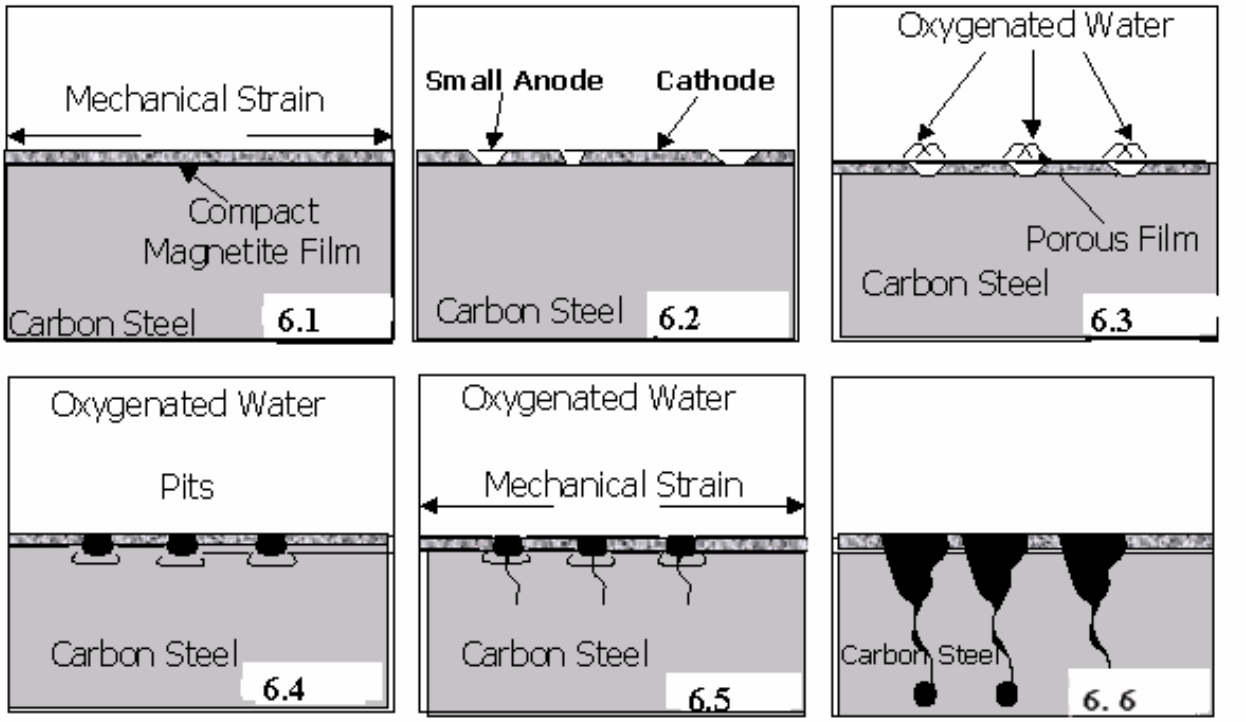

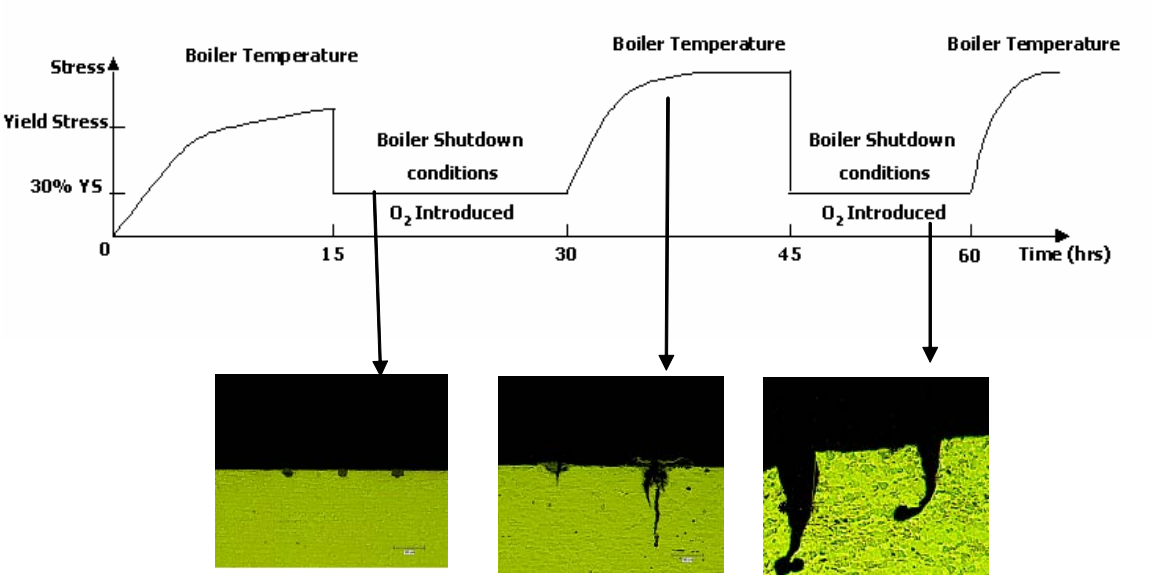

Figure 3.5.23**. Interrupted slow strain rate tests (ISSRT) to simulate boiler start up and shutdown conditions. During shutdown simulation, stress was lowered to 30% of yield stress and oxygen was introduced in the autoclave. Micrographs in this figure show crack morphology at certain time during these tests.**

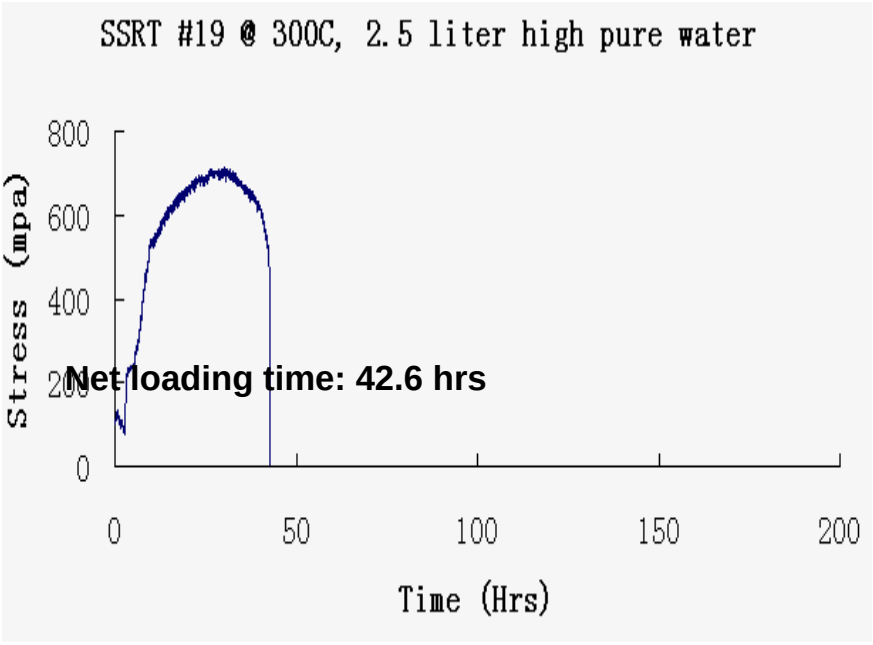

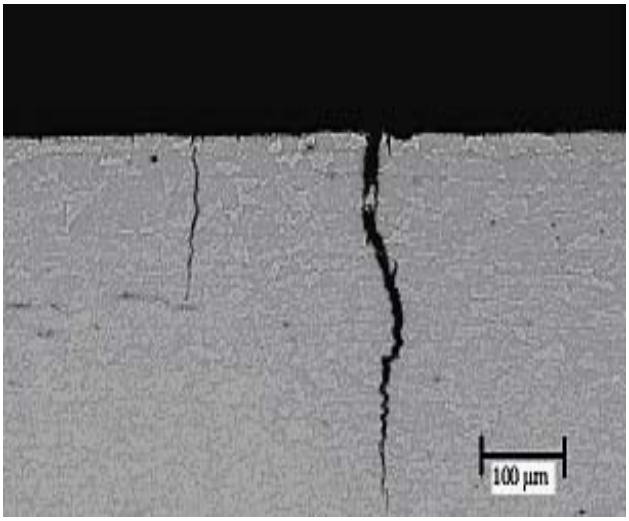

Figure 3.5.24 Sharp crack in SA210 sample tested via slow strain rate test (SSRT) method in boiler water environment.

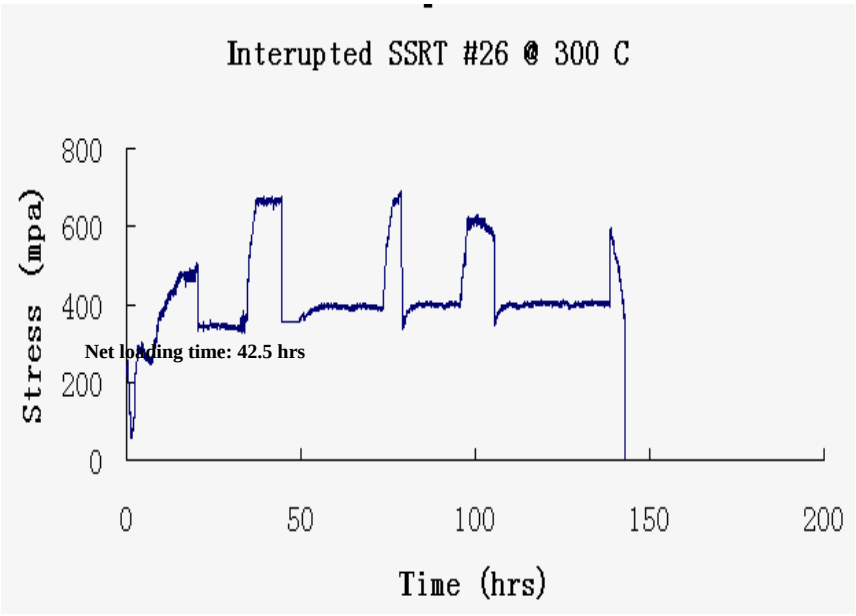

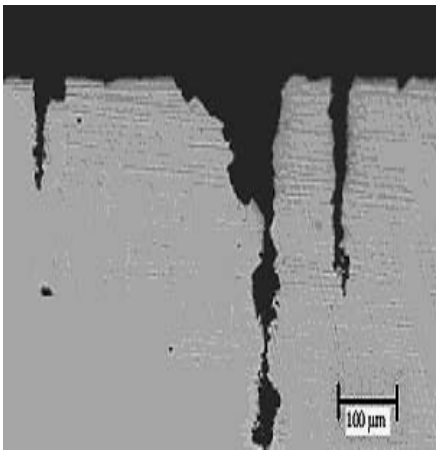

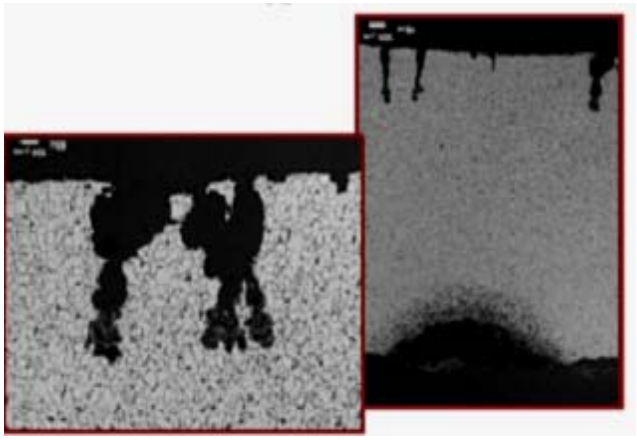

A **B**

Figure 3.5.25 Bulbous SAC crack in SA210 sample tested in interrupted slow strain rate test (ISSRT) method in boiler water environment. (A) simulated cracks were similar morphology to the cracks in (B) found in boiler tubes.

3.5.8 Conclusions on SAC Controlling Factors

- Results from the SSRT tests indicate that dissolved O_2 level higher than 5 ppb in the water is necessary for crack initiation and growth in boiler water environment. With dissolved O_2 in the water, the crack velocity and density increase with temperature.
- Tensile specimens at higher temperature and with cyclic stresses are more susceptible to environmentally induced crack initiation. Both high frequency low-amplitude and low frequency and high- amplitude cyclic loading promote early crack initiation and growth.
- Strain rates have significant affect on stress corrosion cracking of carbon steels in boiler water environments. The SAC crack initiation is dominant on the surface of carbon steel specimen under low strain rate loading in oxygenated boiler water environments.
- Stress assisted corrosion in industrial boilers can be controlled by controlling O_2 to levels below 5 ppb and stress localization near attachment welds below the threshold values need to damage magnetite film in local areas.
- Results from the SSRT tests showed that dissolved O_2 in the water is necessary for crack initiation in boiler water environment. With dissolved O_2 in the water, the crack velocity and density are higher at higher temperatures.
- For carbon steel in boiler water environments relative anode/cathode area ratio can have significant effect on the magnetite film morphology. Small ratios will likely produce a compact, protective film whereas large area ratio favors porous non-protective film.
- Sharp corrosion fatigue cracks and blunt SAC cracks seem to have the same initiation and growth mechanism; however the shape differs due to the differences in the shutdown conditions. Availability of oxygen during the shutdown may lead to crack blunting due to preferential corrosion and result into the bulbous shape of SAC cracks.

3.5.9 References on SAC Controlling Factors

[1]. D. J. Duquette, in “Fatigue and Microstructure”, pp.335-363, American Society for Metals, Metals Park, Ohio, 1979

[2]. Dooley, R. B., Power Engineering 1992 (March), 33

[3]. Dooley, R. B., Power Engineering 1992 (March), 41

[4]. Robertson, J., “The Mechanism of High Temperature Aqueous Corrosion of Steel”, Corrosion Science, Vol. 29, no. 11/12, 1989, pp. 1275-1291

[5]. Nagata, N., “Environmentally Assisted Cracking of Structural Materials for Light Water Reactors,” NRIM Special Report, No. 94-01, Tokyo, Japan, 1994

[6]. Atkinson, J.D. and Forrest, J. E., “Factors Influencing the Rate of Growth of Fatigue Cracks in RPV Steels Exposed to a Simulated PWR Primary Water Environment,” Corrosion Science, Vol. 25, No. 8/9, 1985, pp633-650

[7]. Wu, Xinqiang; Katada, Yasuyuki. "Corrosion Fatigue Behavior of Low-Alloy Pressure Vessel Steels in High Temperature Water under Multi-Factor Conditions," Journal of Pressure Vessel Technology (2004), 126(4), 466-472.

[8] E. M. Field, R. C. Stanley, A. M. Adams and D. R. Holmes, "The Growth, Structure and Breakdown of Magnetite Films on Mild Steel"

[9] Bloom, M. C., Newport, G. N., Journal of the Electrochemical Society 1957, 111, 1343

[10]. Potter, E. C., Mann, G. M. W., Proc., 1st International Congress on Metallic Corrosion, 1961, (London) Butterworths, London, UK, 417

[11]. Field, E. M., Stanley, R. C., Adams, A. M., Holmes, D. R. Proc., 2nd International Congress on Metallic Corrosion, 1963 (New York), Butterworths, London, UK, 829

[12]. Potter, E. C., Mann, G. M. W., Proc., 2nd International Congress on Metallic Corrosion, 1963, (New York) Butterworths, London, UK, 872)

[13]. Preet M. Singh, Jorge J. Perdomo, Jamshad Mahmood, Pablo Conde, "Stress-Assisted Corrosion Simulation in the Laboratory", Power Plant Chemistry, 2005, 7(3))

[14]. Higuchi, Makoto; Sakamoto, "Effects of temperature and dissolved oxygen on cyclic crack growth rate of carbon and low alloy steels in high temperature water". PVP (American Society of Mechanical Engineers) (1998), (Fatigue, Environmental Factors, and New Materials), 241-248

[15]. Vosikovsky, O.; Neill, W. R.; Carlyle, A. "The effect of seawater temperature on corrosion fatigue-crack growth in structural steels". Canadian Metallurgical Quarterly (1987), 26(3), 251-7

[16]. Bloom M. C., Newport G. N., and Fraser W. A., Journal of the Electrochemical Society, Vol. 111, 1957, p 1343.

[17]. Potter, E.C. and G.M.W. Mann, "Oxidation of Mild Steel in High-temperature Aqueous Systems", Proc. 1st Int. Cong. Metall. Corrosion, London, Butterworks, 1961, p. 417

[18]. Potter, E.C. and G.M.W. Mann, "Mechanism of Magnetite Growth on Low-Carbon Steel in Steam and Aqueous Solutions up to 550 Degrees C.", Proc. 2nd Int. Cong. Metall. Corrosion, London, Butterworks, 1963, p. 872.

[19]. Castle J. E. and Mann G. M. W., Corrosion Science, Vol. 6, pp 253-262, 1966.

[20]. Marsh T. F. Journal of the Electrochemical Society, Vol. 113, April 1966, pp 313-318.

[21]. D. J. Duquette, "Corrosion Fatigue Crack Initiation Processes: A State-of-Art Review", "Environmental-induced Cracking of Metals, NACE-10", Oct. 1988

4 ACCOMPLISHMENTS

Main accomplishment of this project is the mechanism of the stress assisted corrosion of carbon steel in boiler water environment. This work has shown important parameters in terms of water chemistry, stress and microstructure that are important in prevention of SAC in the industrial environment.

Work from this project has been published and presented in following conferences and journals.

4.1 JOURNAL ARTICLES PUBLISHED:

1. Preet M. Singh, Jorge J. Perdomo, Jamshad Mahmood, Pablo Conde, Stress Assisted Corrosion Simulation in Laboratory. *Power Plant Chemistry*, Vol. 7, pp.155-161, March **2004.**

4.2 CONFERENCE PUBLICATIONS:

1. Dong Yang, Preet M. Singh, Richard W. Neu, Role of Microstructure on Corrosion Fatigue of Carbon Steel in Boiler Water Environment, 9th International Congress on Fatigue, Atlanta, GA. May 14-19 2006

2. Gorti B. Sarma, Steven J. Pawel, and Preet M. Singh, Modeling of Recovery Boiler Tube Wall Panels to Investigate the Effect of Attachment Welds on Stress-Assisted Corrosion, CORROSION-2006, Paper No. 06240, San Diego, CA, USA, March 2006.

3. Dong Yang, Preet M. Singh, Richard W. Neu, Corrosion Fatigue and Stress Assisted Corrosion of Carbon Steel in Boiler Water Environments. CORROSION-2006, Paper No. 06241, San Diego, CA, USA, March 2006.

4. Gorti B. Sarma, Steven J. Pawel, and Preet M. Singh, Modeling of Recovery Boiler Tube Wall Panels to Investigate the Effect of Attachment Welds on Stress-Assisted Corrosion, Accepted for the Proceedings of TAPPI Engineering Conference, Philadelphia, PA, August 2005.

5. Preet M. Singh, Jorge J. Perdomo, Jamshad Mahmood, Pablo Conde, Stress Assisted Corrosion in Laboratory, Paper #04518, Corrosion-04. New Orleans, March 2004.

6. S. J. Pawel, A. W. Willoughby, H. F. Longmire, P. M. Singh, An Experience with Detection and Assessment of SAC in a Recovery Boile, Paper #04519, Corrosion-04. New Orleans, March 2004.

4.3 PRESENTATIONS:

1. Dong Yang, Preet M. Singh*, Jamshad Mahmood, Richard W. Neu, Effect of Boiler Water Chemistry on Corrosion and Corrosion Fatigue of Carbon Steels, 16th International Corrosion Congress proceedings, Paper # 06-20, Beijing, China. September 2005.

2. Toronto University, Pulp and Paper Center, Toronto, ON, Canada, November 10, 2005, "Stress Assisted Corrosion of Carbon Steel Tubes in Industrial Boilers".

3. NACE-Corrosion-04. New Orleans, March 2004. "Stress Assisted Corrosion in Laboratory." (with Jorge J. Perdomo, Jamshad Mahmood, Pablo Conde).

4. NACE-Corrosion-04, New Orleans, March 2004. "An Experience with Detection and Assessment of SAC in a Recovery Boiler." (with S. J. Pawel, A. W. Willoughby, H. F. Longmire).

5 CONCLUSIONS

Based on failure analysis of carbon steel boiler tubes from over ten different boilers, it can be summarized that the in selected tubes, SAC cracks were found on the inner surface of the waterwall tubes where some attachments were welded on the cold side of the tube. Cracks in all tubes examined were in the longitudinal direction, irrespective of the weld attachment direction. Cracks were generally blunt and had bulbous growth indicating discontinuous growth. Cracks were predominantly transgranular and did not follow grain boundaries.

In a number of tubes, large grains were associated with SAC attack. In these tubes, the maximum length of crack was roughly equal to the thickness of the large grained layer. Large grained layer was in both outer and inner surfaces of some tubes whereas in other tubes they were only found on the inner surface. In some sections of the tube, large grained layer on the inner surface did not have even thickness and was also discontinuous in some regions. Observations from eight failed tubes from three different boilers have shown that further investigation is required to understand the conditions (Heat treatment) under which these microstructural changes are possible during the tube manufacture, during attachment welding, or during boiler operations.

An array of non-destructive techniques, including two ultrasonic wave methods, radiography, and borescope inspection, proved to be generally ineffective for locating SAC on boiler tubes removed from service. In part, this was due to inability to confirm the presence of SAC until destructive evaluation (metallography) had taken place, so specimens bearing SAC were not exposed with equal frequency to all inspection methods. Limitations of each method for field inspection were identified, and the reliable detection of SAC in an operating boiler remains problematic.

Wall penetrations of up to 30% of the wall thickness were found associated with SAC among the boiler tubes examined after removal from service. All SAC penetrations were located immediately adjacent to a scallop-type attachment weld and exhibited a significant accumulation of somewhat porous, mixed oxide filling/covering the SAC penetrations. Invariably, the SAC penetrations were transgranular and essentially straight (non-branching), with bulbous and/or rounded features, and filled with alternating layers (Fe_2O_3 and Fe_3O_4) of oxide, indicating changing corrosion conditions during the propagation of the SAC. A decarburized layer was observed on the ID surface of most of the boiler tubing which was somewhat softer than the bulk material and which may encourage the initiation of SAC due to its lesser strength compared to the nominal steel.

Data from gages on tubes near/around a substantial scallop-type attachment weld in an operating boiler suggest that shutdown/restart events (4 in almost 13 months of data gathering at this mill) generate by far the most significant strains associated with operation. Proximity and orientation relative to the position of the attachment weld was a significant factor in strain response to operational events. Much more modest process upsets, involving a temperature drop/return of between 10 and 95ºC (41 in almost 13 months) were more numerous but much less threatening in terms of strain change associated with each. Although the failure criteria for the internal oxide on the tubes is not known, it seems likely that it is primarily the shutdown/restart events that lead to initiation and/or propagation of SAC.

The results of the initial modeling simulations showed that the stress distribution in a wall tube is significantly altered by the presence of an attachment weld. Without an attachment weld, or on portions of the wall tube removed from the attachment by more than about 2 cm, residual stresses (thermal/mechanical) tend to remain small and compressive on the tube ID at the end of each operating cycle. However, immediately adjacent to an attachment weld, residual stresses on the tube ID tend to increase and become tensile following an operating cycle. The location of the maximum tensile hoop stress in the model – confined to a distance within about 2 cm of the attachment weld – and the location of longitudinally-oriented SAC on boiler tubing are identical, lending credibility to the model results. The presence of a tensile hoop stress when the tubes are cooled from operating temperature, combined with potential water chemistry upsets during shutdown periods, provides conditions under which SAC can initiate and propagate.

The initial model results for co-extruded composite tubing (carbon steel with a outer layer of 304L stainless steel) suggest a much different stress distribution following an operation cycle. In contrast to the carbon steel tubes, the composite tubing tends to exhibit residual compressive hoop stress (or at least smaller tensile stresses) adjacent to attachment welds following an operation cycle, consistent with field observations that composite tubes do not seem as susceptible to SAC as carbon steel tubes.

Laboratory facilities were designed and developed to simulate boiler water environments in the laboratory. Specially designed slow strain rate test rig could be used to study factors affecting SAC in boiler water at temperatures up to 320^{o}C. Results from the SSRT tests indicate that dissolved O_2 level higher than 5 ppb in the water is necessary for crack initiation and growth in boiler water environment. With dissolved O_2 in the water, the crack velocity and density increase with temperature.

Stability of magnetite film on the inner tube surface is very important for the protection of boiler tubes against general corrosion as well as against SAC. For carbon steel in boiler water environments relative anode/cathode area ratio can have significant effect on the magnetite film morphology. Small ratios will likely produce a compact, protective film whereas large area ratio favors porous non-protective film. Tensile specimens at higher temperature and with cyclic stresses are more susceptible to environmentally induced crack initiation. Both high frequency low-amplitude and low frequency and high- amplitude cyclic loading promote early crack initiation and growth. Results have indicated that the strain rates have significant affect on stress corrosion cracking of carbon steels in boiler water environments. The SAC crack initiation is dominant on the surface of carbon steel specimen under low strain rate loading in oxygenated boiler water environments.

Mechanism of sharp corrosion fatigue cracks and blunt SAC cracks was found to be similar. However the crack morphology differs due to the differences in the availability of oxygen during the boiler shutdown. When tubes are still loaded and water has dissolved oxygen in it, these conditions lead to crack blunting due to preferential corrosion at the crack tip and result into the bulbous shape of SAC cracks. Crack growth was found not to occur during this shutdown condition. However, in both cases, stress assisted corrosion in industrial boilers can be controlled by controlling O_2 to levels below 5 ppb and stress localization near attachment welds below the threshold values need to damage magnetite film in local areas.

6 RECOMMENDATIONS

Information from this study has been published and presented to industrial boiler owners as well as other industrial representatives. However, awareness of SAC problems in the pulp and paper industry as well as other industrial boilers is not adequate. It will be important for the end-users to know about the factors that can be controlled to avoid SAC.

There is some concern about the effect of chemical cleaning of boiler tubes on SAC initiation and propagation. Although our results from this study clearly show that the bulbous crack morphology can be due to the presence of dissolved oxygen, but role of acids used for chemical cleaning is not very clear. Acids used in the industry vary as well as their concentration. Depending upon the method used, effect can be from minimal to significant. Work needs to be done to understand the role of chemical cleaning on SAC initiation and re-initiation of SAC cracks.

There is anecdotal evidence that the composite tubes used in the industrial boilers do not undergo SAC. However, this may be due to the longer incubation time or due to residual stresses due to thermal mismatch. The initial model results for co-extruded composite tubing (carbon steel with a outer layer of 304L stainless steel) suggest a much different stress distribution following an operation cycle. In contrast to the carbon steel tubes, the composite tubing tends to exhibit residual compressive hoop stress (or at least smaller tensile stresses) adjacent to attachment welds following an operation cycle, consistent with field observations that composite tubes do not seem as susceptible to SAC as carbon steel tubes. Attempts to modify the model to examine the effects of attachment weld variables and surface decarburization on stress distributions revealed inconclusive results, suggesting further model development as an area for future work.

7. APPENDICES

7.1 BIBLIOGRAPHY ON SAC RELATED TOPICS (ALPHABETIC ORDER)

Adams, N.J.I. "An Analysis and Prediction of Failure in Tubes." In *Third International Conference on Pressure Vessel Technology, Part* 2, *Materials and Fabrication,* held in Tokyo, Japan, April 19-22, 1977. New York, NY: American Society of Mechanical Engineers (ASME),(1) 1977, pp. 685-694.

Ames, W.C., and J.A. Lux. "An Experimental Investigation of Hydrogen Damage in Boiler Tubing." In *Proceedings of the 29th Annual Meeting of the American Power Conference.* Chicago, IL: Illinois Institute of Technology, 1967, pp. 763-777.

Balakhovskii, M.B. , and L. V. Nadtsyna. "Role of Hydrogen in the Fatigue Failure of Power Equipment Units at Moderate Temperatures." *Fiziko-Khimiches- kaya Mekhanika Materialov 17,* 1 (1981): pp.26-28.

Barcikowski, G.F. , et. al. "Locate Problems in Radiant and Convective Sections Early to Improve Availability." *Power* 122,3 (March 1978): pp.40-46.

Barer, R.D. "Boiler and Turbine Component Failures." In *Proceedings of Symposium on Metallography in Failure Analysis,* held in Houston, Texas, July 1977, p. 207

Bates, A.J., et. al. "Waterside Corrosion and Its Prevention in Inclined Tubes in Fawley/Pembroke Power Station Boilers." In *Proceedings of the 40th Annual Meeting of the American Power Conference.* Chicago, IL: Illinois Institute of Technology, 1978, pp. 943-963.

Berman, I., and M.S.M. Rao. "Sensitivity of Estimated Tube Life to Material Property Variation." *Journal of Pressure Vessel Technology* (ASME) 105, 1 (February 1983): p. 73.

Bonner, E.H. "Water Treatment for the Prevention of Water Side Corrosion in Boiler Plant." *Power Works Engineering* 19,1 (January 1979): pp.10-11.

Bruno, F. "Some Aspects of Boiler Water Composition on Stress Corrosion of a Steam Drum." Fifth International Symposium on Corrosion in the Pulp and Paper Industry, held in Vancouver, BC, 1986. Houston, TX: NACE, 1986, p. 41

Castle, J.E., and G.M.W. Mann. "Mechanism of Formation of a Porous Oxide Film on Steel." *Corrosion Science* 6, 6 (1966): pp.253-262.

Chakrapani, D.G., and H. Czyzewski. "Some Unusual Corrosion Fatigue Failures in Industrial Equipment: A Few Case Histories." In *Metallic Corrosion,* Eighth International Congress on Metallic Corrosion, vol.II. Mainz, West Germany Dechema Deutsche Gesell schaft fur Chemisches Apparatewesen, 1981, pp.1412-1417

Chojnowski, B., and R.D.B. Whitcutt. "Corrosion Failure: One Cause and a Cure in an Operational Boiler." (CEGB Research, December, 1975) *Combustion* 48, 5 (November 1976): pp. 28-33.

Dooley, R.B., et al. "Ontario Hydro Experience with Dissimilar Metal Welds in Boiler Tubing." *Welding Journal: Welding Research Supplement* 61, 2 (February 1982): pp.45S-49S.

Eberle, F., and C.H. Anderson. "Scaling Behavior of Superheater Tube Alloys in ASME High Temperature Steam Research Tests at 1100-1500°F." *Journal of Engineering for Power* 84, 3 (July 1982): pp. 223-257.

Elonka, S.M. *Standard Plant Operators' Manual.* 3rd ed. index" for quick cross-referencing. New York, NY: McGraw-Hill, Inc., 1980, pp. 8-19.

French, D.N. "Microstructural Degradation in Boiler Steels." In *Environmental Degradation of Engineering Materials in Aggressive Environments.* Blacksburg, VA: Laboratory for the Study of Environmental Degradation of Engineering Materials, Virginia Polytechnic Institute, 1981, p. 417.

Frey, D.A. "Case Histories of Corrosion in Industrial Boilers." *Materials Performance* 20, 2 (1981): p. 49.

Gabrielli, F. "An Overview of Water-Related Tube Failures in Industrial Boilers." *Materials Performance* 27,6 (1988): pp.51-56.

Gailey, R.H. "Case Histories of Metal Failures in Boilers and Related Equipment." *Microstructural Science* 4, 7 (1979): pp.42-48.

Heitmann, H.G., and W. Kastner. "Erosion-Corrosion in Water-Steam Cycles-Causes and Countermeasures." *V GB Kraftwerkstechnik* (English Issue) 62, 3 (1982): p. 180.

Heitz, E. and C. Kyriazis. “Reactions during Corrosion of Metals in Organic Solvents.” Ind. Eng. Chem. Prod. Res. Dev., vol. 17, no.1, 1978, p. 37.

Herman, K. W. "Causes and Cures of Waterside Problems in Industrial Boiler Systems." *Combustion* 50, 2 (August 1978) : pp. 9-15.

Hinchley, P. "Waste Heat Boilers: Problems and Solutions." *Chemical Engineering Progress* 73, 3 (1977): p. 90.

Holmes, D.R., and G.M.W. Mann. "Critical Survey of Possible Factors Contributing to Internal Boiler Corrosion." *Corrosion* 21, 11 (November 1965): pp. 370-377.

Huijbregts, W .M.M. "Erosion-Corrosion of Carbon Steel in Wet Steam." *Materials Performance* 23, 9 (October 1984): pp. 39-45.

Jackson, C.M., and R.D. Buchheit. "Failure Analysis of Industrial Equipment and Products." *Mechanical Engineering* 106, 7 (July 1984): pp.32-37.

Jackson, J.J. *Steam Boiler Operation Principles and Practice.* Englewood Cliffs, NJ: Prentice-Hall, 1980.

Klein, H.A. "Corrosion of Fossil Fueled Steam Generators." *Combustion* 44, 7 (January 1973): pp.5-20.

Kunze, E., and J. Nowak. "Erosion Corrosion Damages in Power Plants." *Werkstoffe und Korrosion* 33, 5 (May 1982): pp. 262-273.

Lee, W .R., H.J. Westwood, M.D. Moles, and W.H.S. Lawson. "Fracture Characteristics of 2 114 Cr -1.0 Mo Welds Under Thermal Fatigue Conditions." In *Fracture Problems and Solutions in the Energy Industry: Proceedings of the 5th Canadian Fracture Conference,* held in Winnipeg, Canada, September1981. New York, NY: Pergamon Press Ltd., 1982, pp. 85-95.

Lewis, M.W.J. "Failure Diagnosis-I." *Chemical Engineering,* vol. 91, #14 (July) 1984: pp.117-120.

Lewis, M.W.J. "Failure Diagnosis-II." *Chemical Engineering,* vol. 91, #16 (August) 1984: pp.87-90.

Madeyski, A. "A Systematic Approach to Failure Analysis-Part I." *Metal Progress* 125, 6 (May 1984): pp.57-61.

Mann, G.M.W. "History and Causes of On-Load Waterside Corrosion in Power Boilers." *British Corrosion Journal* 12, 1 (1977): pp. 6-14.

Marsh, T.F. "The Morphology of Magnetite Growth on Mild Steel in Alkaline Solutions at 316°C." *Journal of the Electrochemical Society* 113, 4 (1966): pp. 313-318.

Mayer, P., and A. V. Manolescu. "Measurement of Dissolved Hydrogen to Monitor Corrosion in High-Pressure Boilers." *Materials Performance* 24, 2 (1985): pp. 38-46.

Mitchell, D. A. and T.P. McGee. "Determining the Need to Chemically Clean Black Liquor Recovery Boilers." *Materials Performance* June, 1982, pp. 49-50

Partridge, E.P. "Hydrogen Damage in Power Boilers." ASME Transactions, *Journal of Engineering for Power* 86, 3 (July 1964): pp. 311-324.

Port, R.D. "Identification of Corrosion Damage in Boilers." *Materials Performance* 23, 12 (1984): pp. 45-51.

Robinson, J.N., and C.A. Rau. "Analyzing Failures - Some Advice and Examples." *Mechanical Engineering* 106, 7 (July 1984): pp.22-31.

Schoch, W., and H. Spahn. "On the Role of Stress-Induced Corrosion and Corrosion Fatigue in Water-Wetted Boiler Components." In *Corrosion Fatigue: Chemistry, Mechanics, and Microstructure.* Houston, TX: NACE, 1972, pp. 52-64

Tatone, O.S., et al. "Steam Generator Tube Performance: Experience with Water-Cooled Nuclear Power Reactors During 1981." *Nuclear Safety* 25, 3 (May-June 1984), pp. 373-398.

Tomlinson, L. "Mechanism of Corrosion of Carbon and Low Alloy Ferritic Steels by High Temperature Water." *Corrosion* 37, 10 (1981): pp.591-596.

Westwood, H.J., and D.M.C. Moles. "Creep-Fatigue Problems in Electricity Generating Plants." *Canadian Metallurgical Quarterly* 18 (April-June 1979): pp. 215-

230.

Whalley, B.G. "The Analysis of Service Failures." *The Metallurgist and Materials Technologist* (June 1983): pp. 273-277

"Scale and Mud." Power Plant Engineer's Guide, pp. 407-408

References Related to Magnetite Film Formation and Corrosion Fatigue

Castle, J.E. and G.M.W. Mann, "The Mechanism of Formation of a Porous Oxide Film on Steel", *Corrosion Science,* vol. 6, 1966, pp.253-262. [TA462 .C659]

Dooley, R.B., "A Vision for Reducing Boiler Tube Failures", *Power Engineering,* March, 1992, pp. 33-37.
[TJ1 .P77]

Dooley, R.B., "A Vision for Reducing Boiler Tube Failures: Part II", *Power Engineering,* March, 1992, pp. 41-42. [TJ1 .P77]

Dooley, R.B., "Cycle Chemistry Related Boiler Tube Failures and Reduction", *Proceedings of the International Water Conference, 50th Annual Meeting,* held in Pittsburgh, Pennsylvania, October 23-25, 1989. [TD201 .I57x]

Dooley, R.B. and A. Bursik, "State of the Art in Fossil Plant Cycle Chemistry", *12th International Conference on Water and Steam,* held in Orlando, FL, September, 1994, Begel House "Physical Chemistry of Aqueous Systems".

Field, E.M., R.C. Stanley, A.M. Adams, D.R. Holmes, "The Growth, Structure, and Breakdown of Magnetite Films on Mild Steel", *Proc. 2nd Int. Conf. Metallic Corrosion,* New York, 1963, p.829 [IPST]

Fuji, C.T. and R.A. Meussner, "The Mechanism of the High-Temperature Oxidation of Iron-Chromium Alloys in Water Vapor", *Journal of the Electrochemical Society,* volume 111, 1964, p.1215 [IPST]

Goldstein, P., "A Research Study on Internal Corrosion of High Pressure Boilers", *Trans.* ASME 90(A), 1, 1968, pp.23-37 [TJ1 .A7]

Goldstein, P. and C.L. Burton, "A Research Study on Internal Corrosion of High

Pressure Boilers – Final Report", *Trans. ASME* 91(A), 1969, pp. 75-101. [TJ1 .A7]

Hancock, P., "Mechanical Considerations of the Growth and Breakdown of Surface Metal Oxide Films", *Werk. And Korr.,* Vol.21, 1970, p. 1002 [TA401 .W45]

Hurst, R.C., M. Davies and P. Hancock, "The Determination of Fracture Strains of Growing Surface Oxides on Mild Steel at High Temperatures", *Oxidation of Metals,* vol. 9, no. 2, 1975, p. 161. [QD171 .O93]

Jaffee, R.I., "Metallurgical Problems and Opportunities in Coal Fired Steam Power Plants", *Met. Trans.,* Volume 10A, May, 1979, pp. 139-165

Masterson, H.G., J.E. Castle and G.M.W. Mann, "Waterside Corrosion of Power Station Boiler Tubes", *Chemistry and Industry,* Sept. 6, 1969, pp. 1261-1266 [TP1 .S6332]

Molgaard, J. and W.W. Smeltzer, "Thermal Conductivity of Magnetite and Haematite", *Journal of Applied Physics,* Vol. 42, 1971, p. 3644 [QC1 .J88]

Pandey, R.K., V. Raghavan and S.K. Gupta, "Case Studies in Failure Analysis", *Transactions of the Indian Institute of Metals,* vol. 35, no. special, April 1982, p. 47

Potter, E.C. and G.M.W. Mann, "Oxidation of Mild Steel in High-temperature Aqueous Systems", *Proc. 1st Int. Cong. Metall. Corrosion,* London, Butterworks, 1961, p. 417 [TA462 .I5]

Potter, E.C. and G.M.W. Mann, "Mechanism of Magnetite Growth on Low-Carbon Steel in Steam and Aqueous Solutions up to 550 Degrees C.", *Proc. 2nd Int. Cong. Metall. Corrosion,* London, Butterworks, 1963, p. 872. [TA462 .I52 IPST]

Robertson, J., "The Mechanism of High Temperature Aqueous Corrosion of Steel", *Corrosion Science,* Vol. 29, no. 11/12, 1989, pp. 1275-1291 [IPST]

Sylvester, W.R. and G. Sidla, "Waterside Stress-Assisted Corrosion Cracking in Boilers", *Pulp and Paper Canada*, 91:6 (1990) p. T248-T252

C-E Service Information Letter # 388, "Waterside Corrosion Fatigue Cracking (In Recovery Boilers)"

ABB Service Information Letter # 6-92, “Waterside Stress-Assisted Corrosion Cracking in Chemical Recovery Boilers”

Sylvester, W.R., “Waterside Corrosion Fatigue Cracking – Is There a Single Cause and Solution?,” ABB C-E Services, Inc., TIS 8318, Combustion Engineering, Inc., Windsor, CT